Univerzita Karlova v Praze

Přírodovědecká fakulta

Buněčná a vývojová biologie

Ing. Rastislav Dzijak

Jaderná dynamika a interakce myozinu 1c

Nuclear dynamics and interactions of myosin 1c

Disertační práce

Školitel: Prof. Pavel Hozák, Ph.D., D.Sc.

Praha, 2012

Prohlášení:

Prohlašuji, že jsem závěrečnou práci zpracoval samostatně a že jsem uvedl všechny použité informační zdroje a literaturu. Tato práce ani její podstatná část nebyla předložena k získání jiného nebo stejného akademického titulu.

V Praze, 06.01.2012

Podpis

This work started at the Department of Cell Ultrastructure and Molecular Biology of the Institute of Experimental Medicine and most of it was then accomplished at the Department of Biology of the Cell Nucleus of the Institute of Molecular Genetics v.v.i, Academy of Sciences of the Czech Republic under the supervision of Prof. Pavel Hozák, Ph.D., D.Sc., head of the departments.

I would like to thank here to all the people that influenced me during elaboration of this thesis. I am very thankful to my supervisor Prof. Hozák for allowing me to join his team. He gave me the opportunity to experience the world of great science and generously supported my passion for learning new techniques. Last but not least I thank him for forcing me to work and think as an independent scientist.

I had the luck to meet experienced and skilled people. I am particularly grateful to Michal Kahle who was excellent partner in scientific discussions. He taught me how to look at things from a distance and how to think critically, which I value most.

I am also indebted to Zdeněk Hodný and especially to his "JEZINKY" team. Zorka Nováková, Lenka Rossmeislová and Janička Dobrovolná were the angels who often kept me alive when my happy scientific dreams turned into heavy nightmares with no end in sight. My dears, thank you for showing me that besides science, there is also something called life ☺.

I want to acknowledge Helena Fulková, Vendy Strádalová, Lenka Jarolimová, Magduška Skalníková, Janka Rohožková, Bjetuschka Kalendová, Tomáš Venit, Pavel Marášek, Pavel Kríž Iva Jelínková and all the members of our lab for creating family-like atmosphere, and especially for bravely resisting my critical and sometimes skeptical comments ☺.

Last I would like to thank my parents and family without their constant support this would never exist.

When you have eliminated the impossible,

whatever remains, however improbable,

must be the truth.

Sherlock Holmes

Abbreviations

AA, amino acid
ADP, adenosine diphosphate
ATP, adenosine triphosphate
BEST, bidirectional expression of short transcripts
CaM, calmodulin
CTNND1, catenin (cadherin-associated protein), delta 1
DTT, dithiothreitol
EIF4B, Eukaryotic translation initiation factor 4B
GAPDH, glyceraldehyde-3-phosphate dehydrogenase
GFP, Green fluorescent protein
Glut4, Glucose transporter type 4
GNB2L1, Guanine nucleotide-binding protein subunit beta-2-like 1
GTP, Guanosine triphosphate
HSC70, heat shock cognate 71 kDa protein
HSP90 beta, heat shock protein 90 beta
IPO5, importin 5
IPO7, importin7
KPNB1, karyopherin beta1 (importin-β1)
LAT1, large neutral amino acid transporter
mTOR, Mammalian target of rapamycin
Myo1c, myosin 1c
NM1, Nuclear myosin 1
N-WASP, Neural Wiskot-Aldrich syndrome protein
PBS, Phosphate buffer saline
PCNA, Proliferating cell nuclear antigen
PH domain, pleckstrin homology domain
Pi, inorganic phoshate
PIP2, phosphatidylinositol 4,5-bisphosphate
PKC, protein kinase C
Pol I, RNA polymerase I
Pol II, RNA polymerase II
Rictor, Rapamycin insensitive companion of mTOR
RICTOR, Rapamycin-insensitive companion of mTOR
RT-qPCR, Reverse transcriptase quantitative polymerase chain reaction
SDS, Sodium dodecylsulfate
SH3, Sarc homology type 3
SLC3A2, solute carrier family 3 member 2
SOX9, Sry-related HMG box 9
SRY, Sex-determining region Y
STAT, Signal transducer and activator of transcription
TBP, tata box binding protein
TH1, tail homology domain I
TH2, Tail homology domain II,
TIF-1A, transcription initiation factor I A
WB, Western blotting
WSTF, Williams syndrome transcription factor

Contents

1. ABSTRAKT 9

2. ABSTRACT 10

3. GENERAL INTRODUCTION 11

3.1. THE MYOSIN SUPERFAMILY 11
3.2. THE MYOSIN WORKING CYCLE 11
3.3. BIOCHEMICAL CHARACTERISTICS OF CLASS I MYOSINS 12
3.4. STRUCTURE OF CLASS I MYOSINS 13
3.4.1. The head domain *13*
3.4.2. The neck domain *14*
3.4.3. The tail domain *14*
3.5. REGULATION OF MYOSIN I MOTILITY 15
3.6. DISCOVERY OF NM1 15
3.7. NM1/MYO1C GENE 16
3.8. MYO1C PROTEIN 17
3.8.1. Cellular functions of Myo1c *18*
3.9. NM1 PROTEIN 20
3.9.1. Cellular functions of NM1 ..... *21*
3.10. OTHER MYOSIN MOTOR PROTEINS IN THE NUCLEUS 22

4. MOTIVATION 24

5. SPECIFIC AIMS 24

6. RESULTS 25

6.1. EXPERIMENTAL PART I - EXPRESSION AND LOCALIZATION PATTERN OF NM1 IN MOUSE TISSUES 25
6.1.1. NM1 is ubiquitously expressed and its amount in tissues varies *25*
6.1.2. The expression of NM1 is stimulated by serum *27*
6.1.3. The lifespan of NM1 is longer than 16 h *28*
6.1.4. The specific N-terminal sequence of NM1 is identical in mammals and conserved in vertebrates *29*
6.2. EXPERIMENTAL PART II – IDENTIFICATION OF THE NUCLEAR LOCALIZATION SIGNAL OF NM1 32
6.2.1. NM1 is transported to the nucleus after mitosis *32*
6.2.2. First two IQ domains are needed for nuclear transport of NM1 ..... *34*
6.2.3. The second IQ domain contains a novel NLS sequence *35*
6.2.4. Myo1c is able to translocate into the nucleus *37*
6.2.5. Importins bind the NM1 neck region *39*
6.2.6. NM1 nuclear import does not follow the canonical nuclear import pathway *40*
6.2.7. Overexpression of calmodulin negatively influences NM1 nuclear import *42*
6.3. EXPERIMENTAL PART III - IDENTIFICATION OF NOVEL NM1 INTERACTING PROTEINS 43
6.3.1. Endogenous NM1 and Myo1c are distributed in the cell equally *43*
6.3.2. NM1/Myo1c expression is different in tissues and cell lines *46*
6.3.3. NM1/Myo1c tissue expression is associated with epithelial and endothelial cells *48*
6.3.4. Identification of NM1 associated proteins in whole cell lysates of A549, HeLa, H1299 and HUVEC cells *50*

6.3.5. NM1 associated proteins co-localize with NM1/Myo1c at the leading edge.....*51*
6.3.6. Myo1c is able to functionally substitute NM1 .....*53*

7. DISCUSSION 54
7.1. DISCUSSION PART I - EXPRESSION AND LOCALIZATION PATTERN OF NM1 IN MOUSE TISSUES.....54
7.2. DISCUSSION PART II - IDENTIFICATION OF THE NUCLEAR LOCALIZATION SIGNAL OF NM1 56
7.2.1. NM1 contains NLS within the IQ domain *56*
7.2.2. Role of IQ2 in plasma membrane localization of NM1/Myo1c.....*57*
7.2.3. Mechanism of NM1 nuclear import.....*57*
7.2.4. Nuclear localization of NM1/Myo1c *58*
7.3. DISCUSSION PART III - IDENTIFICATION OF NOVEL NM1 INTERACTING PROTEINS.....59
7.3.1. NM1/Myo1c expression.....*59*
7.3.2. NM1 associated proteins.....*60*

8. GENERAL DISCUSSION 62

9. CONCLUSION.....64
9.1. WHAT IS THE EXPRESSION AND LOCALIZATION PATTERN OF NM1 IN MOUSE TISSUES? ..64
9.2. WHICH NM1 DOMAIN IS RESPONSIBLE FOR THE NUCLEAR LOCALIZATION OF THE PROTEIN? 64
9.3. WHAT IS THE COMPOSITION OF PROTEIN COMPLEXES CONTAINING NM1? 65

10. OVERVIEW OF MATERIALS AND METHODS 66
10.1. ANTIBODIES.....66
10.2. CELLS AND SERUM ACTIVATION 66
10.3. CELLS AND TRANSFECTIONS 67
10.4. CELL SYNCHRONIZATION 67
10.5. PLASMID DNA PREPARATION 67
10.6. ANIMALS 68
10.7. IMMUNOFLUORESCENCE MICROSCOPY 68
10.8. IMMUNOBLOTS 69
10.9. RNA ISOLATION AND RT-QPCR 70
10.10. RACE 70
10.11. SEQUENCE SEARCHES, ALIGNMENT, AND CONSTRUCTION OF PHYLOGENETIC TREES ..71
10.12. PULL-DOWN ASSAYS AND IMMUNOPRECIPITATION 71
10.13. PROTEOLYTIC DIGESTION AND SAMPLE PREPARATION 73
10.14. MASS SPECTROMETRIC ANALYSIS.....74
10.15. GENERATION OF THE NM1 KNOCK-OUT MICE 74
10.16. ISOLATION OF NUCLEI FROM MOUSE LIVER.....74

11. REFERENCES.....76

12. APPENDIX.....82

1. ABSTRAKT

Myosiny jsou proteiny, které přeměňují chemickou energii uloženou v ATP na mechanickou sílu, která se aplikuje na vlákna aktinu. Jaderný myosin 1 (NM1) byl první myosin detekován v jádře buňky. Spolu s jaderným aktinem hraje důležitou roli při transkripci DNA a remodelaci chromatinu. Nicméně, molekulární mechanismy funkce NM1 jsou zatím neznámé. K získání dalších poznatků o tomto molekulárním motoru jsme studovali expresi a distribuci NM1 v tkáních, mechanismus jeho jaderné lokalizace a také jeho další molekulární interakce.

V první části byla studována exprese NM1 v různých tkáních myší. Bylo prokázáno, že NM1 se vyskytuje v buněčných jádrech všech myších tkání, přičemž do studia nebyly zahrnuty buňky v terminálním stádiu spermatogeneze. Kvantitativní PCR a western blot prokázaly, že exprese NM1 je různá v jednotlivých myších tkáních a nejvyšší je v plicích. NM1 je izoforma dříve objeveného myosinu 1c (Myo1c), který byl popsán nejprve jako protein cytosolový. Jediný známý rozdíl mezi těmito dvěma proteiny je přítomnost 16 aminokyselin na N-konci NM1. V další části byl proto studován vliv NM1 domén, včetně N-koncového peptidu, na subcelulární lokalizaci tohoto proteinu. Zjistili jsme, že N-koncový peptid NM1 není nezbytný pro jeho vstup do jádra. Jaderný lokalizační signál jsme objevili v doméně NM1 která také váže lehký řetězec, kalmodulin. Tato doména je přítomna také v "cytoplasmatické" isoformě, v proteinu Myo1c. Potvrdili jsme přítomnost obou izoforem v buněčném jádře. Použitím polyklonálních protilátek proti N-konci NM1 a monoklonální protilátky proti ocasu NM1/Myo1c bylo ukázáno, že endogenní NM1 a Myo1c kolokalizují ve zvýšené míře v jádře a na plazmatické membráně. Nakonec jsme použitím techniky ko-imunoprecipitace identifikovali nové interakční partnery NM1 zejména aktin- a fosfolipid-vázajících proteiny. Zajímavé je, že některé z identifikovaných proteinů byly rovněž popsány v komplexu s Myo1c. Závěrem vyslovujeme hypotézu, že NM1 a Myo1c by mohly být stejné funkční varianty jednoho genu.

V této práci jsou prezentovány výsledky, které zvýšily naše znalosti o expresi a lokalizaci NM1 v tkáních, mechanismu jeho jaderné lokalizace a jeho molekulárních interakcí. Nejzajímavějším výsledkem je, že NM1 je více podobný Myo1c, než bylo původně předpokládáno. Proto cílem dalších experimentů bude ověřit, zda NM1 a Myo1c jsou funkčně totožné proteiny.

2. ABSTRACT

Myosins are proteins that convert chemical energy stored in ATP into mechanical force that is applied on an actin filament. Nuclear myosin 1 (NM1) was the first myosin detected in the cell nucleus. Together with nuclear actin they were shown to play important roles in DNA transcription and chromatin remodeling. However, the molecular details of the NM1 functions are largely unknown. To expand our knowledge about this molecular motor we studied tissue expression, mechanism of nuclear localization and molecular interactions of this myosin motor.

In the first part we examined the expression pattern of NM1 in various mouse tissues. We demonstrated that NM1 is present in cell nuclei of all mouse tissues examined except for cells in terminal stages of spermatogenesis. Quantitative PCR and western blots demonstrated that the expression of NM1 in tissues varies, with the highest levels in the lungs. NM1 is a nuclear isoform of earlier identified myosin 1c (Myo1c), which was described initially as a cytosolic, and plasma membrane associated protein. The only known difference between these two proteins was the presence of additional 16 amino acids at the N-terminus of NM1. Next we focused on the influence of NM1 domains, including the N-terminus, on the subcellular localization of this protein. We found out that N-terminus is not required for nuclear entry. Surprisingly, we found a nuclear localization sequence placed within calmodulin-binding motif of NM1. This sequence is also present in the "cytoplasmic" Myo1c protein. We confirmed the presence of both isoforms in the nucleus. The notion that overexpressed NM1 and Myo1c could localize to the cell nucleus prompted us to inspect their colocalization in cells and tissues. Using polyclonal antibodies toward the N-terminus of NM1 and a monoclonal antibody against the tail domain we found that endogenous NM1 and Myo1c colocalize to a high extend in nucleus and at the plasma membrane. Finally, we looked for new interaction partners of NM1 using co-immunoprecipitation. We found set of actin- and phospholipid- binding proteins as the proteins that co-purified from the cell extracts with NM1. Interestingly, some of the identified proteins were also found in complex with Myo1c. We hypothesized that NM1 and Myo1c could be functionally similar transcript variants of the same gene.

The most intriguing result is that NM1 is more similar to Myo1c than previously imagined. Therefore one of the most interesting future questions would be to verify whether NM1 and Myo1c are functionally identical. Naturally, this requires further experiments.

3. GENERAL INTRODUCTION

3.1. The myosin superfamily

Myosins are unique proteins that have the ability to transform free chemical energy stored in ATP into mechanical force. They are best known as engines that power the muscle contraction. In addition to "conventional" muscle myosin, there is a whole family of other myosins called "unconventional" myosins. The first unconventional myosin was isolated from *Acanthamoeba* (Pollard and Korn, 1973). This myosin displayed differences from the muscle myosin in being of lower molecular weight and having only single motor domain. It was named myosin-I. Since that time many other unconventional myosins (termed myosin III – XVII) have been isolated and the family became larger (**Figure I**). Importantly, in organisms the expression of these motor proteins is not restricted to muscle cells but is found in almost all cell types of the body.

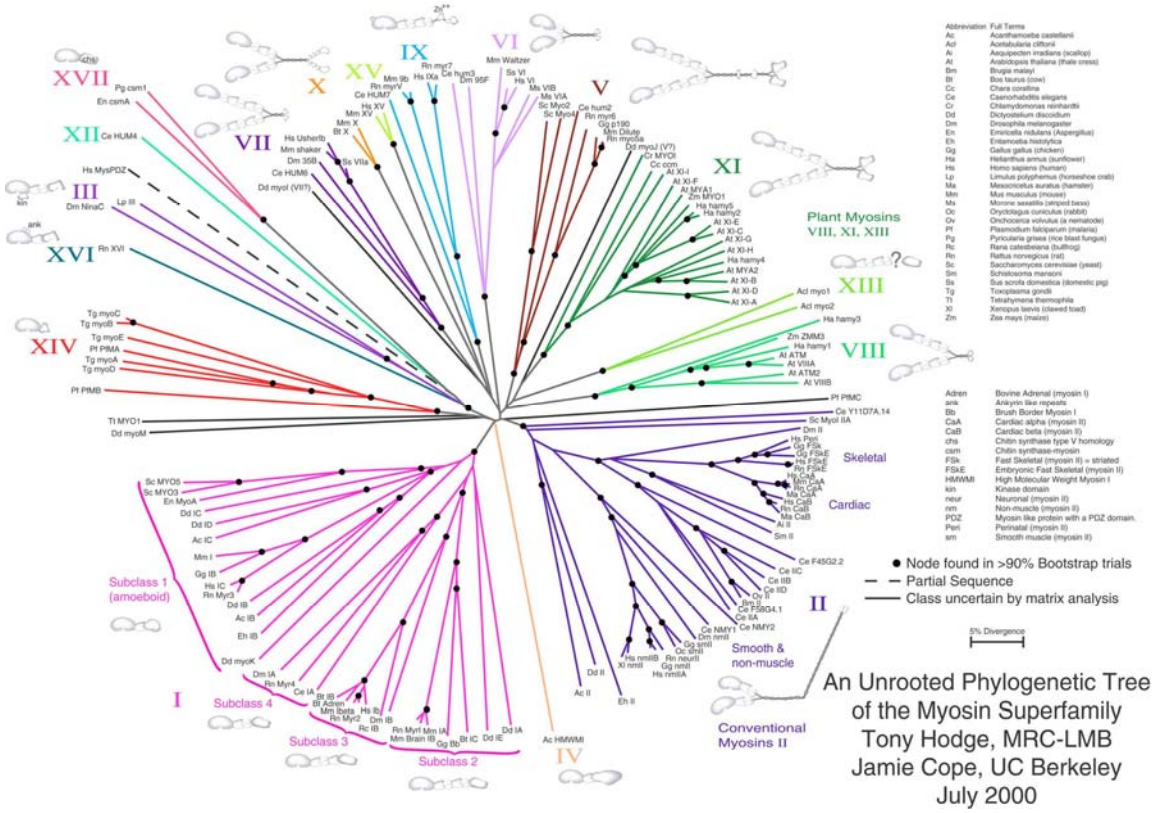

Figure I. Myosin superfamily.

3.2. The myosin working cycle

Every myosin is in fact an ATPase that binds ATP, cleaves it into ADP and inorganic phosphate (Pi) and releases the products of cleavage in a stepwise manner. This cycle is

many fold faster in the presence of actin, therefore myosins are actin-activated ATPases. During the ATPase cycle the myosin head undergoes also substantial conformational changes that in turn alter its affinity for actin as a result, myosin cycles between strong and weak actin binding states. The nucleotide-free head binds strongly to actin. This state is called rigor (from *rigor mortis* - stiffness of the dead body). The actin-myosin crossbridge is dissociated by binding of ATP to the head of myosin. Upon detachment from actin, the head cleaves ATP into ADP*Pi and myosin recocks itself for the power stroke. At this state it binds stereospecifically between two adjacent actins in the actin filament. Concomitantly with the release of Pi a series of conformational changes cause swinging of so called converter domain that results in movement of the tail. During this state myosin generates force (Geeves and Holmes, 1999), ADP is released from the head and the ATPase is ready for another cycle. The ATPase cycle is depicted on the **Figure II** below.

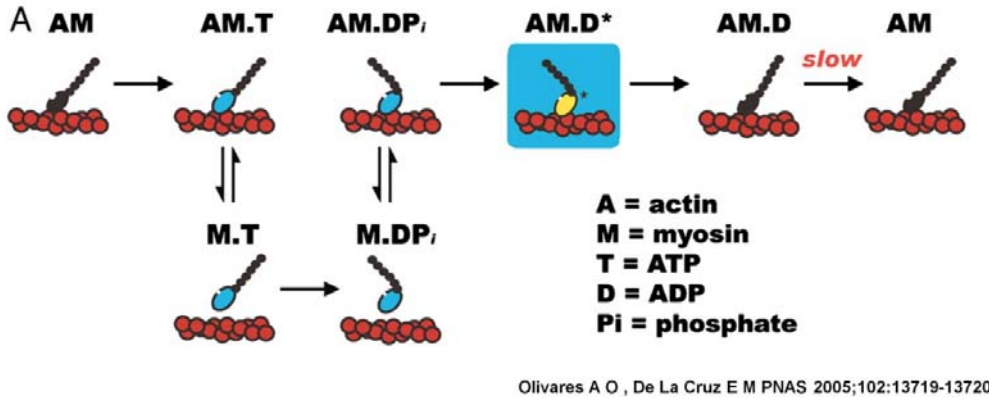

Figure II. The myosin ATPase cycle

3.3. Biochemical characteristics of class I myosins

The lifetimes of strong and weak actin binding states together with duty ratio (fraction of total ATPase cycle where myosin is tightly bound to actin) are important characteristics describing the motile properties of a given myosin. Class I myosins are cleaving ATP slowly and spend small fractions of their ATPase cycle tightly bound to actin. Another characteristic of molecular motors is the processivity; defined by the number of ATPase cycles that the motor spends tightly associated with its track. As can be already deduced from the myosin ATPase cycle, a single molecule of myosin is non-processive because it requires detachment from the actin track in order to continue in ATPase cycle. Processivity is thus arranged by association of myosin molecules into large arrays. Subclass 2 of myosin I´s contains a short tail and is therefore unable to dimerize. There must be at least

50 molecules of these myosins attached to the cargo and actin filament at the same time in order to achieve processivity (O'Connell et al., 2007).

In conclusion, myosin I family members are monomeric, non-processive, slow rate and low duty ratio motors.

3.4. Structure of class I myosins

Phylogenetically, myosin I class could be divided into two subclasses. Subclass I members have long tails consisting of tail homology 1 (TH1), tail homology II (TH2) and SH3 domains. On the other hand subclass II has only short tail containing TH1 domain (**Figure III**). Nuclear myosin 1 (NM1) belongs to the subclass II. Based on their motor domain sequences, the class I myosins can be further sub-divided into two subclasess. In vertebrates, the long tailed (Myo1E) forms the subclass I, and the short tailed (Myo1A, Myo1B, and Myo1C) form the subclass 2 (De La Cruz and Ostap, 2004).

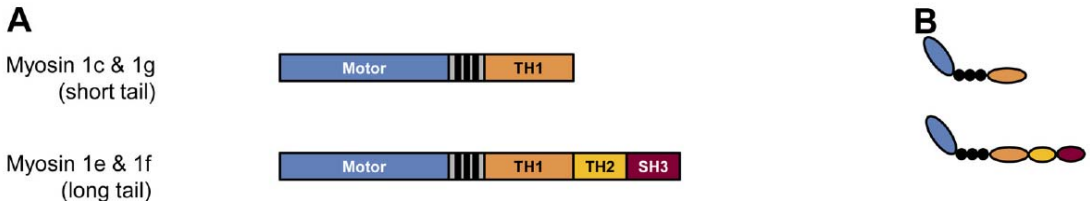

Figure III. Domain organization of class I myosins

3.4.1. The head domain

The ATPase cycle of subclass 2 myosins has an interesting property which results in a power stroke that has two steps (Veigel et al., 1999; Batters et al., 2004a). Rapid and large displacement of lever arm is followed by an additional swinging of the lever arm that leads to smaller displacement. Optical trap measurements revealed that the second step is accompanied by ADP release. Interestingly, in the presence of opposing force (i.e applied against the power stroke direction) the ADP is trapped in the head and myosin stays tightly bound to actin. The power stroke is finished only when the strain is relieved and the actin filament moves in the direction of power stroke. This property could be used in maintaining a sustained tension (Batters et al., 2004b) or a directional movement. If the mechanical load is applied on myosin I, it can switch from a low to a high duty ratio motor (Laakso et al., 2008), which means that it stays bound longer to the actin filament. Subclass II of myosin I molecules do not have the ability to "walk" along the actin filaments, thus they are not able to pull a cargo constantly. However, acting as "ratchets"

they can support unidirectional movement of a load that would be otherwise moved back and forth by diffusion. This knowledge has led to a model where myosin I molecules support the unidirectional movement of their cargoes acting as Brownian ratchets (Nambiar et al., 2010).

3.4.2. The neck domain

Neck domain (also the regulatory domain or the light chain binding domain) of myosins is continuation of the converter domain that transmits the movements produced by conformational changes in the head further to the tail. It consists of helical sequences that are bound by small proteins called the light chains. The function of light chains is to stabilize the lever arm of myosin and ensure that mechanical force is transmitted to the tail. In most class I myosins the light chains are calmodulins that bind to so called IQ motifs. These are short peptides (~25 residues in length), containing isoleucine and glutamine residues. The consensus motif is IQXXXRGXXXR, where residues X vary and may to a great extend modify the mechanism of calmodulin binding (Houdusse et al., 2006). Myosin I class members have 1-6 IQ motifs and it is believed that the length of neck determines the size of displacement steps (Kohler et al., 2003). Crystal structure of first two IQ motifs of myosin V in complex with calmodulin revealed that the calmodulin binds neck in calcium-free state wrapping around the IQ motif with its C-terminal lobe (Houdusse et al., 2006). Binding of calcium to calmodulin weakens the binding of calmodulin to the neck which leads to dissociation of some calmodulin molecules from the tail (Manceva et al., 2007). Besides binding calmodulins the IQ motifs of myosin 1c were shown direct its subcellular localization and binding to yet unknown receptors in the plasma membrane of mechanosensitive hair cells of the inner ear (Cyr et al., 2002). Discovering IQ-binding proteins will allow us to obtain better insight into the molecular functions of myosin-I.

3.4.3. The tail domain

The tail domain is the most divergent part of a myosin molecule that fundamentally influences its functions. Given the nature of their ATPase cycles all myosin motors are non-processive but the long tail with coiled-coil motif of class II members enables the bundling of many heads into one filament. This is increasing the probability of having more heads attached to the actin filament and executing power stroke while the others are just positioning themselves for another ATPase cycle. Only few unconventional myosins have the ability homodimerize via their tails (e.g. myosin V, myosin VI) and move along the actin filament processively. Most tails of class I myosins contain specific binding sites

for cargoes. The tail of subclass II is short, basic and has the affinity toward the acidic phospholipids such as PIP2 (Tang et al., 2002; Hokanson and Ostap, 2006). Interestingly, the tail domain seems to adopt different conformations in response to calcium as shown by cryo-electron microscopy analysis of the Myo1a protein (Whittaker and Milligan, 1997).

3.5. Regulation of myosin I motility

Proposed mechanism of the regulation of myosin predicts that the light chains which bind the neck part, stabilize the lever arm of myosin, thus the force generated by head could be transmitted to the tail (Barylko et al., 2005). Both the ATPase activity and the myosin motility are influenced by calcium. Elevated Ca^{2+} levels stimulate the ATPase activity of myosin several times (Lieto-Trivedi and Coluccio, 2008). Although this might suggest that the motility is stimulated by calcium, the opposite is true. Micromolar concentration of free Ca^{2+} inhibited the movement of actin filaments in an actin-gliding assay (Zhu et al., 1998). This is because the calcium also causes dissociation of one calmodulin from the neck of myosin while the other changes the conformations. In agreement with the lever arm model, calmodulin dissociation from myosin weakens the lever arm and force generation is inhibited. At the present it is not clear which calmodulin dissociates from the neck of Myo1c as the first, but based on biochemical studies (Manceva et al., 2007), it was proposed that the first IQ in the vicinity of the head domain binds the Ca^{2+}-calmodulin with the lowest affinity. Further *in vivo* studies supported this model by the fact that elevated calcium not only causes dissociation of calmodulin but also provokes phosphorylation of serine in the first IQ. Addition of phosphate group to the serine residue within the first IQ by casein kinase increases negative charge and results in electrostatic repelling of calmodulin. That leads to more stabile inactivation of the motility (Yip et al., 2008) . Also protein kinase C was shown to be able to phosphorylate myosin I (Swanljung-Collins and Collins, 1992; Williams and Coluccio, 1995) however, this modification did not influence the actin sliding.

3.6. Discovery of NM1

Nuclear myosin 1 (also Nuclear myosin 1 beta) was discovered accidentally in 1997 (Nowak et al., 1997). The original intention of investigators was to prepare polyclonal antibody against a myosin 1 that was purified from bovine adrenal gland. Surprisingly, the affinity purified antibody against adrenal myosin 1 preparation had a strong immunoreactivity against the cell nucleus. It also recognized band on western blot with

approximate molecular weight of 120 kDa. Similarly to other myosin I family members, the partially purified protein bound calmodulin, ATP and actin. In order to identify the recognized protein, 3T3 nuclear extracts were subjected to immunoprecipitation with the polyclonal sera. The mass spectrometric analysis of the immunopurified protein showed high homology to a member of the myosin 1 family, the Myo1c (myr2, myosin 1 beta) known to be associated with plasma membrane (Wagner et al., 1992). Interestingly, the micro-sequencing also revealed the presence additional 16 amino acids at the N-terminus of NM1. Affinity purified antibody generated against the N-terminal 16 amino acid peptide specifically labeled nuclei of different cell types. Due to the fact that this was the first myosin identified in the cell nucleus the protein was named Nuclear myosin 1 (NM1) (Pestic-Dragovich et al., 2000).

3.7. NM1/Myo1c gene

Human *Myo1c* gene is located at reverse strand of chromosome 17. Mouse *myo1c* is located at chromosome 11. Alternative start of transcription and splicing gives rise to two mRNAs (**Scheme 1 and Figure IV**) that differ in their 5' ends (Pestic-Dragovich et al., 2000). The NM1 mRNA contains an upstream start of translation that brings about the additional 16 amino acids that were found in protein by microsequencing. This additional start of translation is found in exon -1. The transcription of Myo1c gene starts more upstream in, and is the resulting mRNA containing exons -2 and 1, possibly due to alternative splicing. Downstream sequence of Myo1c and NM1 is essentially the same. The NM1 gene contains 13 exons.

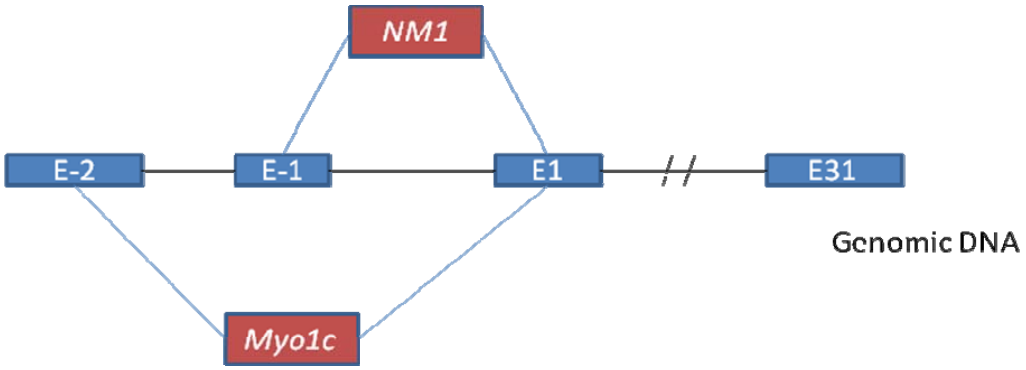

Scheme 1. Genomic organization of NM1/Myo1c gene

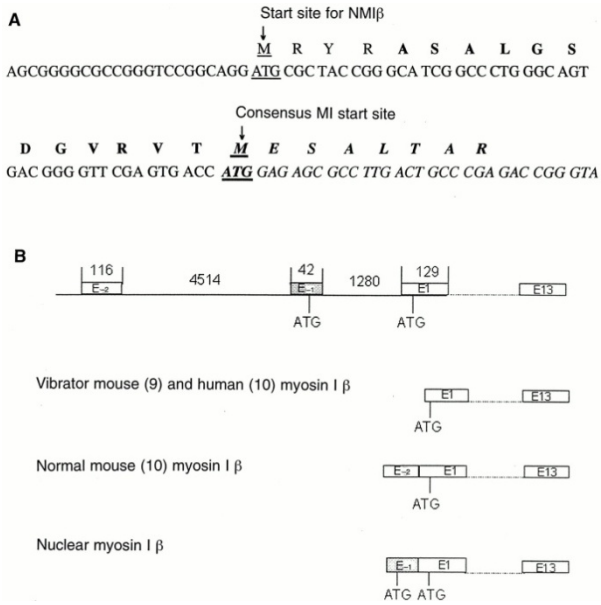

Figure IV. Translation starts of NM1 and Myo1c (Pestic-Dragovich et al., 2000).

3.8. Myo1c protein

Myo1c was discovered independently by several investigators earlier than NM1 (Wagner et al., 1992; Gillespie et al., 1993; Zhu and Ikebe, 1994; Ruppert et al., 1995). Firstly, it was named based on the source tissue or animal (mammalian myosin 1beta, myr2 – rat brain, BAGMI-bovine adrenal gland myosin 1). After unification of the myosin nomenclature it is called Myosin 1c (Gillespie et al., 2001).

Myo1c is a short-tailed class I unconventional myosin, unable to form dimers. The overall structure (**Scheme 2)** consists of the head domain (ATPase), the neck domain (transmission) and the short tail (binding cargoes). It binds directly ATP and actin via the head and up to three calmodulin molecules via the neck (Gillespie and Cyr, 2002).

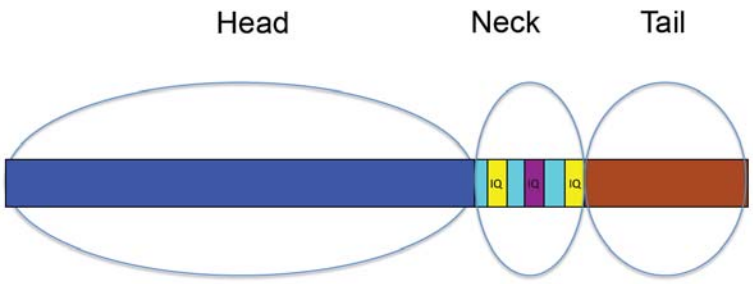

Scheme 2. Domain structure of Myo1c

The tail domain of Myo1c binds tightly and specifically to negatively charged lipids such as PIP2 *in vivo* and *in vitro* (Hokanson et al., 2006; Hokanson and Ostap, 2006). The energy of the PIP2-Myo1c bond is higher than is needed for extraction of the lipid from the bilayer (Pyrpassopoulos et al., 2010). Besides PIP2 there are also protein interaction partners that were shown to bind directly to myo1c tail.

3.8.1. Cellular functions of Myo1c

This protein shows wide expression in variety of rat tissues (Wagner et al., 1992; Ruppert et al., 1995). The molecular function of Myo1c had been studied thoroughly in number of different cell types and was mostly connected dynamic events at the cytoplasmic membrane.

Perhaps the most extensively studied is the function of myo1c the process of hearing. The hair cells located in inner ear form the apparatus that is able to transform mechanical pulses into electrical ones. These impulses are processed by brain into perception of sound. Myo1c was observed in clusters along actin-rich protrusions emanating from the hair cell body (Garcia et al., 1998) with highest concentration at the tips of these so-called stereocilia. Stereociliary tips are connected together with proteinaceous link that opens mechanically gated ion channels when the stereocilia move. The flow of ions through the channel induces neuronal impulse. In noisy environment stereocilia bend and channels are open. In order to percept further changes in sound, ion channels need to be closed first and then re-open by promoted bending of stereocilia. This is called adaptation. Myosin 1c was shown to have direct function in this process since upon its inhibition the adaptation is slow and inefficient (Stauffer et al., 2005) (**Figure V**). Interestingly, a clinical study focused on identification of mutation in this protein revealed 6 missense mutations in Myo1c that were associated with bilateral hearing loss (Zadro et al., 2009).

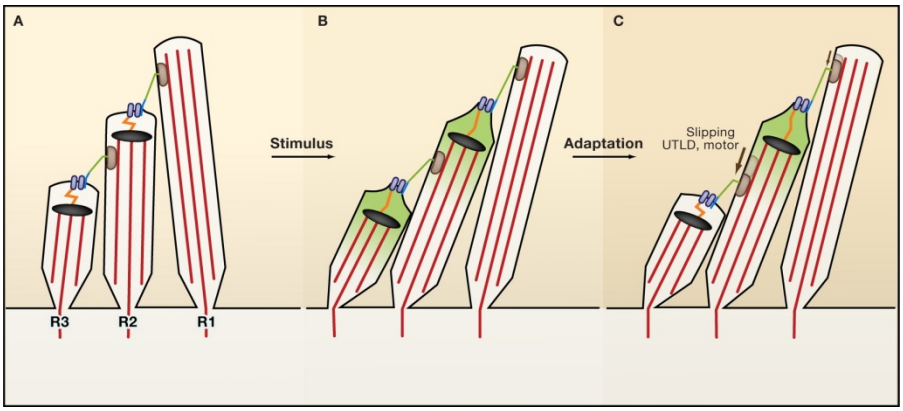

Figure V. Schematic overview of the adaptation process (Gillespie and Muller, 2009)

Several research groups studied function of myosin 1c in adipocytes. Initially, the group of Michael Czech provided evidence that Myo1c facilitates the transport of glucose across the plasma membrane. Stimulation of adipocytes with insulin leads to translocation of the glucose transporter GLUT4 from perinuclear region toward the plasma membrane. Myosin 1c was shown to be necessary for incorporation of the transporter into the plasma membrane (Bose et al., 2002; Bose et al., 2004). It was shown later that insulin-stimulated glucose transport requires the activation of small G protein RalA (**Figure VI**) and its interactions with both the exocyst complex and Myo1c (Chen et al., 2007).

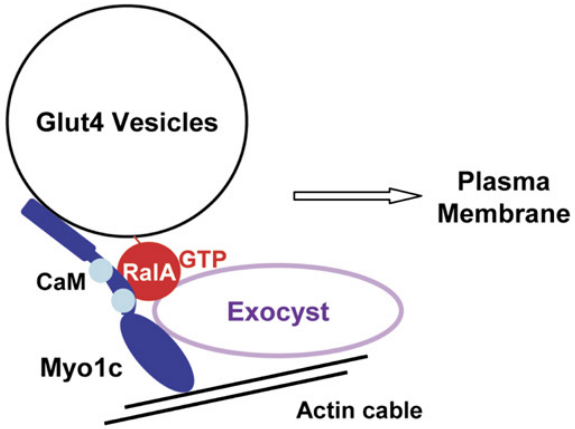

Figure VI. Glut4 incorporation into plasma membrane requires Myo1c (Chen et al., 2007)

Expression of myosin 1c was also detected in different cell types of kidney (Wagner and Molitoris, 1997). In epithelial cells lining up the surface of kidney collecting ducts, myosin 1c was shown to regulate sodium transport. Similarly to function of glut GLUT4 transport, the role of Myo1c could be the regulation of epithelial sodium channel insertion into plasma membrane (Wagner et al., 2005). In addition to collecting ducts, Myo1c expression in podocytes appears to be necessary for the formation of cell-cell junctions and tightening of the glomerular filtration barrier (Arif et al., 2011).

The above mentioned functions myosin 1c are extended by regulation of cortical actin dynamics in Xenopus oocytes (Sokac et al., 2006), maintaining tension in neuronal growth cones (Diefenbach et al., 2002; Wang et al., 2003), phagocytosis in macrophages (Allen and Aderem, 1995) and formation of the immunological synapse in B type lymphocytes (Maravillas-Montero and Santos-Argumedo, 2011).

Taken together, the shorter isoform of the two myosins - myosin 1c - appears to be involved mainly in exocytosis and maintenance of the cytoskeleton-plasma membrane adhesion.

3.9. NM1 protein

NM1 protein shares the same sequence as Myo1c with one exception, which is the presence of additional 16 amino acids at the N-teminus of NM1. It is known to bind actin, ATP and calmodulin (Nowak et al., 1997) while direct binding partner of the positively charged tail domain is yet to be identified. Nevertheless, there is some evidence that it could bind electrostatically to naked DNA (Hofmann et al., 2006a) or RNA (Obrdlik et al., 2010). On the other hand, the sequence of Myo1c and NM1 tails are essentially the same, therefore one could reasonably expect that NM1 is able to bind PIP2 as well. Interestingly, NM1 protein was shown to associate with the principal controller of RNA polymerase I transcription, with TIF1A (Philimonenko et al., 2004). However it is not known whether the interaction is direct or mediated via some of the NM1 direct binding partners. The biochemical characteristics of this protein are yet to be measured, but based on the high sequence similarity between Myo1c and NM1 one can assume that NM1 is also a non-processive low duty ratio motor, with slow rate of the ATP hydrolysis. Mechanistically, one can expect that its basic function is to maintain tensions as proposed for Myo1c (Laakso et al., 2008). The exact function of the N-terminal extension in NM1 molecule that makes the only known difference from Myo1c is uncertain. However, the observation that NM1 is localized mainly in the nucleus and Myo1c at the plasma membrane has led to the opinion that the N-terminus could function as a nuclear targeting or nuclear sequestering sequence (Pestic-Dragovich et al., 2000) (**Scheme 3**).

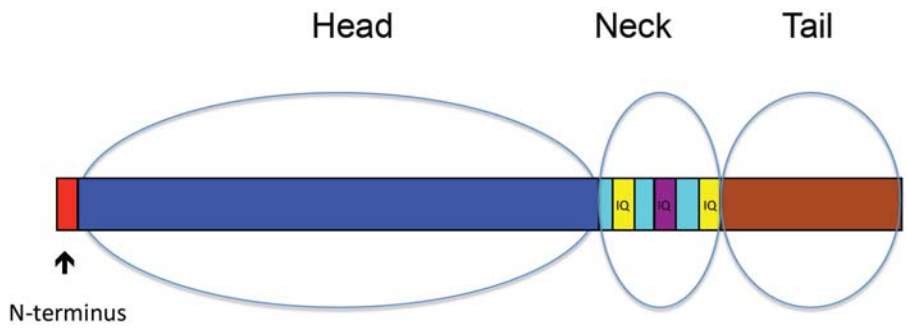

Scheme 3. Domain structure of NM1 protein

3.9.1. Cellular functions of NM1

The main difference from Myo1c was that in addition to plasma membrane, NM1 localized as the first myosin ever also to the cell nucleus (Nowak et al., 1997). Initial hinting on NM1 functions revealed that it is involved in control of DNA transcription. To date, there is ample evidence for involvement of NM1 in transcription by RNA polymerase I and II (Pol I and Pol II). NM1 co-localized with both polymerases at the sites of transcription (Nowak et al., 1997; Fomproix and Percipalle, 2004; Philimonenko et al., 2004; Kysela et al., 2005; Philimonenko et al., 2010), and physically associates with both Pol I and Pol II complexes (Philimonenko et al., 2004; Hofmann et al., 2006b). In-vivo rate of transcription is affected by NM1 overexpression, knock-down and nuclear microinjections of anti-NM1 antibodies. In an in-vitro transcription system, anti-NM1 antibodies inhibit transcription by both polymerases in a dose-dependent manner, whereas adding purified NM1 increases transcription (Pestic-Dragovich et al., 2000; Philimonenko et al., 2004). Transcription initiation assays have revealed that NM1 exerts its function in early steps of Pol I and II transcription, after the formation of pre-initiation complexes (Hofmann et al., 2006b; Ye et al., 2008). Indeed, NM1 interacts with Pol I transcription factor TIF-IA, which is present only in initiation-competent fraction of Pol I complexes (Grummt, 2003), and actin that is associated with RNA polymerase I independently of transcription. According to (Grummt, 2006), the binding of NM1 to Pol I via actin may help to initiate transcription by recruiting TIF-IA to pre-initiation complex (**Figure VII)**.

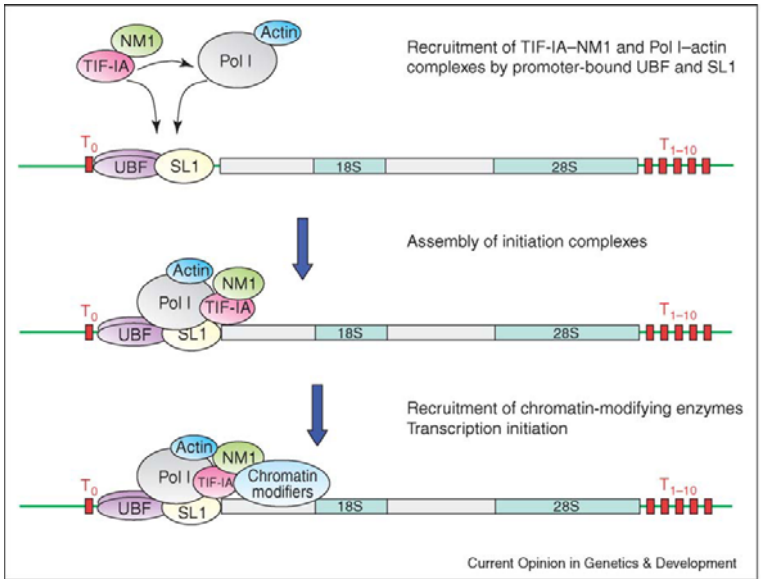

Figure VII. Acto-myosin interaction at the rDNA promoter. from (Grummt, 2006)

This model is further supported by the fact that functional motor domain is needed for interaction of NM1 and Pol I (Ye et al., 2008). In addition to transcription initiation, NM1 is also involved in Pol I transcription elongation since it associates with the chromatin remodeling complex WSTF-SNF2h and might therefore recruit this complex to the actively transcribing genes (Percipalle and Farrants, 2006).

Interestingly, nascent ribosomal particles seem to be accompanied by NM1 during transport from nucleolus toward the nuclear pores (Obrdlik et al., 2010). Furthermore, blocking of NM1 or actin by antibodies results in nuclear retention of small ribosomal subunits (Cisterna et al., 2006; Cisterna et al., 2009).

A role of acto-myosin motor in repositioning of chromosomes is also emerging (Hu et al., 2008; Mehta et al., 2010). In pioneering work, (Chuang et al., 2006) and co-workers showed that labeled artificial gene loci move upon activation toward the center of nucleus and that overexpression of mutated NM1 that lacks motor activity inhibits this effect. However, the exact mechanism behind these translocation phenomena is not clear.

Of particular interest is emerging role of NM1 in estrogen signaling. NM1 was shown to be involved in chromosomal interaction of estrogen-activated genes (Hu et al., 2008). It was also co-purified with estrogen receptor α (Ambrosino et al., 2010).

3.10. Other myosin motor proteins in the nucleus

Currently, there are 5 other myosin molecules that were observed in the nucleus (myosin VI, Va, Vb, XVIb, and XVIIIb) (**Figure VIII**).

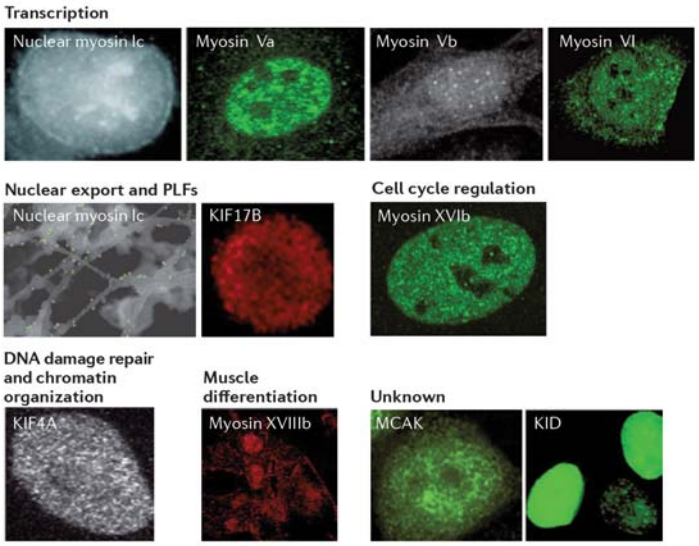

Figure VIII. Molecular motors in the nucleus from (Simon and Wilson, 2011)

They have some interesting properties. Myosin VI that was shown to be associated with RNA polymerase II is able to move along actin to the opposite direction compared to other myosins (Vreugde et al., 2006).

Myosin V localizes to the nucleolus and nucleoplasm, associates with RNA pol I (Lindsay and McCaffrey, 2009). Interestingly, it is able to dimerize and to move a cargo over long distances processively. Initial experiments with myosin XVIb revealed that it co-localizes with the proliferating cell nuclear antigen (PCNA) and its overexpression slows down S-phase of cell cycle (Cameron et al., 2007). Sequence analysis of this protein predicts low ATPase activity and suggests that it could serve rather as a scaffold then as a motor.

4. MOTIVATION

The key motivation behind this dissertation was the fact that nuclear myosin I function has been studied only in cultured cells. However, nothing was known about the tissue expression and distribution of this myosin. Since it differs from the cytoplasmic myo1c only by 16 AA at the N-terminus another interesting question was: What is the function of this N-terminal extension? Naturally, one could predict that these 16 AA are bringing NM1 into the nucleus. However, solid data supporting this hypothesis were missing. And least but not last, despite the evidence that NM1 is involved in control of transcription the exact mechanism how it fulfills this functions is unknown. To understand it in detail, we decided to identify the proteins that associate with NM1 (either directly or indirectly). During the course of conducting the experiments another interesting questions arose. These will be discussed.

5. SPECIFIC AIMS

What is the expression and localization pattern of NM1 in mouse tissues?

Which NM1 domain is responsible for the nuclear localization of the protein?

What is the composition of protein complexes containing NM1?

6. RESULTS

6.1. Experimental part I - Expression and localization pattern of NM1 in mouse tissues

To extend the amount of information available about nuclear myosin, we investigated the tissue expression pattern, the tissue localization pattern of this protein as well as the regulation of NM1 expression. High degree of evolutionary conservation usually points to some important function; therefore we searched for NM1 othologues in different species.

6.1.1. NM1 is ubiquitously expressed and its amount in tissues varies

Different levels of NM1 expression in tissues could suggest certain tissue-specific functions. We have therefore screened eleven mouse organs: small intestine, pancreas, brain, kidney, skin, heart muscle, testis, striated muscle, spleen, liver, and lungs by immunofluorescence microscopy (**Fig. 1**). We observed nuclear staining in all cell types examined but no obvious differences in signal intensity were observed in nuclei of various cell types. There was only one exception - cells in the latest stages of spermatogenesis, which were completely negative.

We also examined the expression of NM1 in these tissues by Western blot (**Fig. 2b**). Intriguingly, the amount of NM1 in lungs was many times higher than in any other tissue. Relatively high levels of NM1 were also found in the small intestine, kidney, skin, heart, testis, spleen, and liver. Low levels were detected in pancreas, brain, and skeletal muscle.

Next, we compared the tissue levels of NM1 and cytoplasmic Myo1c. Since Myo1c differs from NM1 only by missing 16 amino-acid epitope, there is no antibody available that would recognize Myo1c specifically. We used therefore an antibody directed against the tail of Myo1c recognizing both Myo1c and NM1. The tissue levels in this case were similar to NM1, however, the signal in lungs is not so prominent and there is relatively stronger signal in intestine, pancreas, kidney, heart, and liver. We were also able to separate the two myosin isoforms in 3T3 cells and liver tissue by SDS-PAGE. Two distinct bands were distinguished when stained by the antibody recognizing Myo1c tail while the anti-NM1 antibody recognized only the upper band. In both 3T3 cells and mouse liver sample (same as in **Fig. 2b**) the NM1 band was about two to three times weaker than Myo1c band (data not shown).

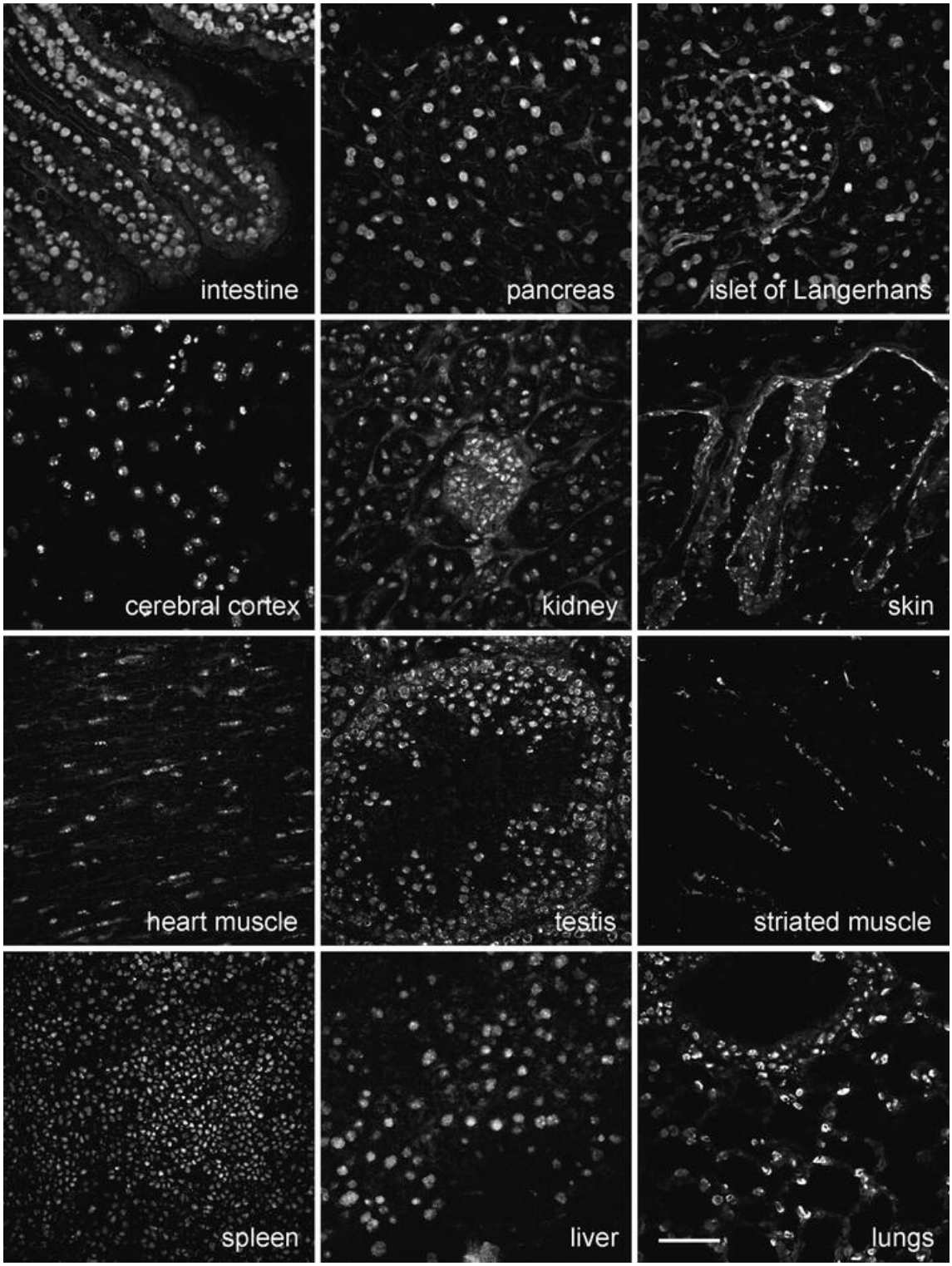

Fig. 1 NM1 is present in nuclei of all mouse tissues. Confocal immunofluorescence microscopy on cryosections shows that NM1 is present in nuclei of all tissues tested with one exception—there is no signal in cells in latest phases of spermiogenesis. *Bar* 50 μm

To quantify the NM1 mRNA, we performed real-time RT-qPCR in the same tissues as above. The primers were designed to anneal to 5′ region unique to NM1 and therefore they detected NM1 mRNA specifically. The amounts of NM1 mRNA are shown relatively to total RNA in samples. We found the highest levels of NM1 mRNA in lungs, medium in heart, testis, and spleen, and low in other tissues (**Fig. 2a**).

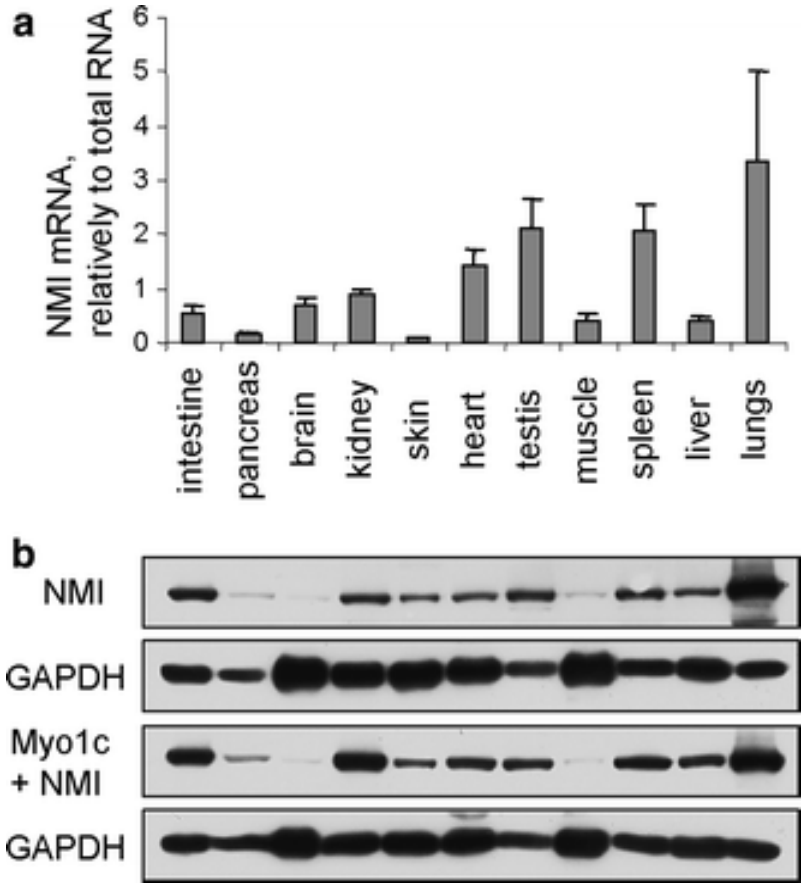

Fig. 2 Expression of NM1 varies in mouse tissues. a) Total RNA was isolated from mouse tissues and identical amounts were analyzed by quantitative RT-PCR. Measurements were repeated with samples from five to eight animals except for skin where only one sample was of sufficient quality, and lungs where samples from two animals were taken only after finding of the high expression on the blot. Averages and standard errors are shown. **b)** Western blot of NM1 and Myo1c in the same tissues. A total of 65 µg of proteins were loaded, β-actin serves as loading control

6.1.2. The expression of NM1 is stimulated by serum

To test the connection of NM1 expression with cell proliferation, we measured the response of NIH 3T3 cells to serum. The cells were first starved in 0.1% serum medium for 48 h and then stimulated by addition of medium containing 10% serum. The amount of mRNA for NM1 was then measured by RT-qPCR (Fig. 3a). Results were normalized to total RNA. The levels of glyceraldehyde-3-phosphate dehydrogenase (GAPDH) and β-actin mRNAs are shown for comparison. Actin mRNA was found previously in a similar

experiment not to change relatively to total mRNA levels (Iyer et al., 1999) so it can represent an "average" transcript. The amount of mRNA for NM1 as well as for actin and GAPDH halved during serum starvation but increased during 2–4 h after serum stimulation, and then slightly decreased. NM1 mRNA was activated by serum more than the housekeeping genes' mRNA. Additional RT-qPCR experiments showed that NM1 expression rose gradually during the first two hours of serum activation (data not shown). However, on the protein level, the amounts of NM1 relatively to total protein content did not change significantly as shown by Western blot (**Fig. 3b**).

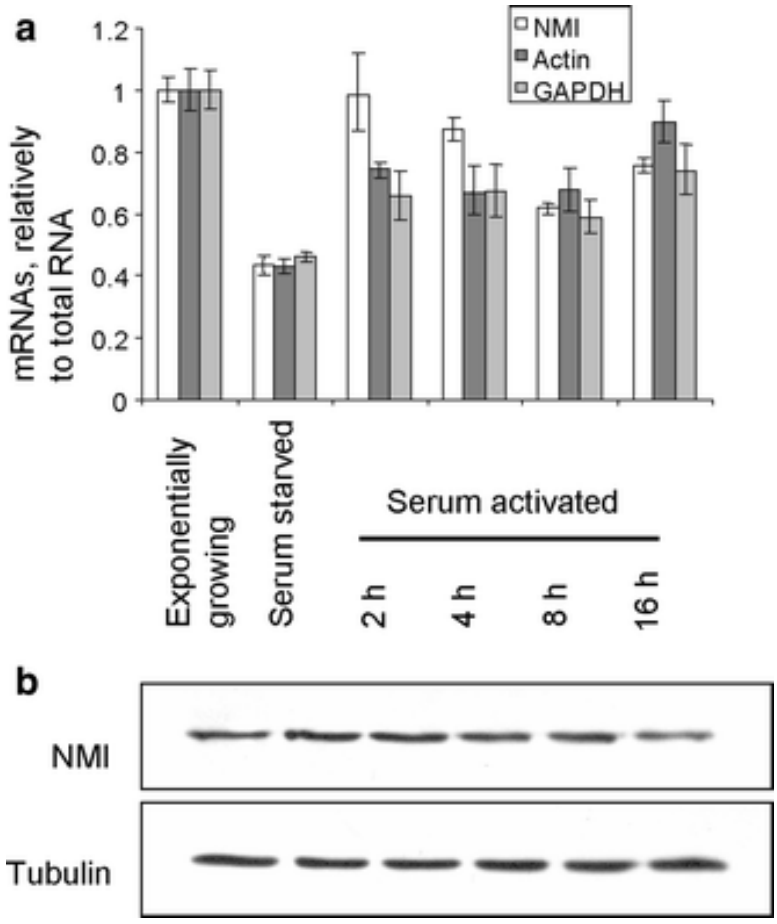

Fig. 3 Transcription of NM1 raises during serum activation. NIH 3T3 cells growing in medium with 10% serum were subjected to 0.1% serum for 48 h and then returned to 10% serum medium. a RT-qPCR quantification of mRNA for NM1, actin, and GAPDH. Samples were run in duplicates, and standard deviations are indicated. b Western blot analysis of NM1 expression. Identical amounts of protein were loaded; tubulin serves as a loading control

6.1.3. The lifespan of NM1 is longer than 16 h

To assess the stability of NM1, we treated NIH 3T3 cells with protein synthesis inhibitor cycloheximide at concentration 2 μg/ml for 16 h and observed the levels of NM1. This concentration of cycloheximide was chosen because half of this concentration was reported

to completely block translation in Chinese Hamster Lung cells (Yildirim and Whish, 1997) and it did not cause morphological signs of apoptosis. The levels of NM1 did not change significantly during 16 h while the amount of control tubulin already started to decrease (**Fig. 4**).This experiment was repeated twice with similar results.

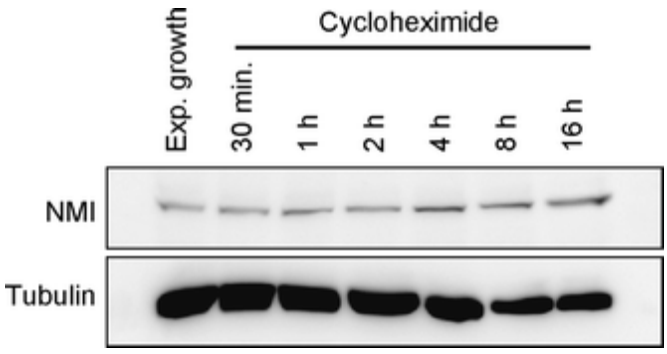

Fig. 4 NM1 is not significantly degraded during 16 h of translation block. Western blot analysis of 3T3 cells treated by 2 μg/ml cycloheximide and harvested in indicated time points

6.1.4. The specific N-terminal sequence of NM1 is identical in mammals and conserved in vertebrates

Information on NM1 phylogenetic conservation could suggest how fundamental is the role of NM1 in transcription. To test this, we examined the expression of NM1 in representatives of various animal classes, namely in human, mouse, chicken, *Xenopus laevis*, zebrafish, and *C. elegans*. Using immunoblot, we found a signal with the mobility corresponding to NM1 in human (HeLa) and mouse (NIH-3T3) cell lines, mouse liver, chicken lungs, but not in chicken liver, *Xenopus* lungs, zebrafish, and *C. elegans* (**Fig. 5**). In the *Xenopus* liver, we found a band with slightly higher mobility than other samples. In chicken, these results can be explained by weak binding of the antibody to varied epitope, which is compensated by a high expression of NM1 in lungs. In *Xenopus* there is no signal in lungs and slightly smaller protein is detected in the liver, therefore we cannot exclude that the antibody does not recognize *Xenopus* NM1, but cross-reacts with another protein in the liver extract.

In the next step, we analyzed the NM1 sequences in the genomic databases of various species. In every model animal, we selected one or two genes homologous to mouse Myo1c by similarity search and then searched in approximately 10–15 kb upstream region of the genomic sequence for an intron coding for a sequence similar to the NM1 N-terminus. Expression of a sequence identical to mouse NM1 N-terminus was predicted by gene prediction software in the genome of human, dog, cow, and rat. Furthermore, similar

NM1 N-terminal sequences were found in a genome of chicken (50% identity), *Xenopus tropicalis* (60% identity), and zebrafish (41% identity). We have also found N-terminal sequences 35% identical to mammalian ones in the genome of pufferfish (*Fugu rubipes*) and *Tetraodon nigroviridis*. In contrast, genomic analysis identified no sequences similar to NM1 N-terminus in urochordate *Ciona intestinalis*, *Drosophila*, or *C. elegans* (**Fig. 6**; for a complete phylogenetic tree, see **Fig. 7**). To test whether these N-terminal sequences are really expressed in the predicted form, we performed a 5′ RLM-RACE analysis in selected species. The results are summarized in the Table 1. We confirmed that a sequence corresponding to NM1 16 amino-acid N-terminus is expressed in human, mouse, chicken, and zebrafish. We have not detected the expression in *Xenopus laevis*, but an expression of sequence coding for 63% similar peptide was described (GenBank AAH44718).

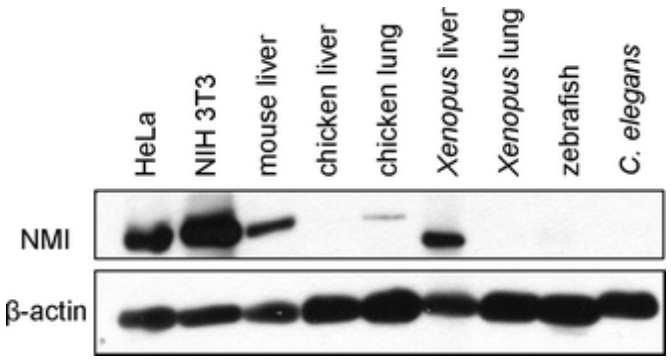

Fig. 5 NM1 in various species as detected by western blot. Total protein (50 µg) extracted from indicated tissues of different organisms were separated by western blot and tested by polyclonal antibody to NM1. β-actin serves as loading control

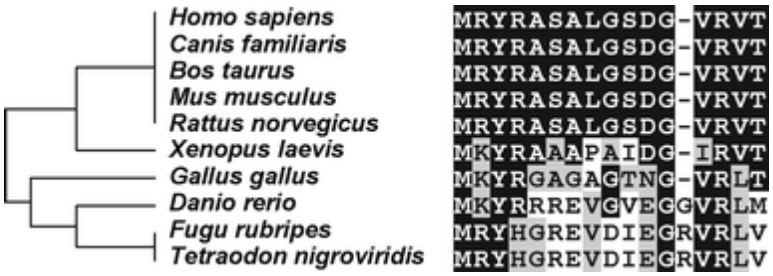

Fig. 6 NM1 is conserved in mammals and expressed in vertebrates. Alignment of NM1 N-terminal sequences from organisms where it was found to be expressed. Residues with *black background* denote identity with consensus, *gray background* marks conservative substitution. The tree on the left shows inferred relations between sequences

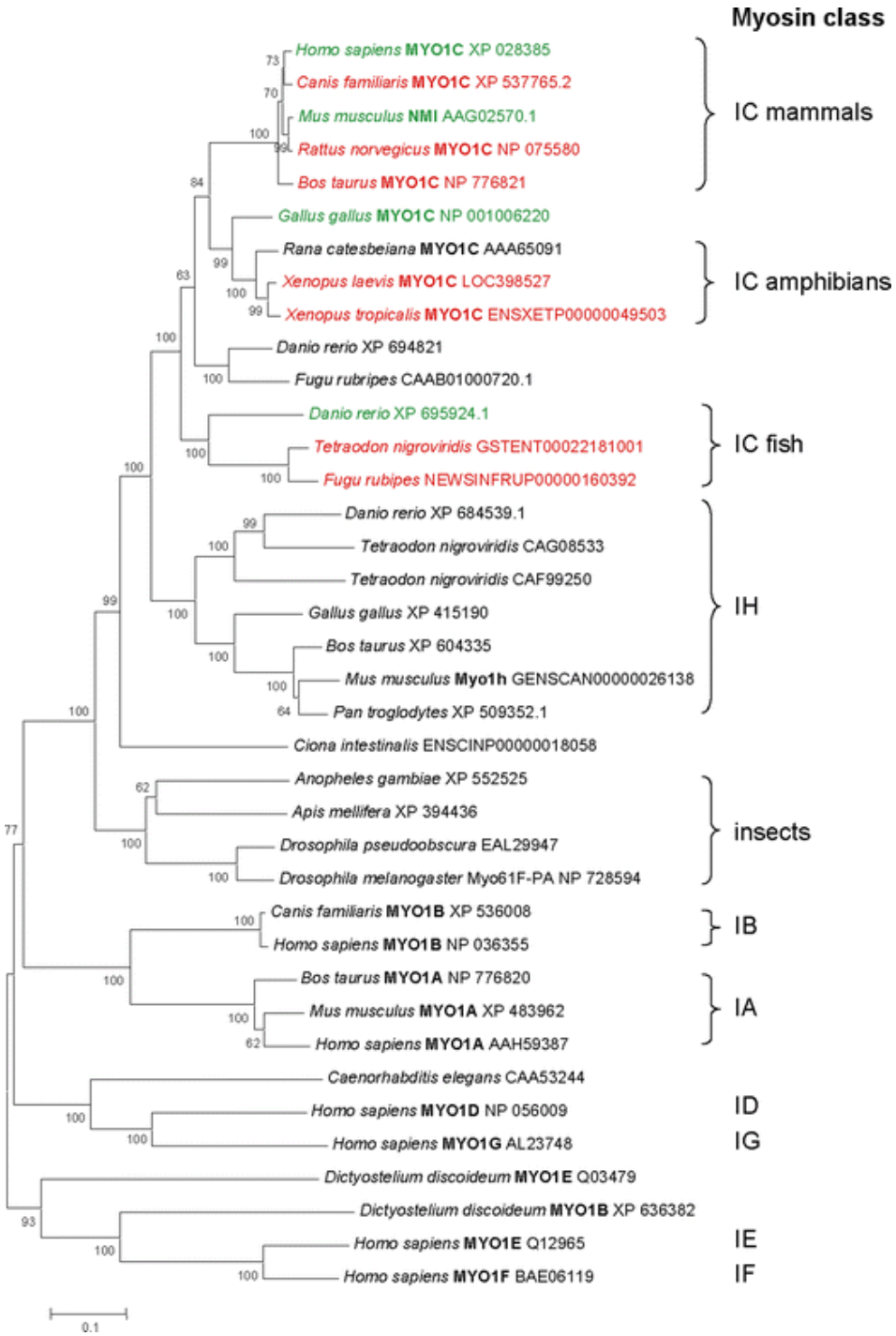

Fig. 7 An unrooted phylogenetic tree of putative Myo1c homologs. Sequences similar to Myo1c were found by BLAST in protein, nucleotide, and genomic databases. Sequences from different organisms most similar to Myo1c were selected and some members of other mammalian myosin I subclasses were added for comparison. Alignment was made by ClustalW, and the tree was constructed and bootstrap tested by minimum evolution algorithm. This tree served to choose candidates for further search for the sequences similar to the NM1 N-terminal. The genes in green were shown to express a sequence similar to N-terminal sequence by RACE, and in red the genes with an exon coding for a similar sequence as found by analysis of genomic sequence. In *Rana catesbeiana*, we did not perform RACE and the genome is not sequenced, therefore we were not able to find the N-terminus. In fish, there are two distinct homologs of Myo1c that probably arose by genome duplication in teleost fish lineage (Jaillon et al., 2004). Only one of these, however, contains the NM1 N-terminal sequence. We have found the N-terminus neither in *Ciona intestinalis* nor in other more distant organisms genomic sequence. *Scale bar* shows evolutionary distance in number of replacements per amino acid. *Numbers in branch points* denote bootstrapping values

Table 1 Results of 5′ RACE of myosin IC genes

Species	NM1	Myo1c
Mouse	EB724369	EB724364-8
Human	EB724371-3	–
Xenopus laevis	–	EB724387
Chicken	EB724384, EB724386	EB724385
Danio rerio	EB724379	EB724375-8

GenBank accession numbers are stated where the RACE matched with database sequences of NM1 and Myo1c

6.2. Experimental part II – Identification of the nuclear localization signal of NM1

Nuclear myosin I (NM1) was the first molecular motor identified in the cell nucleus. Together with nuclear actin, they participate in crucial nuclear events such as transcription, chromatin movements, and chromatin remodeling. NM1 is an isoform of myosin 1c (Myo1c) that was identified earlier and is known to act in the cytoplasm. NM1 differs from the "cytoplasmic" myosin 1c only by additional 16 amino acids at the N-terminus of the molecule. This amino acid stretch was therefore suggested to direct NM1 into the nucleus. We focused here on identification of mechanism that is responsible for nuclear translocation of NM1.

6.2.1. NM1 is transported to the nucleus after mitosis

To study the dynamics of NM1 compartmentalization during cell cycle we followed the localization pattern of the endogenous NM1 during and after mitosis. Immunofluorescent labeling of NM1 in unsynchronized U2OS (**Fig.8A**) and in NIH 3T3 (**Fig.8B**) cells synchronized by mitotic shake off has shown that NM1 did not stay bound to chromatin during the mitosis and that its majority was released into the cytoplasm after the nuclear envelope breakdown in prophase (**Fig. 8B**). Soon after the reconstitution of nuclear envelope in early G1, most of NM1 was in the cytoplasm as shown in **Fig. 8A** and **8B** (Early G1). In unsynchronized population of cells, this pattern was very rarely observed, and the vast majority of cells had clearly nuclear staining of NM1 (**Fig. 8A**, Interphase). This demonstrates that nuclear import of endogenous NM1 is accomplished in G1 phase.

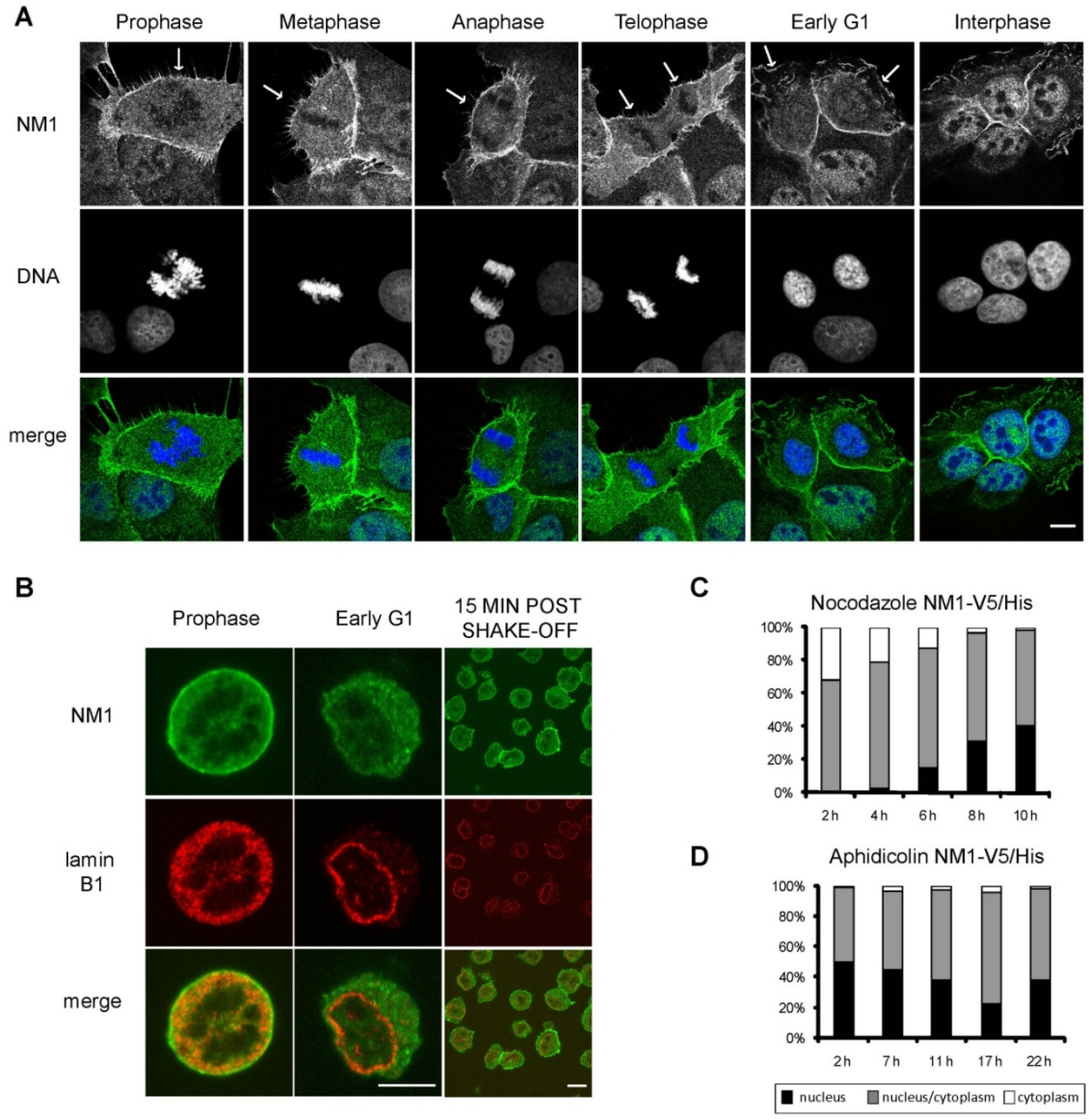

Figure 8: Localization NM1 during mitosis

(**A**) Unsynchronized U2OS cells were fixed and labeled with antibody to NM1. Localization of NM1 is shown at various stages of mitosis. DNA was visualized by DAPI. **(B)** Mitotic NIH 3T3 cell were seeded onto the poly-L-lysine coated coverslips, fixed and labeled with antibodies to NM1 and Lamin B1. Cells fixed immediately after seeding (Prophase) and 15 min after seeding (Early G1, 15 min post shake-off). Nuclear lamina was reconstituted in Early G1 as visualized by Lamin B1 labeling. All immunofluorescence pictures were obtained using confocal microscope, single confocal sections are shown. Scale bar: 10 μm. U2OS cells were transiently transfected with NM1-V5/His. 24 hours after transfection cells were treated with nocodazole (**C**) or aphidicolin (**D**), to stall the cells either in G2/M or in G1/S phase of cell cycle. After the release from the block cells were cultivated for another 24 hours. Samples were taken in indicated time points. Cells were labeled with antibody to V5 tag, patterns counted and divided into three groups according to the localization of fluorescent proteins. More than 100 cells were counted in each time point, experiment was repeated twice with similar result.

To begin identifying import signals in NM1, we first tested the localization of full length NM1 constructs fused to different tags. Untagged overexpressed mouse and human NM1 localized predominantly in the nucleus in 80% of cells, and V5/His-tagged NM1 was predominantly nuclear in 50%, whereas EGFP-tagged or FLAG-tagged NM1 was predominantly nuclear in less than 20% of cells (data not shown). Further studies used the V5/His-tag because it interfered with nuclear import the least.

To visualize the timing of V5/His-tagged NM1 (NM1-V5/His) transport into the nucleus after mitosis, we transfected U2OS cells and the next day added either nocodazole (depolymerizes microtubules) or aphidicolin (DNA polymerase inhibitor) for 16 hours to accumulate cells in M-phase or S-phase respectively, then washed out the inhibitor and used indirect immunofluorescence to localize NM1-V5/His at different times after release from the block (**Fig. 8C,D**). Nocodazole-treated (metaphase-enriched) cells continued with mitosis after washout. The lowest nuclear levels of tagged NM1 were seen at 2 and 4 hours after release, but increased gradually at 6-10 hours after release (**Fig. 8C**). After release from aphidicolin, cells maintained high nuclear levels of NM1-V5/His for ~11 hours, consistent with the expected time needed to complete S-phase and enter G2 (**Fig. 8D**). The lowest levels of nuclear NM1-V5/His were detected 17 hours after release from aphidicolin (**Fig.8D**), when many cells were in mitosis or early G1. Together these results suggested both endogenous and tagged NM1 are released from the nucleus during mitosis. Endogenous NM1 is transported into renewed nuclei shortly after the nuclear envelope reconstitution in the early G1, while nuclear import of the ectopically expressed NM1 with a tag is slower.

6.2.2. First two IQ domains are needed for nuclear transport of NM1

Because the N-terminal part of NM1 was suggested to be crucial for nuclear localization (Pestic-Dragovich et al., 2000), we prepared various deletion and truncation mutants of the NM1 in fusion with V5/His at its C-terminus. We compared their localization in U2OS cells with the full length NM1-V5 which was detected in the cytoplasm and faintly the nucleus (**Fig. 9A**, anti-V5). Surprisingly, the deletion of the neck and the tail domain led to the cytoplasmic retention of the mutant (**Fig. 9B**). This suggested that the NLS sequence is located within the neck or in the tail domains. After deletion of the head domain, we observed enhanced nuclear signal with short C-terminal V5/His (not shown) as well as with the bulky N-terminal EGFP tag (**Fig. 9C**). This suggested that the EGFP-fused myosin neck-tail fragment is imported efficiently. Further deletion of half of the tail

disrupted the plasma membrane association of the protein but not its nuclear translocation (**Fig. 9D**). The tail together with the third IQ domain of the neck stayed out of the nucleus and associated with plasma membrane (**Fig. 9E**) while the construct with first two IQ domains was located exclusively to the nucleus and nucleoli (**Fig. 9F**). This localized a putative nuclear localizing sequence within the first two IQ domains of NM1 neck residues 712-770.

6.2.3. The second IQ domain contains a novel NLS sequence

To pinpoint the exact part of the neck needed for nuclear translocation, we prepared a set of fusion constructs containing GFP and the cytosolic pyruvate kinase (PK) enzyme (Frangioni and Neel, 1993). We used PK to enlarge the proteins so that they would not diffuse passively to the nucleus as GFP alone would (Mohr et al., 2009). The 87 kDa GFP-PK fusion construct was located solely to the cytoplasm (**Fig. 9G)**. When the sequence of the first two IQ domains was added to GFP-PK strong nuclear and nucleolar signal was observed (**Fig. 9H**). Next, we examined the capability of each IQ domain to drive the nuclear transport (**Fig. 2I, J**). Nuclear accumulation was specifically driven by the second IQ motif (**Fig. 9J**), not the first IQ motif (**Fig. 9I**). The IQ2 motif and its C-terminal flanking sequence contain two clusters of basic amino acids. Next, we preserved only the basic amino acid clusters with the intermitting non-polar amino acids, resulting in 13 amino acid peptide, ^{754}GRRKAAKRKWAAQ^{766}. This sequence was sufficient for nuclear translocation (**Fig. 9K**). On the other hand, the N-terminal 16 amino acids from NM1, fused to the N-terminus of the GFP-PK construct, did not localize to the nucleus at all (**Fig. 9L**). To rule out the possibility that it serves as a nuclear retention signal, we fused the N-terminal sequence to EGFP that diffuses freely into nucleus. We did not observe nuclear enrichment of the signal that would be caused by an interaction of the protein inside the nucleus (not shown). In contrast to the full length NM1 (**Fig. 10A**), a C-terminally fused NM1 construct lacking the residues 739-762 accumulated in the cytoplasm of U2OS cells (**Fig. 10B**), supporting an important role for the second IQ. No single K/R-to-A substitution in residues 754-766 was able to disrupt the NLS activity (data not shown). However mutating all 6 basic residues to alanines completely abolished nuclear import (**Fig. 10C**; NM1-V5-mutNLS). NLS Database (Cokol et al., 2000) and literature searches revealed no known NLS homologous to that of NM1. We therefore concluded that NM1 and cytoplasmic Myo1c share a novel type of NLS.

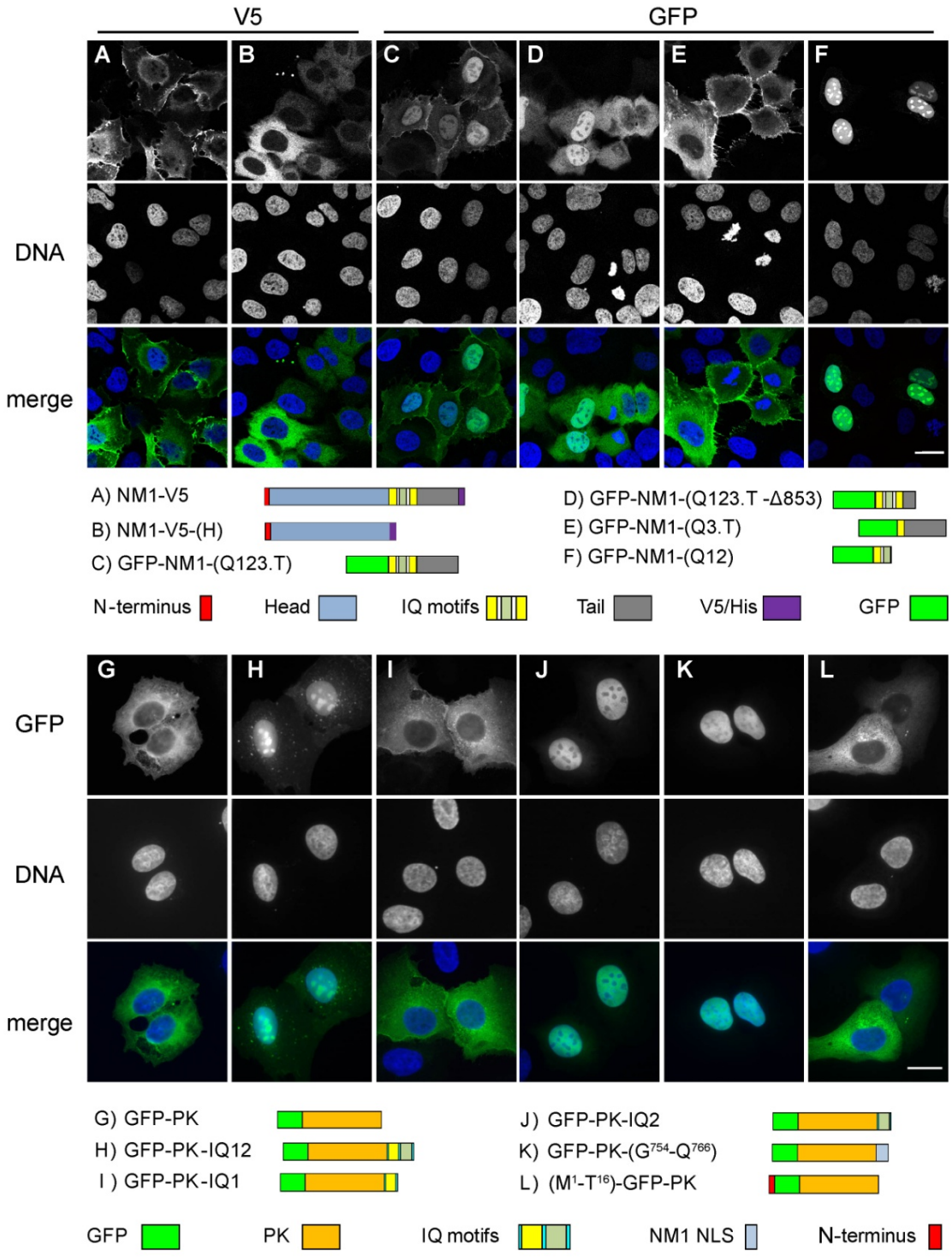

Figure 9: Neck domain of NM1 contains the NLS

U2OS cell transfected with a panel of truncation constructs of full length NM1 (**A-F**) and IQ domains fused to GFP-PK (G-L). Cells were fixed 48 hours post transfection. Below the pictures are schematic representations of the truncations affecting various NM1 domains as well as the GFP-PK phusions. Pictures (**A-F**) were acquired using confocal microscope, single confocal planes are shown. Pictures (**G-L**) were photographed using wide-field fluorescent microscope. Scale bar: 10μm.

6.2.4. Myo1c is able to translocate into the nucleus

N-terminus of NM1 alone did not possess a nuclear localization potential and the NLS was located in region shared by both the NM1 and Myo1c. We therefore inspected the localization of Myo1c under overexpressed condition.

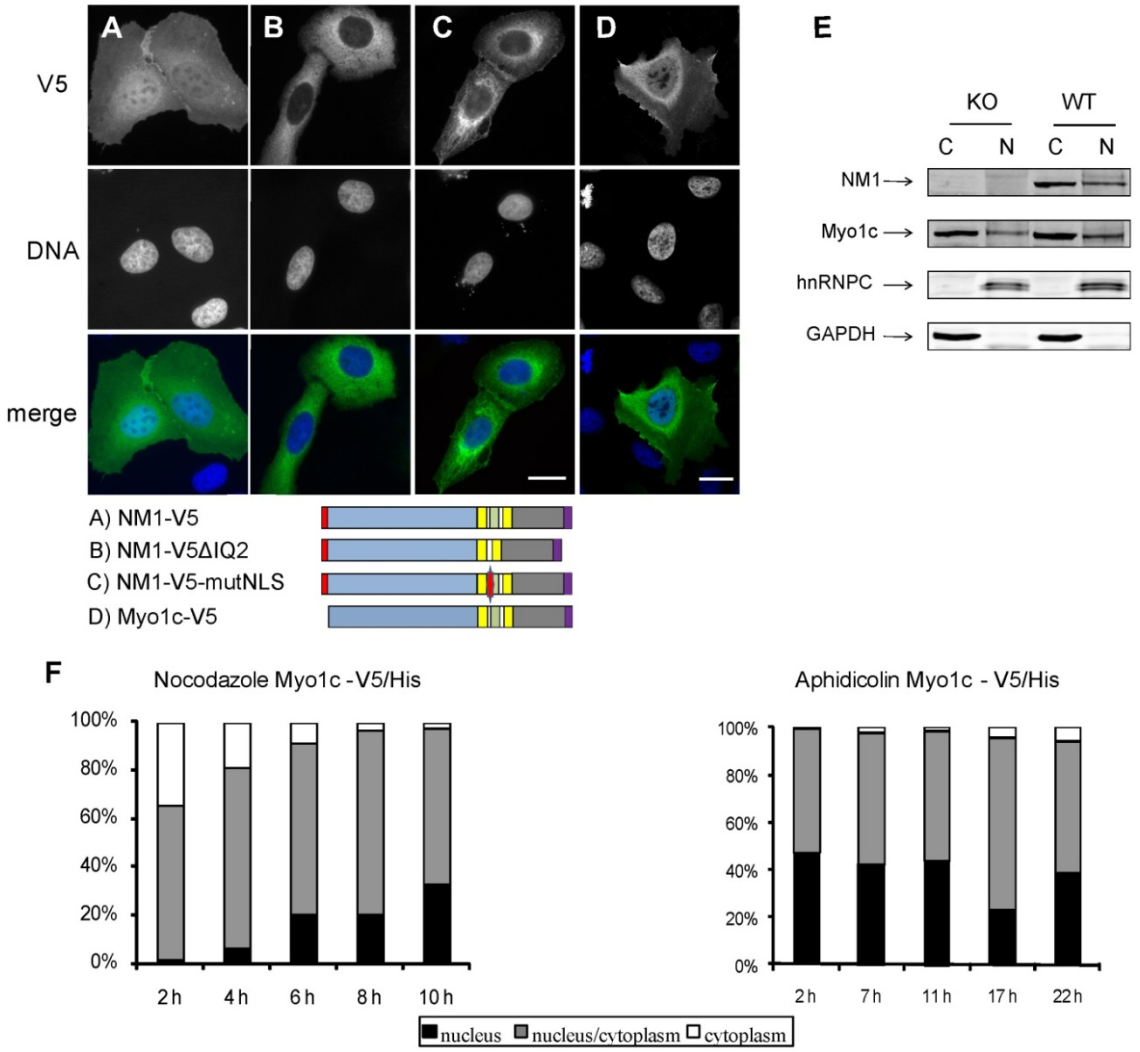

Figure 10: Mutation of basic residues in the neck of NM1/Myo1c abolishes its nuclear import

U2OS cells were transfected with with full length NM1-V5/His (**A**), NM1-V5/His lacking the second IQ motif (**B**), and NM1-V5/His with point mutation of basic amino acids within the NLS into alanines (**C**). Below the pictures are schematic representations of constructs used. Color coding is the same as in Fig. 2. Cells were fixed 48 hours post transfection and labeled with anti-V5 antibody, pictures were obtained using wide-field microscope, scale bar: 10µm (**D**) U2OS cells transiently transfected with Myo1c-V5/His show nuclear localization of the protein Picture is a single confocal plane, obtained by confocal microscope. Scale bar: 10µm. (**E**) Nuclear and cytosolic extracts were prepared from liver of either wild type (WT) or NM1 knock-out (KO) mice. Equal amount of protein was resolved using SDS-PAGE and electro-transferred to nitrocellulose. Membrane was probed with anti-NM1, anti-Myo1c, anti hnRNP C1/C2 and GAPDH antibody. Signal was detected using LI-COR Odyssey infrared imaging system. (**F**) U2OS cells were transiently transfected with Myo1c-V5/His. 24 hours after transfection cells were treated with nocodazole or aphidicolin to stall the cells either in G2/M or in G1/S phase of cell cycle. After the release from the block cells were cultivated for another 24 hours. Samples were taken in indicated timepoints. Cells were labeled with antibody to V5 tag, patterns counted and divided into three groups according to the localization of fluorescent proteins. More than 100 cells were counted in each timepoint, expreriment was repeated twice with similar result.

V5/His tagged Myo1c was localized to the nuclei of transfected U2OS cells (**Fig. 10D**). The nuclear localization of Myo1c-V5/His in nocodazole- or aphidicolin-treated cells was also cell cycle dependent, with profiles (**Fig. 10F**) similar to that of cells that overexpressed NM1 (**Fig. 8C,D**).

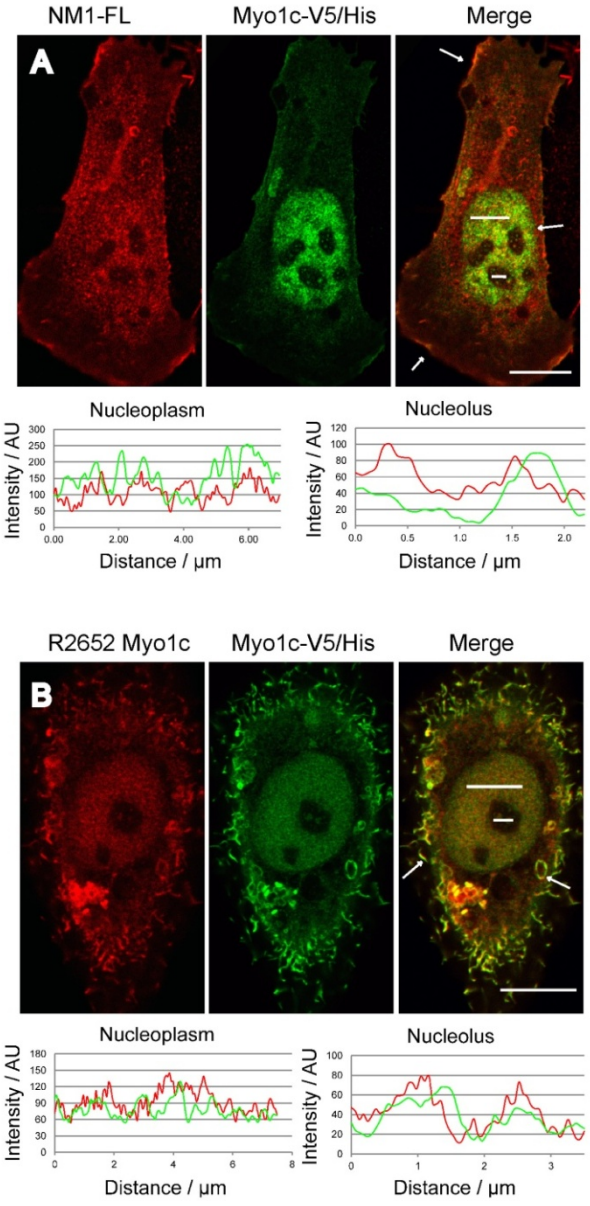

Figure 11: Co-localization of overexpressed NM1 and Myo1c

U2OS cells were co-transfected with FLAG-tagged NM1 (NM1-FL) and V5/His tagged Myo1c (Myo1c-V5/His). Cell showing nuclear localization of NM1 and Myo1c was photographed using confocal microscope (**A**). U2OS were transfected with Myo1c-V5/His. 48h post transfection cells were fixed, and labeled with polyclonal antibody (R2652) directed toward the tail region of NM1/Myo1c and with monoclonal antibody against V5 (**B**). Intensity profiles along the regions of interest in the nucleus and nucleolus are shown under the pictures. White arrows are pointing to regions at the plasma membrane where both proteins are enriched. Scale Bar :10µm

To test the influence of the N-terminal 16 amino acids on NM1 functions we prepared knock-out mice lacking the exon-1 that contains the NM1 translation start codon (Venit et al, in preparation). Resulting mRNA contains only the downstream start of translation which gives rise to Myo1c protein. We used purified liver nuclei from NM1 knock-out mice to confirm that the N-terminus is not required for nuclear transport of endogenous NM1. **Fig. 10E** shows the presence of Myo1c in the purified liver nuclei from NM1 knock-out mice visualized by antibody to the C-terminus of NM1/Myo1c. Weak signal of GAPDH indicates negligible contamination of nuclei with cytosol, while signal of hnRNP C1/C2 shows marked enrichment of nuclear proteins compared to cytosolic liver extract. This shows that both NM1 and Myo1c have the ability to enter the nucleus. Further, we have observed the co-localization of NM1 and Myo1c in a single cell. However, we were not able to co-localize NM1 and myo1c in nuclei of untransfected cells using the polyclonal antibody directed to the tail region of NM1/Myo1c (R2652) (Dumont et al., 2002) since it failed to label endogenous epitopes within nuclear environment. Therefore, U2OS cells were cotransfected with FLAG tagged NM1 and V5/His tagged Myo1c. **Fig. 11A** shows a cell expressing both proteins. Myo1c and NM1 co-localized at the plasma membrane (arrows) and in the nucleus. Interestingly, R2652 antibody revealed the signal in nucleus and nucleolus when Myo1c was overexpressed **Fig. 11B**.

6.2.5. Importins bind the NM1 neck region

The transport of nuclear proteins through nuclear pores is often facilitated by importins that recognize their NLS in cytoplasm (Cokol et al., 2000). To discriminate between cytoplasmic and nucleus/plasma membrane-associated myosin, cells were extracted with buffers containing digitonin that is known to extract cytosolic myosin 1c (Chen and Wagner, 2001). We sought to identify the transport receptors that bind NM1/Myo1c NLS. Using pull down assay with recombinant IQ12 as the bait we identified importin 5 (IPO5) and Heat shock protein 90 beta (HSP90) as the proteins that associate with IQ12 in the cytoplasm of HeLa cells (**Fig. 12A**). To verify the obtained result by another method, we looked for interacting partners of GFP-NM1-(Q123.T) in HEK-293T cells. Mass spectrometry analysis of bands that co-purify specifically with GFP-NM1-(Q123.T) but not with the control Str-GFP contruct, revealed importin 5, importin 7 (IPO7), importin-β1 (KPNB1) and HSP90 beta (**Fig. 12B**). Additional bands that were present on the gel were not identified. To verify that the importin 5, importin 7 and importin-β1, which were found to bind the truncated constructs, recognize also the endogenous protein,

we performed co-immunoprecipitation with a polyclonal antibody directed to N-terminus of NM1. Since most of endogenous NM1 molecules potentially accessible to importins are located in cytosol of the G1 cells (**Fig 8A**), we synchronized the HeLa cells with nocodazole and harvested them 3 hours after nocodazole wash-out. As shown by western blot (**Fig. 12C**), endogenous NM1 specifically binds to importin 5 (IPO5), importin 7 (IPO7), and importin-β1 (KPNB1) in digitonin extracts of the G1 cells. Next, to confirm that importin 5 binds specifically to NM1 NLS via the interaction with positively charged amino acids, we compared the proteins that co-purify with headless NM1 with wild type NLS (GFP-NM1-(Q123.T) ^{NLSwt}) and headless NM1 with all basic residues in the NLS mutated to alanines (GFP-NM1-(Q123.T) ^{NLSmut}) from electroporated HEK293T cells. **Fig. 12D** shows that importin 5 interacts only with GFP-NM1-(Q123.T) ^{NLSwt} and that this interaction occurs in digitonin extract in contrast to triton X-100 that liberates the plasma membrane bound myosin (Chen and Wagner, 2001). Taken together, the aforementioned data show that the importin 5, importin 7 and importin-β1 bind the newly identified NLS.

6.2.6. NM1 nuclear import does not follow the canonical nuclear import pathway

The small GTPase Ran controls the direction of canonical nuclear import pathway. High levels of GTP-loaded Ran in the nucleoplasm cause the dissociation of importin-cargo complex upon translocation through the nuclear pore complex (Pemberton and Paschal, 2005). We probed the stability of the NM1-importin complexes in the presence of RanGTP in order to test whether the nuclear import of NM1 follows the canonical nuclear import pathway.

Complexes containing Str-GFP-NM1-(Q123.T) and associated importins were purified from electroporated HEK293T cells using streptactin affinity column and incubated with recombinant Q69L mutant of Ran, preloaded with GTP. This mutant is not able to hydrolyze GTP (Kutay et al., 1997) and should cause elution of importins from the Str-GFP-NM1-(Q123.T) column The activity of Q69L mutant of Ran was confirmed by its ability to dissociate importin β1 from its well known cargo, SV40 NLS (**Fig. 12E**). In contrast to SV40 NLS, the GFP-NM1-(Q123.T) remained associated with importin 5 even in the presence of RanGTP Q69L. As shown by western blot (**Fig. 12E**), the complex of GFP-NM1-(Q123.T) and importin 5 co-eluted from the column by the addition of biotin that disrupts the binding of Str-GFP-NM1-(Q123.T) to the streptactin resin.

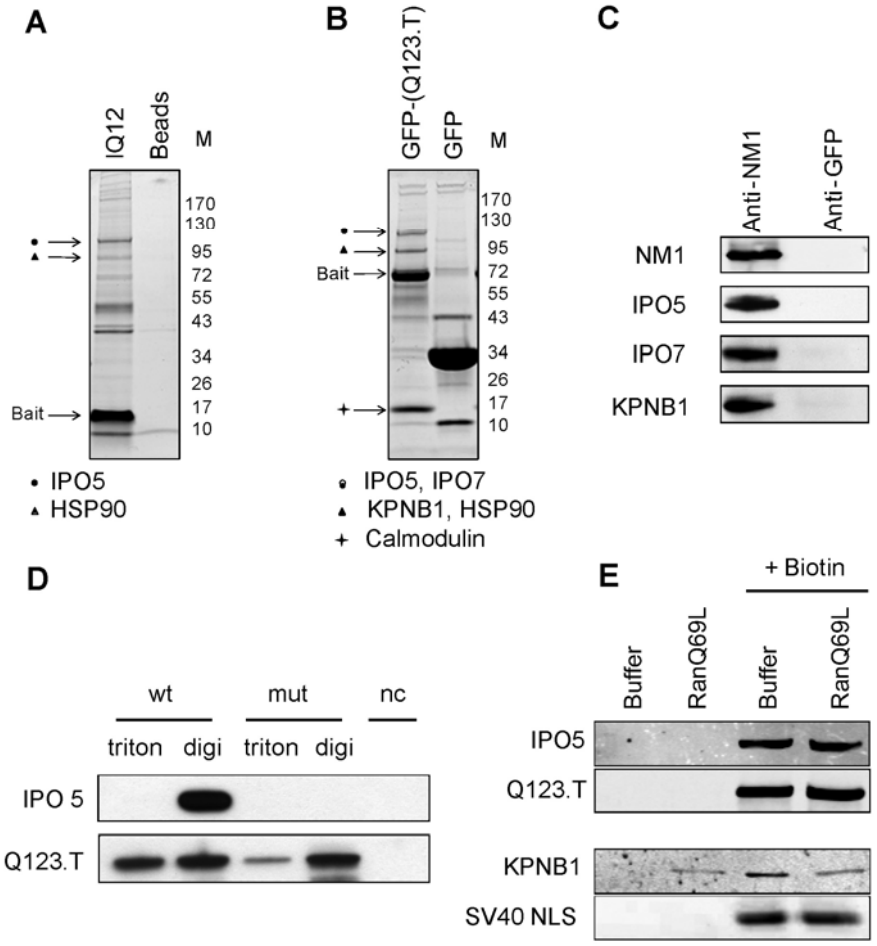

Figure 12: Identification of NM1 interacting proteins in the cytosol

Digitonin extract from suspension HeLa cells was incubated with recombinant Str-IQ12-His peptide containing N-terminal OneStrep tag (IQ12) and Streptactin beads as a control for background binding. Bound proteins were resolved on 4-20% SDS-PAGE gel and stained with SimplyBlue. Mass spectrometric analysis of the protein bands that co-purified with bait (arrows) identified importin 5 and heat shock protein 90 beta (HSP90) (**A**). SimplyBlue stained 4-20% SDS-PAGE gel with proteins that interacted with Str-GFP-NM1-(Q123.T) and Str-GFP as a control in digitonin extract of HEK293T cells. The arrows show positions of bands that contained proteins identified using mass spectrometry as importin 5, importin 7, importin-β1, HSP90 beta and calmodulin (**B**). Proteins that co-immunoprecipitate with antibody to endogenous NM1 from HeLa extracts were resolved using SDS-PAGE and tranferred onto nitrocelulose membrane. Membrane was probed with with anti-NM1, anti-importin 5 (IPO5), anti-importin 7 (IPO7), anti-importin-β1 (KPNB1). Rabbit polyclonal antibody against GFP was used as a control for backgroung binding (**C**). N-terminally Strep tagged GFP-NM1-(Q123.T) ^{NLSwt} (wt), GFP-NM1-(Q123.T) ^{NLSmut} (mut) and GFP as negative control (nc) were expressed in HEK293T cells. Cells were extracted with buffer containing digitonin (digi) to obtain soluble cytosol; pellet was re-extracted with the same buffer containing 1% Triton X-100 (triton). Bound proteins were resolved on SDS-PAGE, transferred to nitrocelulose. Membrane was incubated with antibody to importin 5 ans GFP (**D**). Beads containing Str-GFP-NM1-(Q123.T) and Str-GFP-SV40 NLS and associated proteins were eluted first with buffer containing GTP-loaded RanQ69L or buffer alone and then with biotin containig buffer that liberated Strep-tagged bait proteins from the column. Proteins eluted from the beads were resolved on SDS-PAGE and transferred to nitrocelulose membrane. GFP, importin 5 and importin-β1 signals were detected using specific antibodies (**E**). Signal from secondary antibodies was detected using LI-COR Odyssey infrared imaging system.

Taken together, these data suggested that the NM1 nuclear import does not follow the canonical nuclear import pathway regulated by GTPase Ran.

6.2.7. Overexpression of calmodulin negatively influences NM1 nuclear import

Neck region of NM1 is characterized by the presence of IQ motifs that bind calmodulin in Ca^{2+}-dependent manner (Gillespie and Cyr, 2002). As NLS sequence of NM1 is present within one of these IQ motifs (**Fig13E**), we tested the influence of increased calmodulin levels on the NM1 localization. When GFP-PK-IQ12 was co-expressed with calmodulin in U2OS cells, elevated levels of calmodulin blocked the nuclear import of the IQ12 construct (**Fig. 13B**).

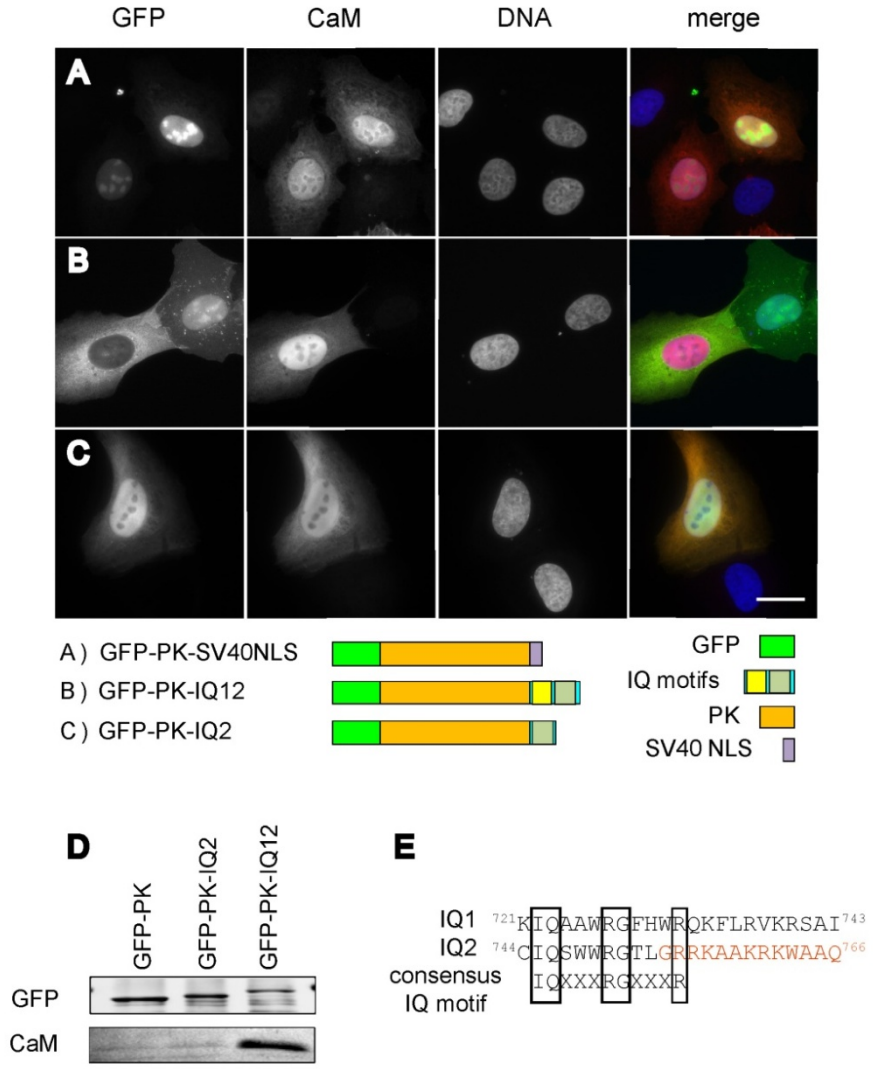

Figure 13: Overexpression of calmodulin influences the nuclear import of NM1

U2OS cells were co-transfected with GFP-PK constructs containing IQ domains, and calmodulin. Calmodulin was visualized using specific antibody (**A,B,C**). Scale bar 10µm. HEK293T cells electroporated with the same constructs as in (**A,B,C**). Whole cell extracts were subjected to immunoprecipitation with anti-GFP nanobody. Bound proteins were resolved on SDS-PAGE and transferred to nitrocelulose. GFP and CaM were visualized using specific antibodies (**D**). (**E**) Comparison of IQ1 and IQ2 sequences. The consensus IQ motif is shown below. The NM1 NLS sequence is highlighted in red.

Calmodulin, on the other hand, did not block the import of GFP-PK-IQ2 (**Fig. 13C**). Importantly, calmodulin did not inhibit the nuclear import of the GFP-PK-SV40 NLS

construct, suggesting that the observed effect is not a general inhibition of nuclear import pathways (**Fig. 13A**). To compare the amount of calmodulin associated with GFP-PK-IQ2 and GFP-PK-IQ12 we immunoprecipitated the proteins from extracts of electroporated HEK293T cells using anti GFP antibody coupled to magnetic beads. As shown in **Fig. 13D**, calmodulin associated with GFP-PK construct only when both IQ domains were present (GFP-PK-IQ12). In conclusion calmodulin binding to IQ12 appears to regulate nuclear import of NM1.

6.3. Experimental part III - Identification of novel NM1 interacting proteins

Nuclear myosin 1 (NM1) is an isoform of myosin 1c (Myo1c), both are monomeric and belong to the class I of unconventional myosins. NM1 and Myo1c display very high degree of sequence similarity, with the only difference; the presence N-terminal peptide at the amino terminus of NM1. Although the molecular structure of the two proteins seems to be very alike, the functions attributed to them differ. Myo1c was shown to work as a dynamic linker between plasma membrane and actin filaments which is a prerequisite for mechanotransduction (Gillespie, 2004), maintenance of actin rich structures such as stereocilia and microvilli (Nambiar et al., 2010), and dynamic plasma membrane events such as exocytosis (Bose et al., 2004; Sokac et al., 2006). On the other hand NM1, was found to play a role in various processes that occur in the cell nucleus. Perhaps the most studied one was the role of NM1 in DNA transcription (Fomproix and Percipalle, 2004; Philimonenko et al., 2004; Hofmann et al., 2006b). Besides its direct binding protein partners, such as actin and calmodulin, NM1 was found to associate with TIF1A, the principal regulator of Pol I transcription (Philimonenko et al., 2004), and with the nuclear import proteins (Dzijak et al., PlosOne, Accepted). Since the binding to different set of proteins could influence the localization, as the next step we identified proteins that associate with NM1 in whole cell extracts. We focused on actin and lipid mediated interactions of NM1.

6.3.1. Endogenous NM1 and Myo1c are distributed in the cell equally

NM1 and Myo1c display very high degree of sequence similarity, with the only difference - the presence N-terminal peptide at the amino terminus of NM1. We have shown that the N-terminus is not responsible for the nuclear localization of NM1. Furthermore, using overexpression we found that the two isoforms do not co-localize entirely (Dzijak et al Plos One, Accepted). Therefore we sought to prove that the co-localization pattern

observed previously with overexpressed proteins applies also to endogenous myosin isoforms at steady state. To co-localize endogenous proteins in one cell, we used monoclonal antibody generated against the tail domain of myosin 1c that recognizes both NM1 and Myo1c (Gillespie et al., 1993). Since we lacked the good quality antibodies to NM1, we generated a polyclonal one against the N-terminal peptide (AA 1-16) that was affinity purified. The specificity of NM1 antibodies was tested using pre-blocking with the N-terminal peptide (**Fig.14**). Surprisingly, at steady state, the localization of NM1 visualized by our newly generated antibody was more cytoplasmic than nuclear (**Fig.14A**).

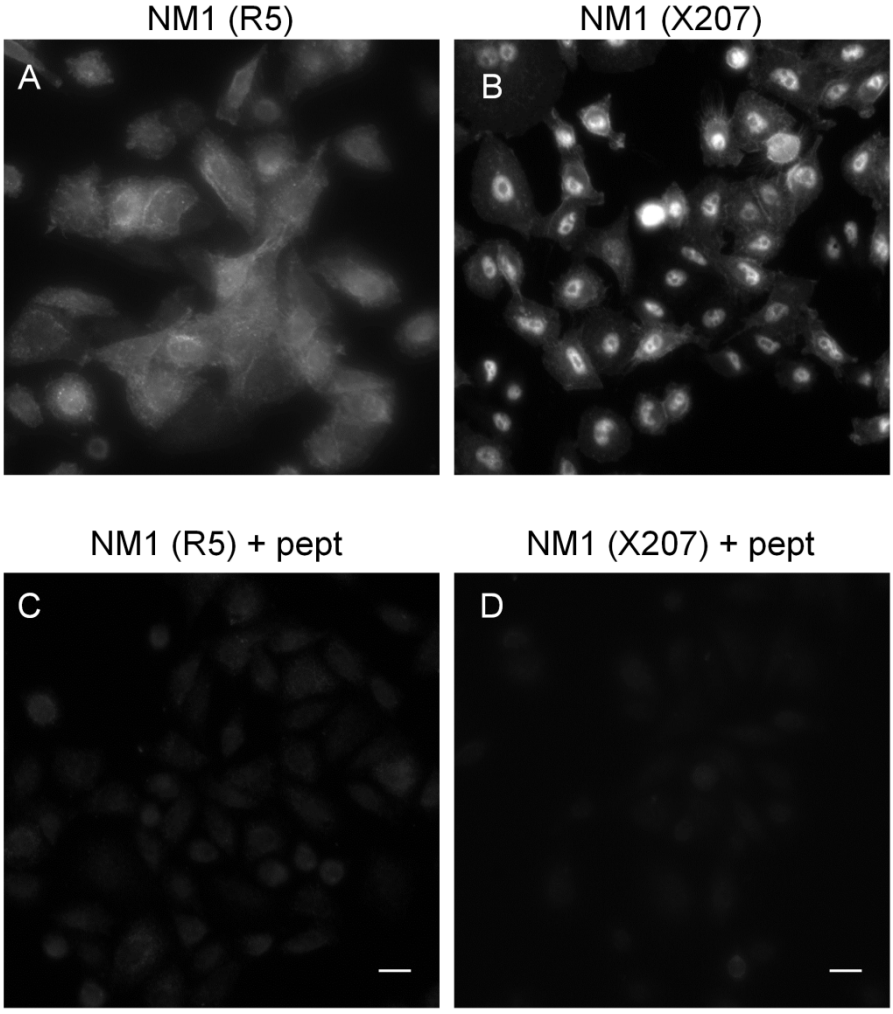

Figure 14. NM1 peptide blocks the signal of NM1 specific antibodies A549 cells were incubated with new anti NM1 antibody (**A**) and X207 anti NM1 polyclonal (Fomproix and Percipalle, 2004) (**B**) polyclonal antibodies. Specific signal was diminished addition of excess of NM1 N-terminal peptide (AA 1-16), (**C,D**).Pictures were taken using a wide field microscope. Scale bar 10 μm.

This was in contrast to previous data obtained by other polyclonal antibodies that labeled NM1 primarily in the cell nucleus (Pestic-Dragovich et al., 2000; Fomproix and Percipalle, 2004). Such a discrepancy could be caused either by a posttranslational modification of the

NM1 N-terminus that masks the epitope in the nucleus, or by a cross-reactivity of the polyclonal antibodies to other nuclear protein. To rule out an influence of posttranslational modification occurring within the N-terminus, we compared the immunofluorecent signal from previously used antibody (Fomproix and Percipalle, 2004) in mouse skin fibroblasts derived from mice lacking the NM1 protein (**Fig.15**). Strikingly, the only obvious difference between $NM1^{-/-}$ and $NM1^{+/+}$ cells was a severe reduction of the signal in cytoplasm of the NM1 knockout cells, while the intensity of the nuclear signal was unchanged. We also repeated the experiment using cells expressing shRNA toward the NM1/Myo1c. In these cells the level of NM1/Myo1c is reduced by 70% compared to the cell expressing control shRNA. The results were identical to those obtained using NM1 knock out cell line (data not shown). Altogether, these data clearly showed that antibodies used previously, cross-reacted with other nuclear protein that was different from NM1.

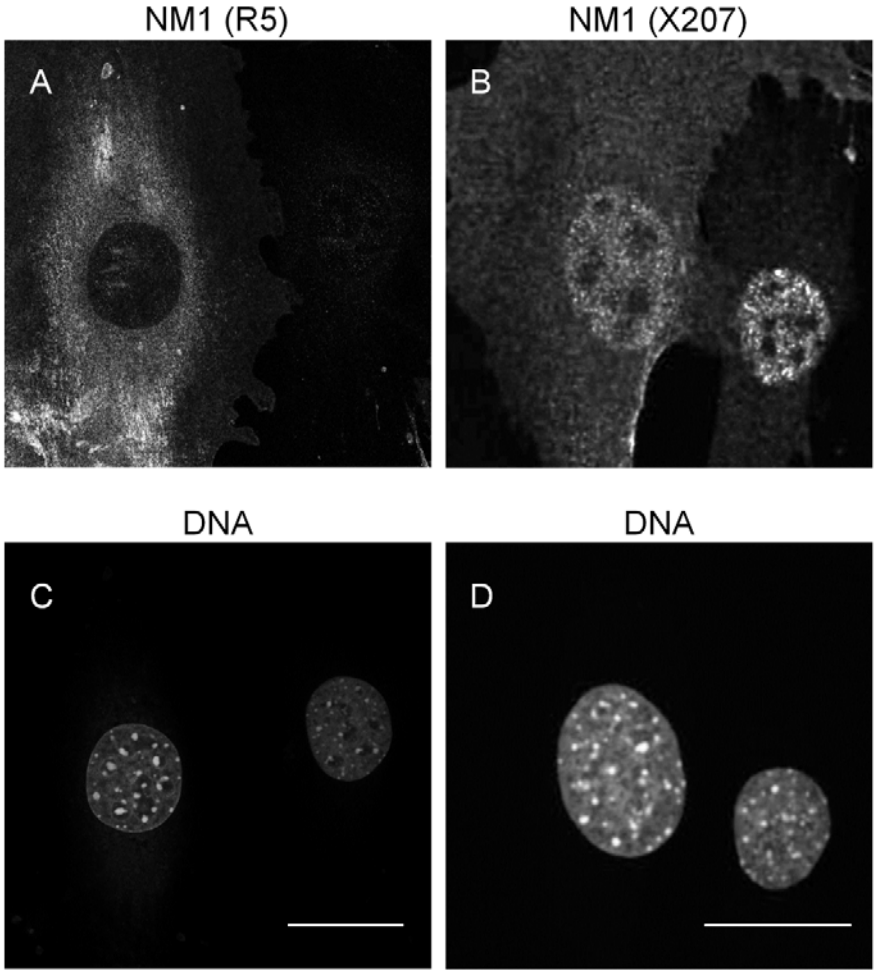

Figure 15 Localization patterns of NM1 antibodies in NM1 wt and knock out cells. Each picture contains a pair of mouse skin fibroblasts derived either from the NM1 WT (Left) or from the NM1 KO mouse (Right). A specific signal by the new anti NM1 (R5) (**A**) and X207 (Fomproix and Percipalle, 2004) (**B**) is present in WT cells. The X207 contains in addition a unspecific signal in the nucleus. (**C,D**) DNA visualised by DAPI. Pictures were taken using confocal microscope, single plane is displayed. Scale bar 10 µm.

Therefore, we used the new antibody for co-localization. Similarly to our previous data, **Fig.16** shows a general high degree of co-localization between NM1 and Myo1c with some regions that do not overlap. Because the distribution of NM1 fluorescent signal in cells was more cytoplasmic than nuclear, we compared the amount of NM1 in cell compartments using biochemical fractionation. In agreement with the immunofluorescence data the biochemical fractionation confirmed that at steady state the distribution of NM1 was more cytoplasmatic than nuclear (80% cytoplasm/20% nucleus) (**Fig.17**). Taken together NM1 and Myo1c have similar cellular distribution and show a high degree of co-localization.

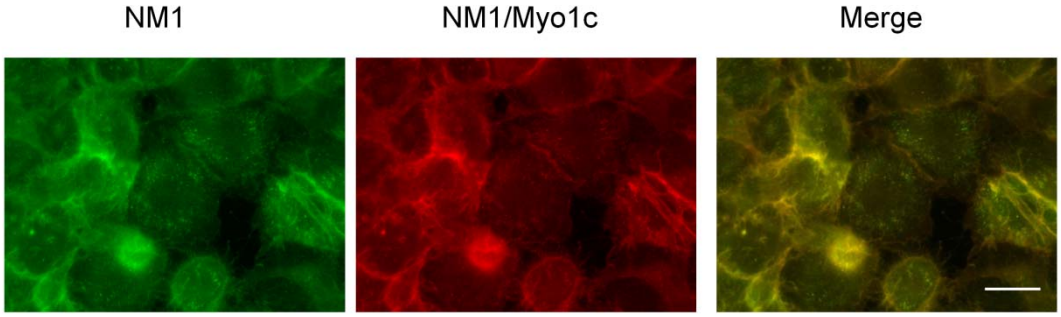

Figure 16 Co-localization of NM1 and Myo1c in A549 cells. A549 cells were incubated with the NM1specific polyclonal antibody (R5) and a monoclonal antibody that recognized the tail domain of NM1/Myo1c (Gillespie et al, 1993).

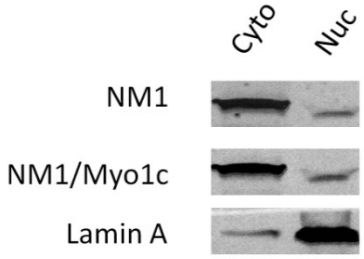

Figure 17 Amount of NM1 and myo1c in cytosolic and nuclear fractions. HeLa cells were fractionated into nuclear and cytosolic freactions. 60 ug of total protein was loaded in each lline. Lamin A was used as a control for cross contamination. NM1 and Myo1c are highly localized in the cytoplasm.

6.3.2. NM1/Myo1c expression is different in tissues and cell lines

NM1 and Myosin 1c are distributed through the cell similarly. We compared the levels of expression of NM1 and Myo1c at the mRNA level previously (Kahle et al., 2007). However, because the molecular weight of NM1 and Myo1c are very close to each other, we were unable to separate the two isoforms efficiently enough to quantify their amounts directly. Therefore, we used Licor Odyssey© fluorescent detection system that enables quantification of fluorescent signal in two separate channels. We used a polyclonal antibody to the N-terminus and a monoclonal antibody that was generated against the tail

domain of NM1/Myo1c. To normalize the signal from the two antibodies, we transfected cells with NM1-GFP construct that has the molecular weight 170 kDa. The intensities of NM1 and Myo1c were compared in the cytosolic and nuclear extracts of HeLa. We found that in this cell line the ratio between NM1 and Myo1c was 1:1 (**Fig.18A**) in both cellular compartments. To confirm this result, we used the advantage of NM1 knockout cell line in which the expression of NM1 is ablated and only Myo1c is expressed. We compared the level of total protein NM1+Myo1c using western blot. In KO cell line, we observed reduction of signal intensity to about 50% of the wild type cells (**Fig.18B**). Similar reduction in fluorescent signal was observed using immunofluorescent labeling with antibody against NM1/Myo1c (data not shown). We also repeated the quantification using NM1 KO lungs and stomach in comparison to WT ones. Here the ratio of NM1 versus Myo1c was shifted more toward the Myo1c (**Fig.18C**).

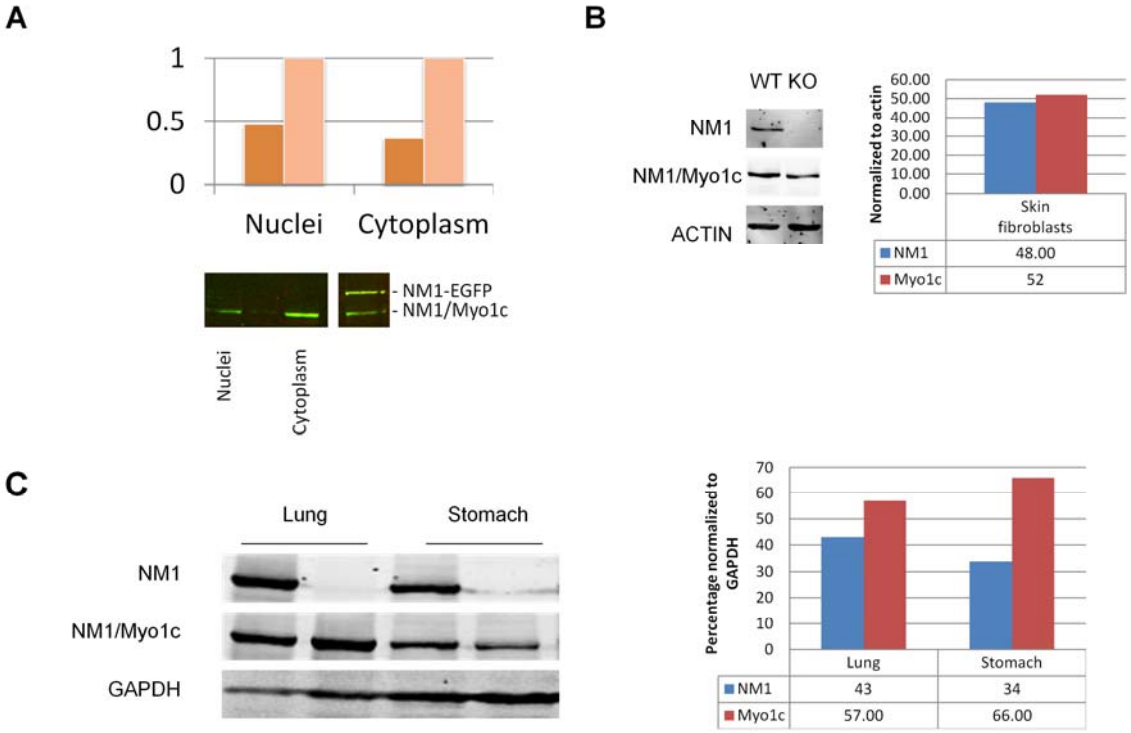

Figure 18 Quantification of NM1/Myo1c expression (**A**) HeLa cells were fractionated into cytosolic and nuclear fractions. NM1 and Myo1c amounts were quantified using double labeling of WB after normalization to NM1-GFP band. (**B**) Amounts of total NM1 + Myo1c were compared in mouse skin fibroblasts derived from NM1 knock-out and NM1 wild type mouse. Graph shows the amount of NM1 and Myo1c after densitometric quantification of bands. Beta actin signal was used as loading normalizer (**C**) Amounts of total NM1 + Myo1c were compared in lungs and stomach from NM1 knock out and NM1 wild type mouse. Graph shows the amount of NM1 and Myo1c after densitometric quantification of bands. GAPDH signal was used as loading normalizer.

Taken together, in cell types such as the fibroblasts and cancer cell lines the NM1 isoform comprises about 50% of total NM1+Myo1c, while the ratio appears to be shifted toward the Myo1c isoform in mouse lungs and stomach.

6.3.3. NM1/Myo1c tissue expression is associated with epithelial and endothelial cells

To obtain a hint about tissue specific functions of NM1, we measured the level of expression of this myosin in various mouse tissues. We identified lungs as the tissue with the highest expression of NM1. However, using the commercial antibody available at that time, we were not able to identify any differences in NM1 expression within this tissue. Therefore, we revisited the tissue localization pattern of NM1 with the antibody that we prepared, and carefully validated. In lungs, NM1 is highly expressed in cells that form alveoli (**Fig.19A**). We also re-inspected NM1/Myo1c localization in other tissues such as brain, striated muscle and stomach using the polyclonal antibody to NM1/Myo1c (Dumont et al., 2002) (**Fig. 19B,C,D**). In these tissues, the expression was the highest in endothelial cells lining up the arteries or forming capillaries (**Fig 19C,D**). In stomach, secretory epithelial cells showed a distinctly high signal, cell-cell contacts of smooth muscle cells were also specifically labeled (**Fig.19B**, and data not shown). Since the highest signal was observed in alveolar epithelial cells of lung, we also investigated the localization of NM1 in the cancer cell line A549, which displays some properties of type II alveolar cells. In subconfluent cells, NM1 was highly localized at the dynamic cell edges called lammelipodia. In confluent culture of alveolar epithelial cell line A549, NM1 was highly enriched at the cell-cell contacts. The endothelium was the second cell type that showed a high expression of NM1. We also inspected the localization of NM1/Myo1c in these cells. We found a dominant plasma membrane localization pattern with occasional clustering of the signal into patch like structures (Data not shown).

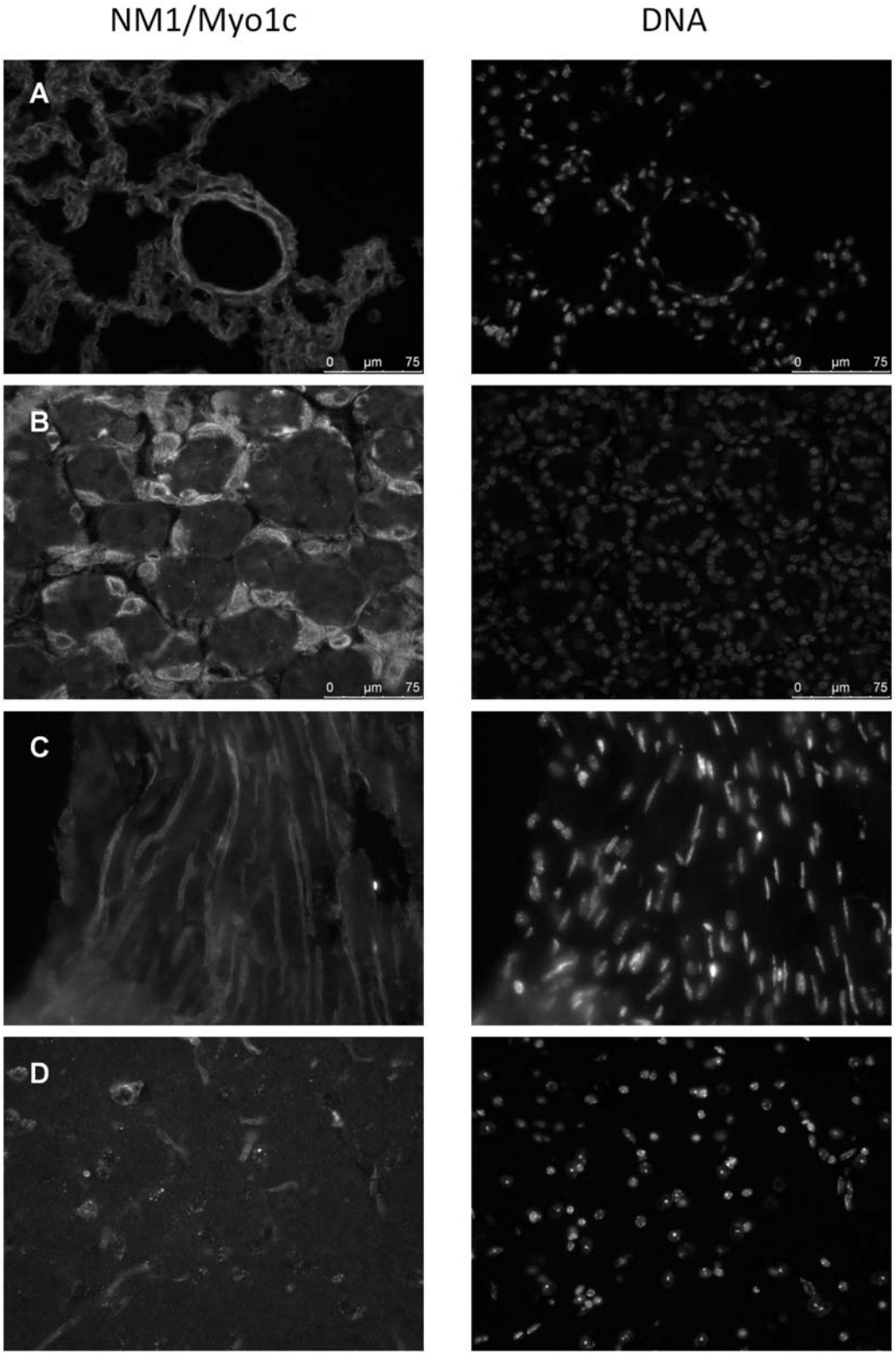

Figure 19 Localization of NM1/Myo1c in mouse tissues

Mouse tissues were fixed in PFA, dehydrated in sucrose and frozen. 7-10 µm sections were prepared using a cryostat. NM1/Myo1c was visualized using antibody directed to the tail domain of NM1/Myo1c. (**A**) a section thru mouse lungs shows labeling in alveoli and endothelial cells of the vein. (**B**) Transversal section of mouse stomach mucosa shows distinct staining of secretory epithelial cells. (**C**) Longitudinal section of mouse striated muscle shows staining in capillaries that intersperse muscular fibers. (**D**) Labeling of capillaries in a section of mouse cerebral cortex. Pictures were obtained using a wide field fluorescent microscope. Scale bar 75 µm.

6.3.4. Identification of NM1 associated proteins in whole cell lysates of A549, HeLa, H1299 and HUVEC cells

NM1 binds directly to actin, calmodulin and acidic phopholipids. These are widely spread adaptor molecules, present in a variety of different complexes that do not suggest directly any specific functions. To obtain a better picture about different cellular processes in which NM1 might play a role we sought to identify proteins that associate with NM1 in a cell. We also used whole cell extracts in co-immunoprecipitation experiments to capture any cytosolic or plasma membrane complexes. Previously, we focused on the identification of proteins that are associated with NM1 in cellular extracts prepared by digitonin.

A

Antibody/CELLS/buffer	NM1m/A549/Triton	NM1p/A549/Triton	NM1m/Lungs/Triton	NM1p/Lungs/Triton	NM1p/Hela/Digitonin
	Filamin A	Alpha actinin 4	FilaminA	Gamma tubulin complex	TPR (translocated promoter region)
	STAT 1	annexin A II	hnRNP A/B	component 3 and 2	PTPRF interacting protein 1
		HSC70			Kinesin 5B
	beta actin	beta actin	beta actin	beta actin	CTNND1
	calmodulin	calmodulin			U2 small nuclear RNA auxiliary splicing factor 2
					tRNA splicing endonuclease Sen34

B

Flag /A549/Triton	Flag/H1299/Triton	Flag/HUVEC/Triton	Flag/A549/ Tween
spectrin			
Myosin heavychain 9		Myosin heavy chain 9	
Filamin A			
Alpha actinin 4		Alpha actinin 4	
Myosin 1B			Gelsolin
UNC45A	UNC54A		UNC 45A
HSP90 beta	HSP90beta		HSP90beta
HSP90 beta			Importin beta
			SLC3A2
			Protein Kinase C alpha
			EIF4B
	HSC70		HSC70
			GNB2L1 (RACK1)
beta actin	beta actin	beta actin	beta actin
			gamma actin
calmodulin	calmodulin	calmodulin	calmodulin

Table 2 Proteins that associate with NM1 (A) A549, whole lungs and HeLa cells were lysed using indicated buffers. We used Triton to efficiently liberate the lipid associated NM1, and digitonin or Tween that do not disturb the binding of NM1 to lipids. Under these conditions we were able to follow the actin, or lipid mediated interactions of NM1. We also used Different antibodies to NM1, (m) Monoclonal (clone #4, Ye et al), and polyclonal (R5) and M3567 (Sigma-Aldrich). (B) We also prepared stable cell lines expressing FLAG-tagged NM1. Cells were lysed in the same buffers as in (A). Bands that appeared on the gel specifically in the IP line were cut out and analyzes by MALDI-FT-ICR instrument. Protein IDs were obtained peptide mass fingerprint using PROFOUND software. At least four peptides were identified in each case.

This method of lysis, however, does not extract the NM1 that is bound to plasma membrane and the nucleus. Therefore, we used also the whole cell extracts prepared by various lysis buffers that extract most of cellular NM1 and sought to identify proteins that associate with NM1. As starting material for immunoprecipitations we used whole cell lysates of the lung cell line A549 that overexpressed FLAG-tagged NM1. We also immunoprecipitated endogenous NM1 from A549 cells using various antibodies generated toward the N-terminus of endogenous NM1. The conditions of extraction and buffer composition were optimized to capture the proteins that could interact with myosin either via actin or the lipid-binding domain. We used various detergents such as digitonin (it extracts the cytosolic NM1), triton X-100 which extracts the lipid bound myosin, and TWEEN-20 (after sonication it solubilized total cellular NM1 but did not disturb the lipid binding). Using this approach we identified various actin and PIP2 binding proteins as the NM1 associated partners (**Table 2**).

6.3.5. NM1 associated proteins co-localize with NM1/Myo1c at the leading edge

Next, we wanted to test where in the cell these proteins co-localize with NM1/Myo1c. We used the antibody directed to the tail part of NM1/Myo1c to co-localize the proteins that were identified by mass spectrometry in intact A549 cells. Most of the identified protein co-localized with NM1/Myo1c at the plasma membrane, more specifically at the leading edge of a cell (**Fig.20**).

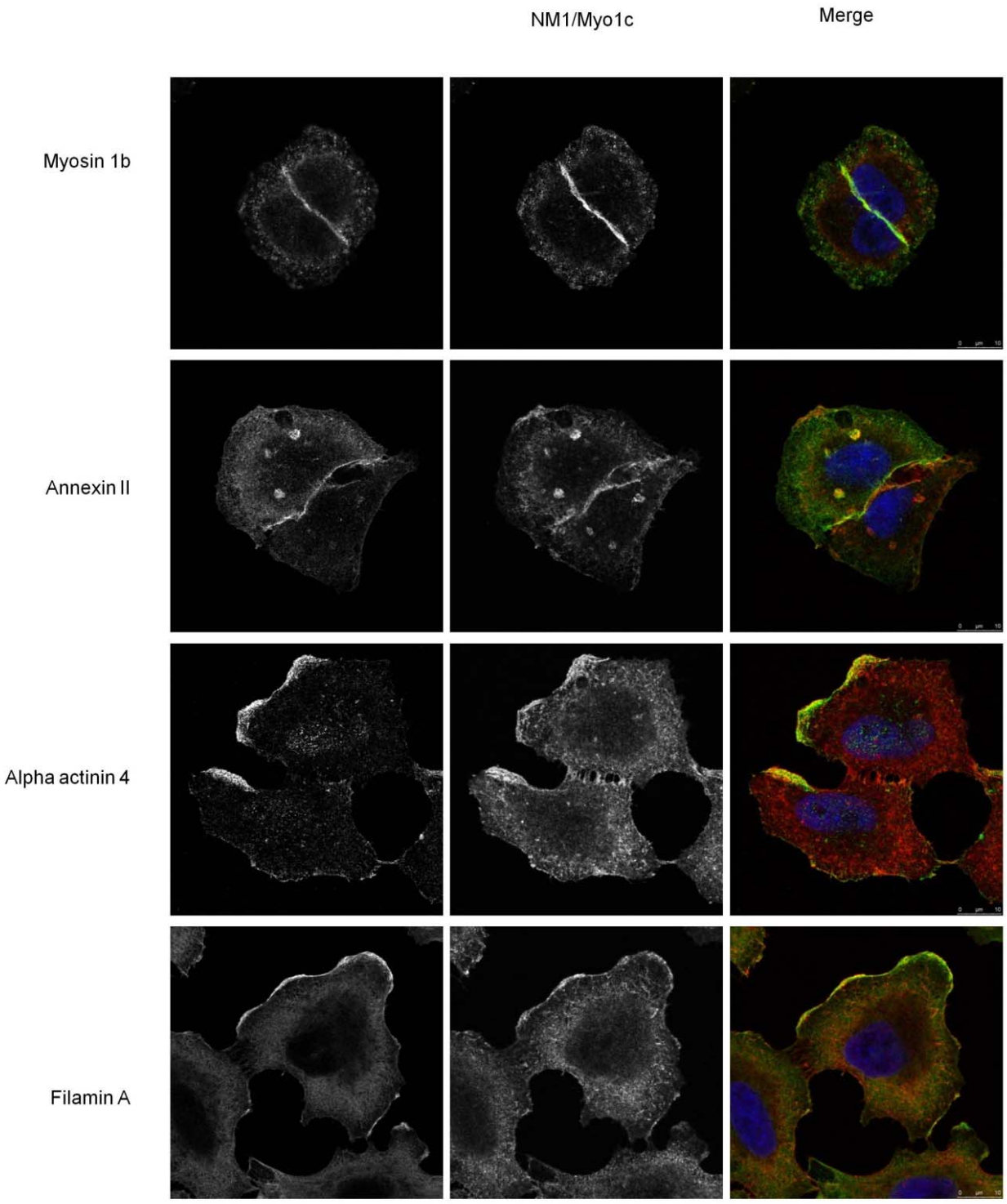

Figure 20 Co-localization pattern of selected NM1-associated proteins

A549 cells were fixed and permeabilized with methanol and labeled with antibody to NM1/Myo1c together with Myosin 1B (A), Annexin II (B), alpha actinin 4 (C) and Filamin A (D). Pictures were photographed using confocal microscope. Scale bar 10 μm.

6.3.6. Myo1c is able to functionally substitute NM1

Since the cellular distribution of NM1 and Myo1c is very similar and the ratio of expression is 1:1, we asked the question whether they are functionally identical. The siRNA mediated depletion of NM1/Myo1c was shown to decrease of RNA polymerase I transcription rate (Philimonenko et al., 2004). We used shRNA against human NM1/Myo1c to induce the PolI deficient phenotype and measured the reconstitution of the phenotype by overexpression of mouse Myo1c that was resistant to the RNAi. We observed the restoration of Pol I transcription rate to almost the endogenous level in RNAi depleted cells reconstituted by overepression of either of Myo1c (**Fig.21**). Taken together Myo1c could compensate for the loss of NM1.

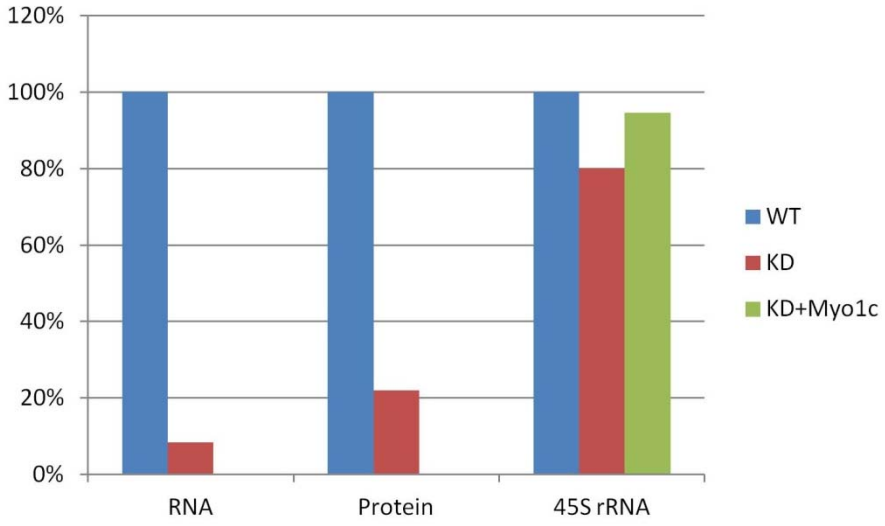

Figure 21 Restoration of Pol I deficient phenotype

Human A549 cell line (**WT**) was transduced with shRNA against human NM1/Myo1c. Total NM1+Myo1c RNA was depleted by 90 % while the protein was depleted by 70% (**KD**). As a result nascent rRNA production was inhibited by 20%. Cells harboring shRNA were transduced with construct encoding for the RNAi resistant mouse Myo1c-GFP. The efficiency of transduction was about 90%. Myo1c expression was able to bring the nascent rRNA production almost to the level of the wild type.

7. DISCUSSION

7.1. Discussion Part I - Expression and localization pattern of NM1 in mouse tissues

Since the discovery of NM1 in 1997, several studies showed that it has important functions in transcription (for reviews, see (de Lanerolle et al., 2005; Percipalle et al., 2006)). However, all data obtained so far have dealt with cell cultures and there is no information on tissue-specific expression or phylogenetic distribution of NM1. This paper aims to fulfill these gaps and provides also additional data on NM1 concerning the protein lifespan and the connection with overall cell metabolism and proliferation.

The tissue distribution of NM1 is interesting because it might answer the question whether NM1 serves a tissue-specific or general role in transcription. These data exist for Myo1c and one can compare them conveniently with those on NM1. Wagner et al. (1992) assayed the distribution of Myo1c in mouse tissues by western blot finding the highest levels in lungs, adrenal gland, and stomach followed by spleen, heart, and esophagus. This study was complemented by (Crozet et al., 1997) who compared similar selection of mouse tissues by Northern blot and found also the highest levels in lungs followed by kidney, spleen, heart, and testis. Similar experiments were performed in rat, and the highest expression of Myo1c was observed again in lung, followed by heart and kidney both by Northern (Sherr et al., 1993) and Western blot (Ruppert et al., 1995). In the data of Yanai (Yanai et al., 2005) who assayed 12 healthy human tissues by Affymetrix GeneChip, the expression of Myo1c was again highest in lungs, followed by prostate, heart, and kidney. As these studies were not designed to distinguish between Myo1c and NM1, they show cumulative levels of both myosin isoforms. In general, our results on the "total" myosin are in agreement with these literature data. In addition, we were able to show the expression of the nuclear isoform separately. If we take in account that in liver NM1 comprises one-quarter to one-third of the "total" pool, we can estimate the ratio of both isoforms also in other organs. Strikingly, in lung, NM1 seems to comprise the large majority of the "total" pool. This suggests some organ-specific functions of the NM1 in lung.

There is a discrepancy between the observation of similar levels of NM1 in the nuclei of different cell types by immunofluorescence microscopy and varied expression detected by quantitative PCR and western blot. The tissues differ in the amount of cytoplasmic and extracellular protein and thus in the ratio of NM1 to total protein. For example, high

amounts of actin and muscle myosin are present in striated muscle while there is much less cytoplasmic and extracellular protein in lung tissue this increases the fraction of nuclear proteins relative to the total protein. However, the many-fold higher expression of NM1 in lungs cannot be explained by this mechanism alone as other nuclear proteins such as Pol II, TATA binding protein (TBP), lamin A and C, and nuclear DNA helicase II do not show such markedly high expression in lungs (data not shown). In addition, the immunofluorescence confocal microscopy has a limited quantitative ability and it is therefore not possible to measure differences between various tissues or cell types, unless they are dramatic like in the latest stages of spermiogenesis.

Because NM1 plays a role in transcription it is important to assess how tightly is NM1 expression regulated in connection with overall transcriptional activity of the cell. We used therefore a convenient model of NIH-3T3 cells subjected to serum starvation and metabolically reactivated following serum addition. During serum starvation, the cells enter G0 phase, and after the addition of serum they reenter the cell cycle while increasing overall transcription. The levels of NM1 after serum activation peak after 2–4 h, and the transcription of NM1 is increased approximately by 30% when compared to an "average" gene like actin or GAPDH. This is a relatively weak response considering that several fold change is not uncommon for other highly regulated genes under these conditions (Iyer et al. 1999). It is, however, stronger response than that of Pol II or TATA-box binding protein (TBP) that respond in a similar fashion as actin (database supplementary to Iyer et al. 1999). It seems, therefore, that the biochemical activity of NM1 is not regulated chiefly on the level of expression but by other mechanisms like calmodulin binding/dissociation (Zhu (Zhu et al., 1998), or phosphorylation (Williams and Coluccio, 1995; Gillespie and Cyr, 2004).

In order to further characterize the dynamic properties of NM1, the stability of NM1 was assessed. Because the treatment with cycloheximide inhibits cytosolic protein synthesis, any observed decrease in NM1 presence should reflect mainly NM1 degradation. No significant change in cellular NM1 levels was observed following 16 h of cycloheximide treatment which indicates that NM1 has a lifespan not shorter than 16 h. In our previous study, we have shown that NM1 reaches its minimum level after 48 h after siRNA inhibition in HeLa cells (Philimonenko et al., 2004). Taken together, we can estimate the lifespan of NM1 molecules between 16 and 48 h. This result is consistent with half-life prediction of about 30 h based on the "N-end rule" (Gonda et al., 1989).

We found the N-terminal sequence of NM1 to be identical in mammals and the rest of the protein is also conserved in mammals with minimum of 95% similarity. The N-terminal peptide is also conserved in all vertebrates tested but we have not found it in urochordate *Ciona intestinalis* or any other more distant species. This means that NM1 N-terminal sequence appears to be a specific achievement of vertebrate evolution.

Altogether, NM1 is evolutionary conserved in vertebrates, it has a lifespan between 16 and 48 h, it is ubiquitously expressed in tissues but with varying intensity, and cellular mRNA levels of NM1 are connected with the level of cellular metabolism. These results suggest that NM1 is universally needed in vertebrate cells and it could have some tissue specific functions especially in lungs. Further studies are needed to elucidate the molecular mechanisms underlying these characteristic features of NM1.

7.2. Discussion part II - Identification of the nuclear localization signal of NM1

Nuclear myosin 1 is ubiquitously expressed protein that localizes to the nuclei of all cell types tested so far with the exception of cells in germinal stage of spermiogenesis (Kahle et al., 2007). Our previous work described the dynamics of intranuclear relocalization of NM1 (Kysela et al., 2005; Philimonenko et al., 2010) and involvement of NM1 in important nuclear processes – namely gene transcription. In this paper, we further contribute to the knowledge of NM1 cellular trafficking by describing the dynamics of its nuclear import and identification of the sequence that is necessary for the nuclear entry of NM1.

7.2.1. NM1 contains NLS within the IQ domain

We used tagged constructs in search for the NLS of NM1. By deletions and truncations of the full length protein, we narrowed down the region of NM1 required for its nuclear import to a short sequence within the second IQ motif of the neck domain (**Fig.13E**). The sequence contains clusters of basic amino acids intermingled with non-polar amino acids and mutation of the basic residues into alanines blocked the nuclear import of NM1. The NLS does not resemble to any of the NLSs already described in the literature and, thus, it might be expected to have some unique properties. Similarly to NM1, also the neck of other unconventional myosin, myosin Vb, contains IQ sequence, that was shown to be responsible for nuclear and nucleolar localization of this myosin. Furthermore, it also mediates interaction with RNA pol I (Lindsay and McCaffrey, 2009). An IQ motif of

another actin and PIP2 binding protein, the neural Wiskot-Aldrich syndrome protein (N-WASP), serves as an NLS (Suetsugu and Takenawa, 2003). In conclusion, the ability to drive nuclear import appears to be common to various IQ motifs.

7.2.2. Role of IQ2 in plasma membrane localization of NM1/Myo1c

NM1/Myo1c neck-tail domain (NM1-(Q123.T)), was shown previously to associate with the plasma membrane through interaction with PIP2. This interaction was assigned to the putative PIP2-specific PH domain in the tail region of myo1c (Hokanson et al., 2006) and/or another less specific to the neck region (Hirono et al., 2004). Interestingly, NM1 mutants which either lacked the second IQ motif or the basic residues within the second IQ sequence were misslocalized from the plasma membrane to the cytosol (**Fig. 10B** and **10C**). These data are in agreement with previously published work that identified the IQ2 as additional plasma membrane binding site (Hirono et al., 2004).

7.2.3. Mechanism of NM1 nuclear import

The basic mechanism of NM1 nuclear import appears to involve karyopherins, because importin 5, importin 7 and importin-β1 were found to be associated with both overexpressed and endogenous NM1. The interaction of importin 5 with NM1 NLS seems to be specific since NM1 mutant lacking the basic amino acids in NLS did not bind this karyopherin.

Canonical importin-mediated nuclear entry is controlled by the nuclear RanGTP which, upon binding to importins, releases their cargos. Surprisingly, the complex of NM1 with importin 5 is stable in the presence of RanGTP (**Fig. 12E**) and its nuclear import is rather dependent on the levels of calmodulin (**Fig. 13B**). This suggests that nuclear import of NM1 is mediated by a non-canonical pathway. Indeed, such a calmodulin-dependent and Ran-independent nuclear import pathway has been shown to regulate the nucleocytoplasmic localization of several transcription factors (SOX9, SRY, c-Rel). The N-terminal domain of SRY and SOX9 contains a calmodulin-binding domain followed by an NLS (Harley et al., 1996). It was shown that calmodulin binding stimulates the nuclear entry of SRY and SOX9 (Argentaro et al., 2003; Sim et al., 2008). On the other hand the NF-κB/Rel family protein c-Rel binds Ca^{2+}-calmodulin via sequence near the NLS and this binding blocks its nuclear accumulation (Antonsson et al., 2003). The NLS of NM1 resides in close vicinity of the second IQ motif. We showed that IQ2 alone is able to drive the translocation of heterologous construct GFP-PK to the nucleus (**Fig. 9J**). Interestingly,

IQ1 seems to play a key role in regulation of NM1 nuclear import (**Fig. 13B**). In presence of elevated levels of calmodulin, IQ1 mediated the inhibition of nuclear import (**Fig. 13B**) and it also substantially increased the binding of CaM the IQ2 (**Fig 13D**).

On the other hand, the crystallographic (Houdusse et al., 2006) and biochemical studies have shown that calmodulin binds the IQ motifs of unconventional myosins in Ca^{2+}-free state and that elevated Ca^{2+} dissociates calmodulin from the neck of Myo1c (Gillespie and Cyr, 2002). More recent study showed that in the absence of calcium, Ca^{2+}-free calmodulin (apo-CaM) was bound to the IQ1 with highest affinity whereas in the presence of calcium IQ1 dissociated Ca^{2+}-CaM most rapidly. Ca^{2+} - induced dissociation of calmodulin molecules from the neck increases ATPase rate and inhibits the motility of Myo1c (Manceva et al., 2007). We propose a scenario in which the calmodulin occupies the IQ12 at low Ca^{2+} cellular levels preventing the importin from binding to NM1. The Ca^{2+} oscilations which occur during G1 phase of cell cycle (Kahl and Means, 2003) or which follow the signal transduction events (Yip et al., 2008) might cause the calmodulins to dissociate from the NM1 neck. As a result, the CaM-free IQ2 will subsequently bind to the import receptor that transports the NM1 to the nucleus. Taken together, at the cellular level, both the motor function of NM1/Myo1c and its localization appear to be dynamically regulated by transient changes in Ca^{2+} concentration. Obviously, further experiments are needed to reveal the details of the mechanism.

7.2.4. Nuclear localization of NM1/Myo1c

The fact that both Myo1c and NM1 contain the same NLS sequence points to the question whether also Myo1c would be present in the nucleus along with NM1. NM1 was first detected in the nucleus in 1997 (Nowak et al., 1997) using the antibody specific to N-terminus of NM1. Myo1c has never been reported in the nucleus since the antibody directed to the C-terminus (Dumont et al., 2002) does not label the nuclei of cells. Intriguingly, upon transfection with either NM1 or Myo1c, the nuclear signal could be readily detected also by this antibody (**Fig. 11B**). One plausible explanation of this discrepancy would be that epitope is probably masked by nuclear binding partners or posttranslational modifications. However, the steady-steate cytosol to nucleus distribution of endogenous NM1 and Myo1c in mouse liver is approximately 70% (cytosol) to 30% (nucleus) Fig 10E. Therefore another possible intepretation is that the level of endogenous nuclear myosins at steady state is below the detection limit of the antibody directed to the C-terminus.

In conclusion, our work revealed a novel NLS sequence responsible for nuclear translocation of NM1. The fact that 16 N-terminal amino acids specific for NM1 are not involved in this process leads to an interesting question whether the two myosins serve the same functions in the nucleus and in the cytoplasm. Obviously, further investigation is needed to answer the question.

7.3. Discussion part III - Identification of novel NM1 interacting proteins

Nuclear myosin 1 (NM1) is an isoform of myosin 1c (Myo1c), both are monomeric and belong to the class I unconventional myosins. Although the molecular structure of the two proteins seems to be very alike, the functions attributed to them differ. Here we further explored the localization, expression and binding partners of the two isoforms of the protein.

7.3.1. NM1/Myo1c expression

We found that localization of both myosins in a cell overlaps to a high degree. Both are localized in nucleus and cytoplasm. Surprisingly, we found that similar to Myo1c also NM1 is more cytoplasmic at steady state. This is in contrast to previously published data (Pestic-Dragovich et al., 2000; Fomproix and Percipalle, 2004) that described NM1 as the predominantly nuclear protein. Here we showed that the previous conclusion was based on the labeling with antibody that also cross-reacted with some other nuclear protein that contained a sequence partially overlapping with the NM1 N-terminal peptide. The distinctly nuclear localization was observed only in small number of cells after forced expression of the NM1 from a plasmid. On the other hand, cells that stably expressed tagged NM1, shoved predominantly cytosolic and plasma membrane localization. Although NM1 is not enriched in nucleus compared to cytoplasm, there are plenty of *in vitro* data that show the direct influence of NM1 on transcription machinery. This indicates that even low levels of this protein are sufficient to exert an effect. We observed previously the increased expression of NM1/Myo1c in lung tissue, and that the ratio between NM1 and Myo1c is not the same in all tissues therefore, it could be regulated. Here we found that in lung about 43 % of total NM1/Myo1c comprises the NM1. Interestingly, similar results were observed in knock-in mice that harbored construct which contained genomic region 4 kilobases upstream the Myo1c start translation start codon (Holt et al., 2002), without the more distal start of transcription (Pestic-Dragovich et al., 2000). In lungs, this construct yielded 35% of total *Myo1c* mRNA while the expression was higher (65%) in

inner ear. We could hypothesize that the genomic organization of NM1/Myo1c gene contains two separate promoters. The proximal one located upstream the exon -1 drives the expression of *NM1* mRNA, and another one about 6 kb upstream close to the exon -2 where the expression of *Myo1c* starts.

7.3.2. NM1 associated proteins

We re-inspected the NM1/Myo1c localization in the mouse tissues and found relatively high expression in epithelial and endothelial cells. We identified a number of proteins that associate with NM1 in the corresponding cell lines. Most of them were either actin or plasma membrane associated proteins. We do not know the functional meaning of the interactions with NM1. Nevertheless, based on high sequence similarity with Myo1c we could hypothesize that the NM1 takes part in the same cytosolic processes as Myo1c. Indeed, some of the identified proteins such as actinin 4, annexin II and protein kinase C alpha were also found to co-purify or co-localize with Myo1c. One extensively studied function of Myo1c is the mediation of mechanotransduction in the inner ear (Spinelli and Gillespie, 2009). Myo1c acts as dynamic linker between the plasma membrane and cytoskeleton that mechanically closes the ion channels and regulates the influx of calcium in response to mechanical stimulus. One possibility is that similarly to Myo1c, NM1 links the membrane to underlining cytoskeleton and is also involved in sensing the mechanical stimuli. But how does mechanical stress of plasma membrane relate to the transcription? Interestingly, it was shown recently that human periotodontal fibroblasts responded to mechanical stretching by attenuation of transcription. Moreover, the investigators also observed the relocalization of NM1 from the nucleus to cytoplasm (Steinberg et al., 2011). This suggests indirectly that NM1 could be involved in response to mechanical stress, but the details of how remain to be solved.

As shown initially, NM1 influenced transcription also in unstressed cells. The acute depletion of NM1/Myo1c in HeLa cells leads to a decreased transcription rate, while overexpression of NM1 stimulated the transcription (Philimonenko et al., 2004). Besides the direct influence of NM1 on transcription apparatus (Hofmann et al., 2006b), the observed changes in transcription could be explained by the cytosolic/plasma membrane activities of NM1. In adipocytes, the Myo1c isoform associates with Rictor (Rapamycin insensitive companion of mTOR) that interacts with the mammalian target of rapamacin mTOR. The mTOR kinase is a major controller of cellular proliferation and growth, which partially exerts its function thru a regulation of RNA polymerase I transcription (Grummt,

2003). Myo1c also facilitates the membrane insertion of a solute carrier protein SLC2A4 which is a glucose importer also known as GLUT4. Interestingly, here we found SLC3A2 as one of proteins that associated with NM1. SLC3A2 comprises the heavy subunits of the large neutral amino acid transporter (LAT1) that is also known as CD98. LAT1 is responsible for the intracellular transport of neutral branched (valine, leucine, isoleucine) and aromatic (tryptophan, tyrosine) amino acids. Interestingly, it was shown previously that leucine is an activator of mTOR (Lynch, 2001). Therefore one attractive hypothesis would be that NM1 regulates a membrane insertion of SLC3A2 which leads to an increased import of leucine that in turn activates mTOR and cell growth. The other way around, the acute depletion of NM1/Myo1c by RNAi leads to a decreased import of leucine and hence lower mTOR activity. It is of interest that similarly to NM1/Myo1c, LAT1 is highly expressed in endothelial cells. Nevertheless, the presented mechanism is entirely hypothetical and requires substantially more work to prove.

In podocytes, Myo1c facilitated the membrane integration of Neph1 and was implied in maturation of cell-cell junctions (Arif et al., 2011). To support the hypothesis of functional similarity between NM1 and Myo1c, we found Catenin delta-1 (CTNND1), a member of Armadillo protein family, which functions in adhesion between cells and in signal transduction (Hartsock and Nelson, 2008), and Receptor-type tyrosine-protein phosphatase F interacting protein 1 (Liprin 1) as proteins that associate with NM1 in digitonin extracts of HeLa cells. Altogether we could hypothesize that in cytosol, NM1 could act in the same processes as Myo1c but associates with different proteins than Myo1c. This could cause slight differences in the localization pattern of NM1 and Myo1c. As a results we do not see complete colocalization between the two isoforms.

8. GENERAL DISCUSSION

NM1 was the first myosin protein identified in the cell nucleus in 1997. As a predominantly nuclear protein, NM1 was shown to have function in transcription by RNA polymerases I and II by us (Hofmann et al., 2006b; Philimonenko et al., 2004) and others (Fomproix and Percipalle, 2004). On the other hand, the cytoplasmic, or more exactly the plasma membrane myosin 1c was discovered in 1992. These two proteins are the product of one gene. The only difference between NM1 and Myo1c are the 16 amino acids at the N-terminus of NM1. Based on different cellular localization of NM1 and Myo1c, previous publications considered the NM1 molecule to be a nuclear protein that is functionally distinct from its cytoplasmic isoform, the Myo1c. In simple words, however, one can say that NM1 is composed of Myo1c +16 amino acids. In this simplistic view, one obvious question popped up. What is the N-terminal piece changing in Myo1c molecule to such an extent that it becomes NM1? The attempt to answer this rather simple question led to the discovery of a number of interesting facts some of which are provocative and prompted us to re-visit or re-interpret the some of the previous data.

The broad expression of NM1 in various mouse tissues strongly suggested that it could serve some important function. In addition to that, the relatively high conservation of N-terminus among vertebrates implied that it might contribute to some important property that was preserved during evolution. Therefore, the next question was whether this preserved property was the ability to localize the myosin molecule into the nucleus. In contrast to some previous data, we found that the N-terminus itself is not an NLS. Moreover, the “cytoplasmic” Myo1c molecule did localize into nucleus even without N-terminal extension. Subsequently, we found that the nuclear translocation is driven by another sequence that is shared by NM1/Myo1c. Importantly, the highly overlapping distribution of endogenous NM1 and Myo1c in a cell strongly suggested that the N-terminus does not contribute to the cellular localization of the isoforms. Thus its function could be in changing some of the molecular properties of NM1. The attachment of N-terminus to head could influence the binding of myosin to actin or the myosin ATPase cycle. Therefore, the next question was whether Myo1c could serve the same functions as NM1. To answer this, we made one simple experiment in which we depleted both proteins and added back only Myo1c. The result suggested that the myosin isoforms could be functionally equal. Another independent notion that supported this hypothesis was the fact that neither the mice nor the fibroblasts derived from NM1 knockout mice displayed any

severe defect in transcription (Venit et al., in preparation). Since the NM1 is not expressed in this mouse, we could hypothesize that the Myo1c is able to replace NM1 functionally. This could be true especially in tissues where the expression of NM1 is not predominant or the lack of one isoform is compensated by another. On the other hand, NM1/Myo1c is highly expressed in cell types that face mechanical tension or fluid shear stress. Therefore, to unmask the possible defect in the NM1- lacking cells, one would have to compare the behavior of KO and WT cells under stress conditions.

Of importance was also the finding that at steady state, NM1 is not predominantly nuclear. This statement is supported by number of observations presented in the last chapter of this thesis. Along with Myo1c, NM1 is localized predominantly in the cytoplasm and at the plasma membrane. None of the previous work describing the functions of Myo1c in cytosol took this into an account, and by depleting Myo1c the investigators were also reducing the level of NM1. Therefore, some of the cytosolic functions of Myo1c could be attributed to NM1. Indeed, we identified a large number of cytosolic or cytoplasmic membrane associated proteins as the proteins that co-purify with cellular NM1. Therefore, in addition to the "nuclear" functions NM1 could play a role in the cytoplasmic processes. On the other hand, since the Myo1c could localize to the nucleus, it could also play a role in transcription.

Myo1c has an interesting molecular property. It could act as a molecular ratchet allowing the attached cargo to move in one direction only. The promoter-proximal pausing of RNA polymerase (RNAP) is a divergent (anti-sense) transcription (Core et al., 2008) known as bidirectional expression of short transcripts (BEST). It was shown to be a general feature of RNA polymerase transcription in mammalian tissues (Seila et al., 2008). Remarkably, the data available so far show that NM1 motor activity is needed during the early stages of transcription initiation (Hofmann et al., 2006b; Ye et al., 2008). Therefore, in a hypothetic scenario the NM1/Myo1c together with actin could form a molecular motor that would act as enhancer of transcription by helping the RNAP to maintain the directionality of transcription. Unfortunately we have only sparse data so far to be able to show it. Nevertheless, the fact that acute depletion of NM1/Myo1c leads to both the reduction of Pol I transcription and proliferation rate suggests that NM1/Myo1c could be involved in the regulation of these processes.

9. CONCLUSION

9.1. What is the expression and localization pattern of NM1 in mouse tissues?

We demonstrated that NM1 is present in cell nuclei of all mouse tissues examined except for cells in terminal stages of spermatogenesis. Quantitative PCR and western blots demonstrate that the expression of NM1 in tissues varies, with the highest levels in the lungs. The expression of NM1 is lower in serum-starved cells and it increases after serum stimulation. The lifespan of NM1 is longer than 16 h as determined by cycloheximide translation block. A homologous protein is expressed in human, chicken, Xenopus, and zebrafish, as shown by RACE analysis. The analysis of genomic sequences indicates that almost identical homologous NM1 genes are expressed in mammals, and similar NM1 genes in vertebrates.

9.2. Which NM1 domain is responsible for the nuclear localization of the protein?

We investigated the mechanism of nuclear import of NM1 in detail. Using overexpressed GFP chimeras encoding for truncated NM1 mutants, we identified a specific sequence that is necessary for its import to the nucleus. This novel nuclear localization sequence is placed within calmodulin-binding motif of NM1, thus it is present also in the Myo1c. We confirmed the presence of both isoforms in the nucleus by transfection of tagged NM1 and Myo1c constructs into cultured cells, and also by showing the presence of the endogenous Myo1c in purified nuclei of cells derived from knock-out mice lacking NM1. Using pull-down and co-immunoprecipitation assays, we identified importin beta, importin 5 and importin 7 as nuclear transport receptors that bind NM1.

Since the NLS sequence of NM1 lies within the region that also binds calmodulin we tested the influence of calmodulin on the localization of NM1. The presence of elevated levels of calmodulin interfered with nuclear localization of tagged NM1. We have shown that the novel specific NLS brings not only the "nuclear" isoform of myosin I (NM1 protein) but also its "cytoplasmic" isoform (Myo1c protein) to the cell nucleus. This opens a new field for exploring functions of this molecular motor in nuclear processes, and for exploring the signals between cytoplasm and the nucleus

9.3. What is the composition of protein complexes containing NM1?

Since NM1 is distributed in nucleus and also in cytoplasm, we sought to identify all possible cellular proteins that could interact with NM1. Using co-immunoprecipitation and mass spectrometry we identified a large number of proteins that associate with NM1 in the cellular extracts of various human cell lines and mouse lungs. Most of the identified proteins were actin and plasma membrane associated. These proteins are involved in mechanical stabilization of cell cytoskeleton, exocytosis and cell-cell contacts. We found that NM1/Myo1c colocalizes with selected proteins mainly at the leading edge of plasma membranes and cell-cell contacts. Thus, similarly to Myo1c, NM1 could also play an important role in the dynamic processes at the plasma membrane.

10.OVERVIEW OF MATERIALS AND METHODS

10.1. Antibodies

NM1 was detected using rabbit polyclonal antibody directed to N-terminal part of NM1 (M3456, Sigma). Polyclonal antibody R2652 and monoclonal antibody mT2 against the tail of Myo1c was a gift from Peter G. Gillespie, Oregon Hearing Research Center and Vollum Institute (Gillespie et al., 1993; Dumont et al., 2002). Antibodies against β-actin (A2066) and γ-tubulin (T6557) were purchased from Sigma; antibody against GAPDH (clone 6G5) is available from Acris. In immunofluorescence and co-immunoprecipitation experiments we used affinity purified antibody directed to the NM1 N-terminus M3567 (Sigma), antibodies to lamin B (M-20, Santa Cruz Biotechnology), V5-tag (Serotec), V5-tag (V8137-Sigma), FLAG-tag (Stratagene) and to calmodulin (Upstate, cat. No. 05-173). Anti-importin 5 (sc-17802), importin beta (sc-1919) and importin 7 (sc-55235) were purchased from Santa Cruz Biotechnology; rabbit polyclonal anti-NM1 for western blots and immunofluorescence in Experimental Part III was kindly provided by Piergiorgio Percipalle (Fomproix and Percipalle, 2004), and EGFP antibody was purchased from Invitrogen (cat. No. A11122). R5 antibody (Exbio Antibodies) was generated against N-terminal peptide of NM1 (AA1-15), serum was affinity purified on the same peptide. We also used monoclonal antibodies to Filamin A (MAB1678, Cheminon); Annexin II (BD Pharmingen™); Lamin A (clone 133A2, kind gift from Yves Raymond); and a polyclonal anti Myosin 1B (HPA013607).

10.2. Cells and serum activation

NIH 3T3 and HeLa cells were grown in Dulbecco's modified Eagle's medium (DMEM) supplemented with 10% fetal calf serum (FCS) and antibiotics in humidified 5% CO_2/air, 37°C environment. The protocol for serum activation experiments was essentially as described (Iyer et al., 1999). Briefly, NIH 3T3 cells were grown on six-well plates. When they reached approximately 50% confluence they were washed two times with phosphate buffered saline (PBS), and low serum medium (0.1% FCS) was added to the plates. The cells did not show morphological signs of apoptosis under these conditions. After 48 h, the medium was replaced with a fresh medium containing 10% FCS. Cells were harvested before the addition of serum (time 0) and after 2, 4, 8, and 16 h of serum stimulation.

10.3. Cells and transfections

Cell lines cells were obtained from American Type Culture Collection. NIH/3T3 (ATCC No. CRL-1658), U2OS (ATCC No. HTB-96), HeLa (ATCC No. CCL-2) and HEK 293T/17 (ATCC No CRL-11268) were kept in DMEM supplemented with 10% fetal bovine serum (FBS) in 5% CO2/air, 37°C, in humidified atmosphere. HeLa S3 (ATCC No.CCL-2.2) were kept in S-MEM supplemented with 5% FBS and grown in spinner flasks. The U2OS cells were transfected with FUGENE 6 (Roche) according to the manufacturer's protocol, fixed after 48 h and either observed directly under the microscope or labeled with antibodies. HEK293T cells were electroporated using GenePulser (Biorad) electroporator as described (Galvez et al., 2001). The efficiency of electroporation was about 90%.

10.4. Cell synchronization

U2OS cells were treated with nocodazole (80 ng/ml or 400 ng/ml) for 16h. Mitotic cells were washed off the dish with medium, spun down and resuspended in fresh medium, and seeded on coverslips. Cells on coverslips were cultivated further in fresh medium and fixed 2,4,6,8, and 10 hours after the nocodazole block. Aphidicolin (1 μg/ml) was applied for 16 hours, cells were washed, cultivated in fresh medium, and then fixed 2, 7, 11, 17, and 22 hours post aphidicolin block. NIH 3T3 cells were synchronized by mitotic shake-off. Harvested cells were seeded on poly-lysine coated coverslips, and allowed to attach for 15 min. HeLa cells, used for co-immunoprecipitation of endogenous NM1, were incubated for 16 hours with nocodazole (400 ng/ml), washed in PBS, and then cultivated in complete medium for additional 3 h prior to the harvest.

10.5. Plasmid DNA preparation

NM1-GFP, GFP-NM1, Myo1c-GFP, NM1-V5, Myo1c-V5 were obtained by ligation of full length mouse NM1 (amino acids 1-1024) and Myo1c (aa 1-1028) (Pestic-Dragovich et al., 2000) cDNA into pEGFP-C3, pEGFP-N3 (Clontech) and pcDNA3.1/V5-His (Invitrogen) vectors. Truncations containing head (H) neck with IQ domains (Q123) and tail (T) domains were generated using inverse PCR. NM1-V5-(H) (aa 1 to 716) was generated from NM1-V5.GFP-NM1-(Q123.T) (aa 712 to 1044),GFP-NM1-(Q3.T) (aa 763 to 1044), GFP-NM1-(Q123.T -Δ853) (aa 712 to 853), GFP-NM1-(Q12) (aa 712 to 770) were constructed from GFP-NM1 using standard cloning methods. For inspection of NLS-peptide localization, we produced a testing construct GFP-PK that contains in-frame fusion

of EGFP and cytosolic enzyme pyruvate kinase (PK) (Frangioni and Neel, 1993), GFP-PK-IQ-12 was produced by ligation NM1-(Q12) sequence into GFP-PK vector. GFP-PK-IQ1 (aa 712 to 740), GFP-PK-IQ2 (aa 739 to 766) GFP-PK-NLS $^{(NM1)}$ (aa 754 to 766) were generated by PCR deletions from GFP-PK-IQ1,2. Nt-GFP-PK was produced by ligation of NM1 N-terminal sequence (aa 1-16) in front of EGFP in GFP-PK vector. Ligation of the OneStrep tag sequence (IBA) in front of EGFP in the pEGFP-C3 vector generated Str-GFP. Str-GFP-NM1-(Q123.T) was produced by ligating the Q123.T (aa 712 to 1044) sequence into Str-GFP vector. Calmodulin cDNA was prepared from HeLa total cell RNA using RT-PCR and cloned into pcDNA3.1 vector (Invitrogen). Bacterial expression vector pET-Str-His was generated by ligation of OneStrep sequence into the pET28b vector (Novagen). Str-IQ12-His was produced by an in-frame ligation of the PCR-amplified fragment of NM1-(Q12) (aa 712 to 770) between the OneStrep- and His-tag. Point mutations in the NLS sequence of NM1 were generated by the site directed mutagenesis protocol (Stratagene). Bacterial expression plasmid pQE-RanQ69L was kindly provided by Prof. Dirk Görlich. Detailed description of all cloning procedures is available upon request. Recombinant proteins were expressed in bacteria and purified using Ni-NTA agarose column as described (Kutay et al., 1997; Manceva et al., 2007).

10.6. Animals

Laboratory mice strain C53/Bl6, four males and three females, 10–16 weeks old were killed by cervical dislocation. Samples of the small intestine, pancreas, brain, kidney, skin, heart muscle, testis/ovary, striated muscle, spleen, liver, and lungs intended for RNA isolation were stored in RNAlater storage solution (Sigma), parts of the tissues intended for subsequent cryostat slicing were frozen in liquid nitrogen. Experiments were performed according to the national and local regulations for use of experimental animals.

10.7. Immunofluorescence microscopy

For immunostaining in Experimental part I, 6 μm cryostat sections were mounted onto glass slides coated with poly-L-lysine, and fixed 15 min in absolute ethanol at room temperature. Sections were then permeabilized in 0.2% Triton X-100 in PBS for 10 min, incubated with antibody against NM1 (16 μg/ml, 1 h at RT), and with FITC-conjugated goat anti rabbit secondary antibody (Jackson ImmunoResearch). Coverslips were mounted with Mowiol (Sigma) containing DABCO (Sigma) as an antifading agent, 0.5 μg/ml

propidium iodide, and 0.1 μg/ml DAPI (Sigma), and observed with confocal microscope Leica TCS SP.

Mouse tissues experimental part III were obtained from mouse fixed by whole body perfusion with 4% PFA in PBS. Tissues excised from the body were further fixed using 4% PFA in PBS over night and dehydrated in sucrose. After freezing in mounting media, 7-10 μm sections were prepared using cryostat. Cryostat sections on slides were incubated 3x5 min with 0.1% sodium borohydride, washed, permeabilised with 0.1% PBS, blocked with 5% BSA, washed 3x in PBS/TWEEN and incubated with indicated antibodies for 1h at room temperature. Signal from primary antibodies was visualize using ALEXA 647 conjugated goat anti rabbit antibody.

In experimental parts II and III

Cells grown on coverslips were fixed with freshly prepared 3% formaldehyde for 10 minutes, permeabilized with 0.1% Triton X-100 in PBS for 10 minutes, incubated with primary antibodies for 1 hour at room temperature. To unmask epitopes for actin, actinin and annexin II, cells in Fig.20 were fixed with -20°C metanol, re-hydrated in PBS/Tween and incubated with primary antibodies diluted in PBS containing 0.05% Tween-20 (PBST) After washing in PBST, coverslips were incubated with ALEXA 488 or ALEXA 647 goat anti-rabbit or goat anti-mouse secondary antibodies (Invitrogen). Coverslips were mounted with Mowiol (Sigma) containing DABCO (Sigma) as an anti-fading agent and 0.1 μg/ml DAPI (Sigma), and observed under fluorescent or confocal microcopes (LEICA DM 6000, LEICA DMI 6000, LEICA TCS SP5 AOBS TANDEM). Brightness and contrast of captured digital images was adjusted with Photoshop software (Adobe).

10.8. Immunoblots

Tissues and cells for the experiments on Figs. 2,5 and 18 were homogenized in SDS lysis buffer (60 mM Tris pH 6.8, 10% glycerol, 2% SDS), lysates were cleared by centrifugation and total protein content was measured using BCA assay (Pierce). In other experiments, cultured cells were lysed in lysis buffer (20 mM Tris pH 7.4, 200 mM NaCl, 1% Triton X-100, 2 mM EDTA, 10 mM EGTA, 10 mM K_2HPO_4, 1 mM PMSF, 10 μg/ml leupeptin, 1 μg/ml pepstatin), briefly sonicated, and cleared by centrifugation. Protein content was measured by Bradford assay (Biorad) of BCA (Pierce). Equal amounts of protein were loaded on 8% gel, proteins were separated by SDS-PAGE and transferred to nitrocellulose membrane. The blots were incubated with antibodies, horseradish peroxidase conjugated

secondary antibodies (Bio-Rad), and the signal was visualized by ECL (Pierce). Where indicated, signal from primary antibodies was visualized using fluorescently conjugated antibodies on an Li-cor Odyssey imaging system.

The two myosin isoforms were separated according to (Rossini et al., 1995) with following modifications. We used a 0.75 mm thick midigel format (Hoefer SE 600 Ruby), 4% stacking gel (15 mm high) and 8% resolving gel. Both gels contained 30% glycerol. Electrophoresis was run for 14 h with maximum power 3 W, maximum voltage 350 V, and with cooling to 8°C by circulator bath.

10.9. RNA isolation and RT-qPCR

Total RNA from cells and tissues was isolated with TriReagent (Sigma) according to manufacturer's protocol. The cells were lysed on plates. Concentration of RNA was measured by spectrophotometry and the integrity of RNA was checked on denaturing agarose gel. A total of 100 ng of RNA was reverse-transcribed with random hexamers as primers using TaqMan Reverse Transcription Reagents (Applied Biosystems). Real-time qPCR was performed in ABI Prism 7300 instrument using SYBR Green PCR Master Mix (all Applied Biosystems). The following primers were used: mouse NM1 CGGCAGGATGCGCTACC and TCAAGGCGCTCTCCATGG, mouse ß-actin GCCCTGAGGCTCTTTTCCA and TGCCACAGGATTCCATACCC, and mouse GAPDH GGAAGGGCTCATGACCACAG and GCCATCCACAGTCTTCTGGG. Data were evaluated with 2-ΔΔ CT method (Livak and Schmittgen, 2001) using control genes as described in Results.

10.10. RACE

RLM-RACE (RNA ligase-mediated rapid amplification of cDNA ends) was performed according to the protocol developed by Invitrogen with minor modifications. Briefly, total RNA was first treated with Shrimp Alkaline Phosphatase (SAP) to remove 5′ phosphates from all uncapped RNAs. RNA was then extracted by phenol:chloroform and treated with Tobacco Acid Pyrophosphatase to remove the cap, yielding 5′ phosphate. After phenol:chloroform extraction, a special RNA adapter oligonucleotide was ligated to 5′ phosphorylated RNAs by T4 RNA Ligase. RNA was extracted once more and reverse-transcribed with random hexamers as primers using TaqMan Reverse Transcription Reagents (Applied Biosystems). PCR was performed as above with touchdown protocol. (Annealing temperature went down every five cycles from 70° to 68°, 65°, and then

remained 63° during the rest of amplification.) Primers were designed to align with homologues of Myo1c in the respective species: human MYO1C (GenBank NM_033375) GTGTCCGCCACGGCAAACAGG and CCGTGCGCAGTGCTCGGTACAC, chicken MYO1C (GenBank NM_001006220) TCACTGGTGAAGTTCTCAAGCAGG, *Xenopus laevis* MYO1C (GenBank BC044718) TCTTTATATGGGTTGACAGAGACC and GCTTCACTTGTATAGTTTTCCAACAG, and *Danio rerio* Myo1c homologues GenBank XM_690832 ATGAAAGCGGCTTCACTGTTGTGG and GenBank XM_689729 GACAAAATCCTGCACACCCACCC. PCR products were separated on 3% agarose gel, bands were excided, isolated by Zymoclean Gel DNA Recovery Kit (Zymo Research), and sequenced on ABI Prism 3100 (Applied Biosystems).

10.11. Sequence searches, alignment, and construction of phylogenetic trees

The sequences similar to NM1 were found in the GenBank and Ensembl databases using TBLASTN (Altschul et al., 1997). Genscan (Burge and Karlin., 1997) was used for gene predictions in genomic DNA. Sequences were aligned with ClustalW and manually refined. The phylogenetic trees were constructed and bootstrap tested by minimum evolution method using molecular evolutionary genetics analysis software MEGA version 3.1 (Kumar et al. 2004).

10.12. Pull-down assays and immunoprecipitation

Digitonin extract from suspension HeLa cells, prepared as described (Kutay et al., 1998), was diluted to 2 mg/ml of total protein in lysis buffer (50 mM HEPES pH 7.4, 150 mM NaCl, 75 mM potassium acetate, 5 mM magnesium acetate, 1 mM DTT, protease inhibitors). After dilution, purified bacterially expressed Str-IQ12-His was added to the lysate. After 3 hours of incubation, the extract was centrifuged to remove precipitated proteins and supernatant was further incubated for 1 hour with StrepTactin Beads (IBA) to capture the bait and associated proteins. Beads were briefly washed 3 times with 1 ml of the lysis buffer followed by brief wash with IBA wash buffer (100 mM Tris pH 7.5, 100 mM NaCl, 1 mM EDTA) and captured proteins were eluted from beads with the wash buffer supplemented with 2 mM biotin. HEK 293T cells electroporated with Str-GFP-NM1-(Q123.T) or Str-GFP were collected by trypsinization into serum-containing medium. After centrifugation 300 g / 3 minutes, the cells were washed twice with ice-cold PBS and extracted twice with lysis buffer containing 50 mM HEPES pH 7.4, 150 mM potassium acetate, 5 mM magnesium acetate, 1 mM DTT, 1 mg/ml digitonin (Fluka),

EDTA-free COMPLETE inhibitors (Roche). After 4 hours of incubation with StrepTactin resin, the captured protein complexes were washed briefly 3 times with 1 ml of the lysis buffer followed by wash with 1 ml of IBA wash buffer. Proteins were eluted from beads with 2 mM biotin added into the wash buffer. The experiments with RanQ69L mutant were performed as described above, with the exception that after the 3rd wash a half of the beads was incubated for 10 min with buffer containing recombinant RanQ69L and the other half was incubated only in buffer. Elution with Ran mutant was repeated twice and remaining proteins were eluted from beads with IBA elution buffer containing 2 mM biotin. Eluates were concentrated ultrafiltration (Ultracel 10K, Milipore) and resolved on 6-20% gradient polyacrylamide gel.

Endogenous NM1 was immunoprecipitated from adherent HeLa cells synchronized with nocodazole. Cells were extracted twice in lysis buffer (50 mM HEPES pH 7.4, 150 mM NaCl, 75 mM potassium acetate, 5 mM magnesium acetate, 1 mM DTT, 1mg/ml of digitonin and protease inhibitors), lysates were clarified by centrifugation (10 min, 16 000g, 4°C), and incubated with beads containing either covalently bound antibody antibody to NM1 (Sigma, cat no M3567) or to EGFP (Exbio, Czech Republic, cat no 11-473-C100). After 3 washes in 1 ml of lysis buffer beads were washed in 1ml of 50 mM amonium bicarbonate pH 7.5 to remove salts and detergent. Bound proteins were eluted twice with 500 µl of 500 mM amonium hydroxide. Eluates were evaporated using SpeedVac concentrator (Savant, Holbrook, NY, USA), dry pellets were resuspended in 20 ul of 1x SDS loading buffer, boiled and resolved on 6-20% gradient SDS PAGE. After transfer to nitrocelulose proteins were visualized using specific antibodies.

GFP-PK constructs in Fig.13D were immunoprecipitated from lysates of electroporated HEK23T cells as follows. Cells were harvested by trypsinization, washed in PBS and lysed in lysis buffer (150 mM NaCl, 50mM Tris-HCL pH-7.5, 10mM EGTA, 2mM EDTA, 1% Triton X-100, protease inhibitors ROCHE). After clarification by centrifugation (10 min, 16 000g, 4°C), supernatans were incubated with 20 µl of GFP-trap magnetic particles (ChromoTek GmbH, Germany). After 5 washes in 1 ml of lysis buffer particles were washed in 1ml of 50 mM amonium bicarbonate pH 7.5 to remove salts and detergent. Bound proteins were eluted twice with 500 µl of 500 mM amonium hydroxide. Eluates were evaporated using SpeedVac concentrator (Savant, Holbrook, NY, USA), dry pellets were resuspended in 20 ul of 1x SDS loading buffer, boiled and resolved on 6-20%

gradient SDS PAGE. After transfer to nitrocelulose proteins were visualized using specific antibodies.

In experimental Part III

Cells were extracted in either in buffer containing 20 mM Tris pH 7.4, 150 mM NaCl, 1% Triton X-100, 2 mM EDTA, 10 mM EGTA, 10 mM K_2HPO_4 (Triton extraction buffer), or 20 mM Tris pH 7.4, 150 mM potassium acetate, 5 mM magnesium acetate, 1 mM DTT, 1 mg/ml digitonin (digitonin buffer) complete protease inhibitors (ROCHE), 20 mM Tris pH 7.4, 150 mM potassium acetate, 5 mM $MgCl_2$, 1 mM DTT, 0.1% Tween 20, protease and phophatase inhibitors (Tween buffer). Cells were disrupted by sonication on ice. Lysates were cleared by centrifugation 14000g/10min/4°C. After 5 washes in 1 ml of lysis buffer particles were washed in 1ml of 50 mM amonium bicarbonate pH 7.5 to remove salts and detergent. Bound proteins were eluted twice with 500 µl of 500 mM amonium hydroxide. Eluates were evaporated using SpeedVac concentrator (Savant, Holbrook, NY, USA), dry pellets were resuspended in 20 ul of 1x SDS loading buffer, boiled and resolved on 6-20% gradient SDS PAGE.

10.13. Proteolytic digestion and sample preparation

Protein bands were cut from the gel, sliced into the small pieces, and decolorized in sonic bath at 60°C several times with 0.1 M 4-ethylmorpholine acetate (pH 8.1) in 50% acetonitrile (ACN). After complete destaining, proteins were reduced by 50mM TCEP in 0.1 M 4-ethylmorpholine acetate (pH 8.1) for 5min at 80°C and alkylated using 50mM iodoacetamide in 0.1 M 4-ethylmorpholine acetate (pH 8.1) for 30min in dark at room temperature. Then, the gel was washed with water, shrunk by dehydration with ACN and reswollen in water. The rehydratation and dehydration of the gel was repeated twice. Next, the gel was reswollen in 0.05 M 4-ethylmorpholine acetate (pH 8.1) in 50% acetonitrile (ACN) and then the gel was partly dried using a SpeedVac concentrator (Savant, Holbrook, NY, USA). Finally, the gel was reconstituted with cleavage buffer containing 0.01% 2-mercaptoethanol, 0.05 M 4-ethylmorpholine acetate (pH 8.1), 10 % ACN, and sequencing grade trypsin (Promega, 10 ng/µl). Digestion was carried out overnight at 37 °C; the resulting peptides were extracted with 30% ACN/0.1% TFA and subjected to mass spectrometric analysis.

10.14. Mass spectrometric analysis

Mass spectra were acquired in the positive ion mode on a MALDI-FTMS APEX-Ultra (Bruker Daltonics, Bremen, Germany) equipped with 9.4 T superconducting magnet and SmartBeam laser. The acquisition mass range was 700 - 3500 m/z and 512k data points were collected. A 280 V potential was applied on the MALDI plate. The cell was opened for 2500 ms, 4 experiments were collected for one spectrum where one experiment corresponds to 300 laser shots. The instrument was externally calibrated using PepMix II peptide standard (Bruker Daltonics, Bremen, Germany). It results in typical mass accuracy below 2 ppm. A saturated solution of α-cyano-4-hydroxy-cinnamic acid in 50% ACN/0.2% TFA was used as a MALDI matrix. A 1 µl of matrix solution was mixed with a 1 µl of the sample on the target and the droplet was allowed to dry at ambient temperature. After the analysis the spectra were apodized using square sin apodization with one zero fill. The interpretation of mass spectra was done using DataAnalysis version 3.4 and BioTools 3.2 software packages (Bruker Daltonics, Billerica, MA). Proteins were identified by peptide mass fingerprinting (PMF) using a search algorithm MASCOT (Matrix Science).

10.15. Generation of the NM1 knock-out mice

To generate NM1-KO mice, loxP-recombination sites were introduced into NM1 gene by homologous recombination in R1 embryonic stem cell line (Nagy et al., 1993). Cre-mediated recombination in germline cells, achieved by cross breeding with the meu-cre expressing mice (Leneuve et al., 2003) resulted in removal of the loxP-flanked exon-1 from the mouse NM1 genomic sequence (sequence from -165 to + 116 base pairs from NM1 translation initiation site). In the mutant NM1 allele, only the start codon initiating the translation of Myo1c is present. As a result, only Myo1c protein is expressed in all tissues. Mice were genotyped using genomic PCR, and the absence of NM1 protein was confirmed by Western blotting (Venit et al., in preparation).

10.16. Isolation of nuclei from mouse liver

Nuclei from mouse liver were isolated as described (Nagata et al., 2010). Briefly, mice were killed by CO_2 and liver was homogenized in ice-cold buffer A (250 mM sucrose, 5 mM $MgCl_2$, 10 mM HEPES pH 8) in glass Dounce homogenizer. The homogenate was spun down (600 g/10 min), the supernatant was taken as the cytosolic fraction and the pellet was washed once in buffer A. The crude nuclear pellet was resuspended in buffer B

(2.0 M sucrose, 1.5 mM $MgCl_2$, 10 mM HEPES pH 8) and centrifuged 30 minutes/16000 g. Purified nuclei were resuspended in buffer Z (62.5 mM Tris pH 6.8, 10% glycerol, 2% SDS), heated to 90 °C for 10 minutes, sonicated, and centrifuged again (16000 g/10 min). The amount of protein in the supernatant was measured using BCA (Pierce).

11. REFERENCES

Allen, L.H., and A. Aderem. 1995. A role for MARCKS, the alpha isozyme of protein kinase C and myosin I in zymosan phagocytosis by macrophages. *J Exp Med*. 182:829-840.

Altschul, S.F., T.L. Madden, A.A. Schaffer, J. Zhang, Z. Zhang, W. Miller, and D.J. Lipman. 1997. Gapped BLAST and PSI-BLAST: a new generation of protein database search programs.

Ambrosino, C., R. Tarallo, A. Bamundo, D. Cuomo, G. Franci, G. Nassa, O. Paris, M. Ravo, A. Giovane, N. Zambrano, T. Lepikhova, O.A. Janne, M. Baumann, T.A. Nyman, L. Cicatiello, and A. Weisz. 2010. Identification of a hormone-regulated dynamic nuclear actin network associated with estrogen receptor alpha in human breast cancer cell nuclei. *Mol Cell Proteomics*. 9:1352-1367.

Antonsson, A., K. Hughes, S. Edin, and T. Grundstrom. 2003. Regulation of c-Rel nuclear localization by binding of Ca2+/calmodulin. *Mol Cell Biol*. 23:1418-1427.

Argentaro, A., H. Sim, S. Kelly, S. Preiss, A. Clayton, D.A. Jans, and V.R. Harley. 2003. A SOX9 defect of calmodulin-dependent nuclear import in campomelic dysplasia/autosomal sex reversal. *J Biol Chem*. 278:33839-33847.

Arif, E., M.C. Wagner, D.B. Johnstone, H.N. Wong, B. George, P.A. Pruthi, M.J. Lazzara, and D. Nihalani. 2011. Motor protein Myo1c is a podocyte protein that facilitates the transport of slit diaphragm protein Neph1 to the podocyte membrane. *Mol Cell Biol*. 31:2134-2150.

Barylko, B., G. Jung, and J.P. Albanesi. 2005. Structure, function, and regulation of myosin 1C. *Acta Biochim Pol*. 52:373-380.

Batters, C., C.P. Arthur, A. Lin, J. Porter, M.A. Geeves, R.A. Milligan, J.E. Molloy, and L.M. Coluccio. 2004a. Myo1c is designed for the adaptation response in the inner ear. *Embo J*. 23:1433-1440.

Batters, C., M.I. Wallace, L.M. Coluccio, and J.E. Molloy. 2004b. A model of stereocilia adaptation based on single molecule mechanical studies of myosin I. *Philos Trans R Soc Lond B Biol Sci*. 359:1895-1905.

Bose, A., A. Guilherme, S.I. Robida, S.M. Nicoloro, Q.L. Zhou, Z.Y. Jiang, D.P. Pomerleau, and M.P. Czech. 2002. Glucose transporter recycling in response to insulin is facilitated by myosin Myo1c. *Nature*. 420:821-824.

Bose, A., S. Robida, P.S. Furcinitti, A. Chawla, K. Fogarty, S. Corvera, and M.P. Czech. 2004. Unconventional myosin Myo1c promotes membrane fusion in a regulated exocytic pathway. *Mol Cell Biol*. 24:5447-5458.

Burge, C., and S. Karlin. 1997. Prediction of complete gene structures in human genomic DNA. *J Mol Biol*. 268:78-94.

Cameron, R.S., C. Liu, A.S. Mixon, J.P. Pihkala, R.J. Rahn, and P.L. Cameron. 2007. Myosin16b: The COOH-tail region directs localization to the nucleus and overexpression delays S-phase progression. *Cell Motil Cytoskeleton*. 64:19-48.

Chen, J., and M.C. Wagner. 2001. Altered membrane-cytoskeleton linkage and membrane blebbing in energy-depleted renal proximal tubular cells. *Am J Physiol Renal Physiol*. 280:F619-627.

Chen, X.W., D. Leto, S.H. Chiang, Q. Wang, and A.R. Saltiel. 2007. Activation of RalA is required for insulin-stimulated Glut4 trafficking to the plasma membrane via the exocyst and the motor protein Myo1c. *Dev Cell*. 13:391-404.

Chuang, C.H., A.E. Carpenter, B. Fuchsova, T. Johnson, P. de Lanerolle, and A.S. Belmont. 2006. Long-range directional movement of an interphase chromosome site. *Curr Biol*. 16:825-831.

Cisterna, B., M. Malatesta, J. Dieker, S. Muller, E. Prosperi, and M. Biggiogera. 2009. An active mechanism flanks and modulates the export of the small ribosomal subunits. *Histochem Cell Biol*. 131:743-753.

Cisterna, B., D. Necchi, E. Prosperi, and M. Biggiogera. 2006. Small ribosomal subunits associate with nuclear myosin and actin in transit to the nuclear pores. *Faseb J*. 20:1901-1903.

Cokol, M., R. Nair, and B. Rost. 2000. Finding nuclear localization signals. *EMBO Rep*. 1:411-415.
Core, L.J., J.J. Waterfall, and J.T. Lis. 2008. Nascent RNA sequencing reveals widespread pausing and divergent initiation at human promoters. *Science*. 322:1845-1848.
Crozet, F., A. el Amraoui, S. Blanchard, M. Lenoir, C. Ripoll, P. Vago, C. Hamel, C. Fizames, F. Levi-Acobas, D. Depetris, M.G. Mattei, D. Weil, R. Pujol, and C. Petit. 1997. Cloning of the genes encoding two murine and human cochlear unconventional type I myosins. *Genomics*. 40:332-341.
Cyr, J.L., R.A. Dumont, and P.G. Gillespie. 2002. Myosin-1c interacts with hair-cell receptors through its calmodulin-binding IQ domains. *Journal of Neuroscience*. 22:2487-2495.
De La Cruz, E.M., and E.M. Ostap. 2004. Relating biochemistry and function in the myosin superfamily. *Curr Opin Cell Biol*. 16:61-67.
de Lanerolle, P., T. Johnson, and W.A. Hofmann. 2005. Actin and myosin I in the nucleus: what next? *Nat Struct Mol Biol*. 12:742-746.
Diefenbach, T.J., V.M. Latham, D. Yimlamai, C.A. Liu, I.M. Herman, and D.G. Jay. 2002. Myosin 1c and myosin IIB serve opposing roles in lamellipodial dynamics of the neuronal growth cone. *J Cell Biol*. 158:1207-1217.
Dumont, R.A., Y.D. Zhao, J.R. Holt, M. Bahler, and P.G. Gillespie. 2002. Myosin-I isozymes in neonatal rodent auditory and vestibular epithelia. *J Assoc Res Otolaryngol*. 3:375-389.
Fomproix, N., and P. Percipalle. 2004. An actin-myosin complex on actively transcribing genes. *Exp Cell Res*. 294:140-148.
Frangioni, J.V., and B.G. Neel. 1993. Use of a general purpose mammalian expression vector for studying intracellular protein targeting: identification of critical residues in the nuclear lamin A/C nuclear localization signal. *J Cell Sci*. 105 (Pt 2):481-488.
Garcia, J.A., A.G. Yee, P.G. Gillespie, and D.P. Corey. 1998. Localization of myosin-Ibeta near both ends of tip links in frog saccular hair cells. *J Neurosci*. 18:8637-8647.
Geeves, M.A., and K.C. Holmes. 1999. Structural mechanism of muscle contraction. *Annu Rev Biochem*. 68:687-728.
Gillespie, P.G. 2004. Myosin I and adaptation of mechanical transduction by the inner ear. *Philos Trans R Soc Lond B Biol Sci*. 359:1945-1951.
Gillespie, P.G., J.P. Albanesi, M. Bahler, W.M. Bement, J.S. Berg, D.R. Burgess, B. Burnside, R.E. Cheney, D.P. Corey, E. Coudrier, P. de Lanerolle, J.A. Hammer, T. Hasson, J.R. Holt, A.J. Hudspeth, M. Ikebe, J. Kendrick-Jones, E.D. Korn, R. Li, J.A. Mercer, R.A. Milligan, M.S. Mooseker, E.M. Ostap, C. Petit, T.D. Pollard, J.R. Sellers, T. Soldati, and M.A. Titus. 2001. Myosin-I nomenclature. *J Cell Biol*. 155:703-704.
Gillespie, P.G., and J.L. Cyr. 2002. Calmodulin binding to recombinant myosin-1c and myosin-1c IQ peptides. *BMC Biochem*. 3:31.
Gillespie, P.G., and J.L. Cyr. 2004. Myosin-1c, the hair cell's adaptation motor. *Annu Rev Physiol*. 66:521-545.
Gillespie, P.G., and U. Muller. 2009. Mechanotransduction by hair cells: models, molecules, and mechanisms. *Cell*. 139:33-44.
Gillespie, P.G., M.C. Wagner, and A.J. Hudspeth. 1993. Identification of a 120 kd hair-bundle myosin located near stereociliary tips. *Neuron*. 11:581-594.
Gonda, D.K., A. Bachmair, I. Wunning, J.W. Tobias, W.S. Lane, and A. Varshavsky. 1989. Universality and structure of the N-end rule. *J Biol Chem*. 264:16700-16712.
Grummt, I. 2003. Life on a planet of its own: regulation of RNA polymerase I transcription in the nucleolus. *Genes Dev*. 17:1691-1702.
Grummt, I. 2006. Actin and myosin as transcription factors. *Curr Opin Genet Dev*. 16:191-196.
Harley, V.R., R. Lovell-Badge, P.N. Goodfellow, and P.J. Hextall. 1996. The HMG box of SRY is a calmodulin binding domain. *FEBS Lett*. 391:24-28.
Hartsock, A., and W.J. Nelson. 2008. Adherens and tight junctions: structure, function and connections to the actin cytoskeleton. *Biochim Biophys Acta*. 1778:660-669.

Hirono, M., C.S. Denis, G.P. Richardson, and P.G. Gillespie. 2004. Hair cells require phosphatidylinositol 4,5-bisphosphate for mechanical transduction and adaptation. *Neuron*. 44:309-320.

Hofmann, W.A., T. Johnson, M. Klapczynski, J.L. Fan, and P. de Lanerolle. 2006a. From transcription to transport: emerging roles for nuclear myosin I. *Biochem Cell Biol*. 84:418-426.

Hofmann, W.A., G.M. Vargas, R. Ramchandran, L. Stojiljkovic, J.A. Goodrich, and P. de Lanerolle. 2006b. Nuclear myosin I is necessary for the formation of the first phosphodiester bond during transcription initiation by RNA polymerase II. *J Cell Biochem*. 99:1001-1009.

Hokanson, D.E., J.M. Laakso, T. Lin, D. Sept, and E.M. Ostap. 2006. Myo1c binds phosphoinositides through a putative pleckstrin homology domain. *Mol Biol Cell*. 17:4856-4865.

Hokanson, D.E., and E.M. Ostap. 2006. Myo1c binds tightly and specifically to phosphatidylinositol 4,5-bisphosphate and inositol 1,4,5-trisphosphate. *Proc Natl Acad Sci U S A*. 103:3118-3123.

Holt, J.R., S.K. Gillespie, D.W. Provance, K. Shah, K.M. Shokat, D.P. Corey, J.A. Mercer, and P.G. Gillespie. 2002. A chemical-genetic strategy implicates myosin-1c in adaptation by hair cells. *Cell*. 108:371-381.

Houdusse, A., J.F. Gaucher, E. Krementsova, S. Mui, K.M. Trybus, and C. Cohen. 2006. Crystal structure of apo-calmodulin bound to the first two IQ motifs of myosin V reveals essential recognition features. *Proc Natl Acad Sci U S A*. 103:19326-19331.

Hu, Q., Y.S. Kwon, E. Nunez, M.D. Cardamone, K.R. Hutt, K.A. Ohgi, I. Garcia-Bassets, D.W. Rose, C.K. Glass, M.G. Rosenfeld, and X.D. Fu. 2008. Enhancing nuclear receptor-induced transcription requires nuclear motor and LSD1-dependent gene networking in interchromatin granules. *Proc Natl Acad Sci U S A*. 105:19199-19204.

Iyer, V.R., M.B. Eisen, D.T. Ross, G. Schuler, T. Moore, J.C. Lee, J.M. Trent, L.M. Staudt, J. Hudson, Jr., M.S. Boguski, D. Lashkari, D. Shalon, D. Botstein, and P.O. Brown. 1999. The transcriptional program in the response of human fibroblasts to serum. *Science*. 283:83-87.

Jaillon, O., J.M. Aury, F. Brunet, J.L. Petit, N. Stange-Thomann, E. Mauceli, L. Bouneau, C. Fischer, C. Ozouf-Costaz, A. Bernot, S. Nicaud, D. Jaffe, S. Fisher, G. Lutfalla, C. Dossat, B. Segurens, C. Dasilva, M. Salanoubat, M. Levy, N. Boudet, S. Castellano, V. Anthouard, C. Jubin, V. Castelli, M. Katinka, B. Vacherie, C. Biemont, Z. Skalli, L. Cattolico, J. Poulain, V. De Berardinis, C. Cruaud, S. Duprat, P. Brottier, J.P. Coutanceau, J. Gouzy, G. Parra, G. Lardier, C. Chapple, K.J. McKernan, P. McEwan, S. Bosak, M. Kellis, J.N. Volff, R. Guigo, M.C. Zody, J. Mesirov, K. Lindblad-Toh, B. Birren, C. Nusbaum, D. Kahn, M. Robinson-Rechavi, V. Laudet, V. Schachter, F. Quetier, W. Saurin, C. Scarpelli, P. Wincker, E.S. Lander, J. Weissenbach, and H. Roest Crollius. 2004. Genome duplication in the teleost fish Tetraodon nigroviridis reveals the early vertebrate proto-karyotype. *Nature*. 431:946-957.

Kahl, C.R., and A.R. Means. 2003. Regulation of cell cycle progression by calcium/calmodulin-dependent pathways. *Endocr Rev*. 24:719-736.

Kahle, M., J. Pridalova, M. Spacek, R. Dzijak, and P. Hozak. 2007. Nuclear myosin is ubiquitously expressed and evolutionary conserved in vertebrates. *Histochem Cell Biol*. 127:139-148.

Kohler, D., C. Ruff, E. Meyhofer, and M. Bahler. 2003. Different degrees of lever arm rotation control myosin step size. *J Cell Biol*. 161:237-241.

Kutay, U., F.R. Bischoff, S. Kostka, R. Kraft, and D. Gorlich. 1997. Export of importin alpha from the nucleus is mediated by a specific nuclear transport factor. *Cell*. 90:1061-1071.

Kutay, U., G. Lipowsky, E. Izaurralde, F.R. Bischoff, P. Schwarzmaier, E. Hartmann, and D. Gorlich. 1998. Identification of a tRNA-specific nuclear export receptor. *Mol Cell*. 1:359-369.

Kumar, S., K. Tamura, and M. Nei. 2004. MEGA3: Integrated software for Molecular Evolutionary Genetics Analysis and sequence alignment. *Brief Bioinform*. 5:150-163.

Kysela, K., A.A. Philimonenko, V.V. Philimonenko, J. Janacek, M. Kahle, and P. Hozak. 2005. Nuclear distribution of actin and myosin I depends on transcriptional activity of the cell. *Histochem Cell Biol*. 124:347-358.

Laakso, J.M., J.H. Lewis, H. Shuman, and E.M. Ostap. 2008. Myosin I can act as a molecular force sensor. *Science*. 321:133-136.

Leneuve, P., S. Colnot, G. Hamard, F. Francis, M. Niwa-Kawakita, M. Giovannini, and M. Holzenberger. 2003. Cre-mediated germline mosaicism: a new transgenic mouse for the selective removal of residual markers from tri-lox conditional alleles. *Nucleic Acids Res*. 31:e21.

Lindsay, A.J., and M.W. McCaffrey. 2009. Myosin Vb localises to nucleoli and associates with the RNA polymerase I transcription complex. *Cell Motil Cytoskeleton*. 66:1057-1072.

Livak, K.J., and T.D. Schmittgen. 2001. Analysis of relative gene expression data using real-time quantitative PCR and the 2(-Delta Delta C(T)) Method. *Methods*. 25:402-408.

Lynch, C.J. 2001. Role of leucine in the regulation of mTOR by amino acids: revelations from structure-activity studies. *J Nutr*. 131:861S-865S.

Manceva, S., T. Lin, H. Pham, J.H. Lewis, Y.E. Goldman, and E.M. Ostap. 2007. Calcium regulation of calmodulin binding to and dissociation from the myo1c regulatory domain. *Biochemistry*. 46:11718-11726.

Maravillas-Montero, J.L., and L. Santos-Argumedo. 2011. The myosin family: unconventional roles of actin-dependent molecular motors in immune cells. *J Leukoc Biol*.

Mehta, I.S., M. Amira, A.J. Harvey, and J.M. Bridger. 2010. Rapid chromosome territory relocation by nuclear motor activity in response to serum removal in primary human fibroblasts. *Genome Biol*. 11:R5.

Mohr, D., S. Frey, T. Fischer, T. Guttler, and D. Gorlich. 2009. Characterisation of the passive permeability barrier of nuclear pore complexes. *Embo J*. 28:2541-2553.

Nagata, T., R.S. Redman, and R. Lakshman. 2010. Isolation of intact nuclei of high purity from mouse liver. *Anal Biochem*. 398:178-184.

Nagy, A., J. Rossant, R. Nagy, W. Abramow-Newerly, and J.C. Roder. 1993. Derivation of completely cell culture-derived mice from early-passage embryonic stem cells. *Proc Natl Acad Sci U S A*. 90:8424-8428.

Nambiar, R., R.E. McConnell, and M.J. Tyska. 2010. Myosin motor function: the ins and outs of actin-based membrane protrusions. *Cell Mol Life Sci*. 67:1239-1254.

Nowak, G., L. Pestic-Dragovich, P. Hozak, A. Philimonenko, C. Simerly, G. Schatten, and P. de Lanerolle. 1997. Evidence for the presence of myosin I in the nucleus. *J Biol Chem*. 272:17176-17181.

O'Connell, C.B., M.J. Tyska, and M.S. Mooseker. 2007. Myosin at work: motor adaptations for a variety of cellular functions. *Biochim Biophys Acta*. 1773:615-630.

Obrdlik, A., E. Louvet, A. Kukalev, D. Naschekin, E. Kiseleva, B. Fahrenkrog, and P. Percipalle. 2010. Nuclear myosin 1 is in complex with mature rRNA transcripts and associates with the nuclear pore basket. *Faseb J*. 24:146-157.

Pemberton, L.F., and B.M. Paschal. 2005. Mechanisms of receptor-mediated nuclear import and nuclear export. *Traffic*. 6:187-198.

Percipalle, P., and A.K. Farrants. 2006. Chromatin remodelling and transcription: be-WICHed by nuclear myosin 1. *Curr Opin Cell Biol*. 18:267-274.

Percipalle, P., N. Fomproix, E. Cavellan, R. Voit, G. Reimer, T. Kruger, J. Thyberg, U. Scheer, I. Grummt, and A.K. Farrants. 2006. The chromatin remodelling complex WSTF-SNF2h interacts with nuclear myosin 1 and has a role in RNA polymerase I transcription. *EMBO Rep*. 7:525-530.

Pestic-Dragovich, L., L. Stojiljkovic, A.A. Philimonenko, G. Nowak, Y. Ke, R.E. Settlage, J. Shabanowitz, D.F. Hunt, P. Hozak, and P. de Lanerolle. 2000. A myosin I isoform in the nucleus. *Science*. 290:337-341.

Philimonenko, V.V., J. Janacek, M. Harata, and P. Hozak. 2010. Transcription-dependent rearrangements of actin and nuclear myosin I in the nucleolus. *Histochem Cell Biol*. 134:243-249.

Philimonenko, V.V., J. Zhao, S. Iben, H. Dingova, K. Kysela, M. Kahle, H. Zentgraf, W.A. Hofmann, P. de Lanerolle, P. Hozak, and I. Grummt. 2004. Nuclear actin and myosin I are required for RNA polymerase I transcription. *Nat Cell Biol*. 6:1165-1172.

Pollard, T.D., and E.D. Korn. 1973. Acanthamoeba myosin. I. Isolation from Acanthamoeba castellanii of an enzyme similar to muscle myosin. *J Biol Chem*. 248:4682-4690.

Pyrpassopoulos, S., H. Shuman, and E.M. Ostap. 2010. Single-molecule adhesion forces and attachment lifetimes of myosin-I phosphoinositide interactions. *Biophys J*. 99:3916-3922.

Rossini, K., C. Rizzi, M. Sandri, A. Bruson, and U. Carraro. 1995. High-resolution sodium dodecyl sulfate-polyacrylamide gel electrophoresis and immunochemical identification of the 2X and embryonic myosin heavy chains in complex mixtures of isomyosins. *Electrophoresis*. 16:101-104.

Ruppert, C., J. Godel, R.T. Muller, R. Kroschewski, J. Reinhard, and M. Bahler. 1995. Localization of the rat myosin I molecules myr 1 and myr 2 and in vivo targeting of their tail domains. *J Cell Sci*. 108 (Pt 12):3775-3786.

Seila, A.C., J.M. Calabrese, S.S. Levine, G.W. Yeo, P.B. Rahl, R.A. Flynn, R.A. Young, and P.A. Sharp. 2008. Divergent transcription from active promoters. *Science*. 322:1849-1851.

Sherr, E.H., M.P. Joyce, and L.A. Greene. 1993. Mammalian myosin I alpha, I beta, and I gamma: new widely expressed genes of the myosin I family. *J Cell Biol*. 120:1405-1416.

Sim, H., A. Argentaro, and V.R. Harley. 2008. Boys, girls and shuttling of SRY and SOX9. *Trends Endocrinol Metab*. 19:213-222.

Simon, D.N., and K.L. Wilson. 2011. The nucleoskeleton as a genome-associated dynamic 'network of networks'. *Nat Rev Mol Cell Biol*. 12:695-708.

Sokac, A.M., C. Schietroma, C.B. Gundersen, and W.M. Bement. 2006. Myosin-1c couples assembling actin to membranes to drive compensatory endocytosis. *Dev Cell*. 11:629-640.

Spinelli, K.J., and P.G. Gillespie. 2009. Bottoms up: transduction channels at tip link bases. *Nat Neurosci*. 12:529-530.

Stauffer, E.A., J.D. Scarborough, M. Hirono, E.D. Miller, K. Shah, J.A. Mercer, J.R. Holt, and P.G. Gillespie. 2005. Fast adaptation in vestibular hair cells requires myosin-1c activity. *Neuron*. 47:541-553.

Steinberg, T., N. Ziegler, A. Alonso, A. Kohl, E. Mussig, S. Proksch, S. Schulz, and P. Tomakidi. 2011. Strain response in fibroblasts indicates a possible role of the Ca(2+)-dependent nuclear transcription factor NM1 in RNA synthesis. *Cell Calcium*. 49:259-271.

Suetsugu, S., and T. Takenawa. 2003. Translocation of N-WASP by nuclear localization and export signals into the nucleus modulates expression of HSP90. *J Biol Chem*. 278:42515-42523.

Swanljung-Collins, H., and J.H. Collins. 1992. Phosphorylation of brush border myosin I by protein kinase C is regulated by Ca(2+)-stimulated binding of myosin I to phosphatidylserine concerted with calmodulin dissociation. *J Biol Chem*. 267:3445-3454.

Tang, N., T. Lin, and E.M. Ostap. 2002. Dynamics of myo1c (myosin-ibeta) lipid binding and dissociation. *J Biol Chem*. 277:42763-42768.

Veigel, C., L.M. Coluccio, J.D. Jontes, J.C. Sparrow, R.A. Milligan, and J.E. Molloy. 1999. The motor protein myosin-I produces its working stroke in two steps. *Nature*. 398:530-533.

Vreugde, S., C. Ferrai, A. Miluzio, E. Hauben, P.C. Marchisio, M.P. Crippa, M. Bussi, and S. Biffo. 2006. Nuclear myosin VI enhances RNA polymerase II-dependent transcription. *Mol Cell*. 23:749-755.

Wagner, M.C., B. Barylko, and J.P. Albanesi. 1992. Tissue distribution and subcellular localization of mammalian myosin I. *J Cell Biol*. 119:163-170.

Wagner, M.C., B.L. Blazer-Yost, J. Boyd-White, A. Srirangam, J. Pennington, and S. Bennett. 2005. Expression of the unconventional myosin Myo1c alters sodium transport in M1 collecting duct cells. *Am J Physiol Cell Physiol*. 289:C120-129.

Wagner, M.C., and B.A. Molitoris. 1997. ATP depletion alters myosin I beta cellular location in LLC-PK1 cells. *Am J Physiol*. 272:C1680-1690.

Wang, F.S., C.W. Liu, T.J. Diefenbach, and D.G. Jay. 2003. Modeling the role of myosin 1c in neuronal growth cone turning. *Biophys J*. 85:3319-3328.

Whittaker, M., and R.A. Milligan. 1997. Conformational changes due to calcium-induced calmodulin dissociation in brush border myosin I-decorated F-actin revealed by cryoelectron microscopy and image analysis. *J Mol Biol*. 269:548-557.

Williams, R., and L.M. Coluccio. 1995. Phosphorylation of myosin-I from rat liver by protein kinase C reduces calmodulin binding. *Biochem Biophys Res Commun*. 216:90-102.

Yanai, I., H. Benjamin, M. Shmoish, V. Chalifa-Caspi, M. Shklar, R. Ophir, A. Bar-Even, S. Horn-Saban, M. Safran, E. Domany, D. Lancet, and O. Shmueli. 2005. Genome-wide midrange transcription profiles reveal expression level relationships in human tissue specification. *Bioinformatics*. 21:650-659.

Ye, J., J. Zhao, U. Hoffmann-Rohrer, and I. Grummt. 2008. Nuclear myosin I acts in concert with polymeric actin to drive RNA polymerase I transcription. *Genes Dev*. 22:322-330.

Yildirim, A., and W.J. Whish. 1997. The role of protein secretion on the adhesion strength of Chinese hamster lung (CHL) cells. *Biochem Soc Trans*. 25:381S.

Yip, M.F., G. Ramm, M. Larance, K.L. Hoehn, M.C. Wagner, M. Guilhaus, and D.E. James. 2008. CaMKII-mediated phosphorylation of the myosin motor Myo1c is required for insulin-stimulated GLUT4 translocation in adipocytes. *Cell Metab*. 8:384-398.

Zadro, C., M.S. Alemanno, E. Bellacchio, R. Ficarella, F. Donaudy, S. Melchionda, L. Zelante, R. Rabionet, N. Hilgert, X. Estivill, G. Van Camp, P. Gasparini, and M. Carella. 2009. Are MYO1C and MYO1F associated with hearing loss? *Biochim Biophys Acta*. 1792:27-32.

Zhu, T., K. Beckingham, and M. Ikebe. 1998. High affinity Ca2+ binding sites of calmodulin are critical for the regulation of myosin Ibeta motor function. *J Biol Chem*. 273:20481-20486.

Zhu, T., and M. Ikebe. 1994. A novel myosin I from bovine adrenal gland. *FEBS Lett*. 339:31-36.

12.APPENDIX

The list of papers that form the basis of the thesis and declaration of applicant participation on the data acquisition.

Research paper I

Kahle M, Pridalova J, Spacek M, **Dzijak R** and Hozak P. Nuclear myosin is ubiquitously expressed and evolutionary conserved in vertebrates. Histochem Cell Biol. 2007 Feb;127(2):139-48.
Impact Factor: 4.727 (2010)
R.Dzijak performed RACE sequence aligment and sequence searches.

Research paper II

Dzijak R., Yildirim S., Kahle M., Novák P., Hnilicová J., Venit T., and Hozák P., Specific nuclear localizing sequence directs two myosin isoforms to the cell nucleus in calmodulin sensitive manner. PlosOne, 2011 Accepted Manuscript.
Impact factor 4.411 (2010)
R.Dzijak designed and performed experiments (Immunofluorescence, plasmid constructions, pull downs) and wrote the manuscript

Research paper III

Dzijak R., Rohozkova J., Venit T., Kalendova A., Novak P., Hozak P. Identification of NM1 interacting proteins in human lung cell line A549. Manuscript.
R.Dzijak designed and performed experiments (immunofluorescence on cultured cells and on the tissue sections, co-immunoprecipitation, pull downs, preparation of samples for mass spectrometry) and wrote the manuscript.

On behalf of all authors Pavel Hozák